THE PATHOLOGY AND PATHOGENESIS OF CANINE CEREBRAL BABESIOSIS

By

Anne Dale Pardini

A dissertation in fulfillment of the requirements of the degree

Master of Science in Pathology

Supervisor: Professor N.P.J. Kriek
Departmental Head
Department of Pathology

Faculty of Veterinary Science
University of Pretoria

April 2000

DEDICATION

For my husband:

Stephan

and my children:

Astrid and Theresa.

CONTENTS

SUMMARY

The pathology of canine cerebral babesiosis was examined at the gross, histological and ultrastructural levels. Gross lesions could be categorised as either global or regional. Congestive brain swelling, diffuse cerebral congestion and diffuse cerebral pallor were classified as global lesions. Multifocal haemorrhage and malacia were classified as regional lesions. Oedema was inconsistently present and could be either focal or diffuse.

The majority of histological changes were observed in both cerebral babesiosis and control cases. Regional lesions were unique to cerebral babesiosis and had specific histological features. Highly localised endothelial injury was the primary lesion. Early lesions were multifocal and strictly associated with the microvasculature. Intermediate lesions, with perivascular haemorrhage and neutrophil infiltration, were suggestive of reperfusion injury. Advanced lesions were locally extensive and similar in appearance to haemorrhagic infarction. It is likely that the pathogenesis of regional lesions is by a process of microvascular infarction, as venous thrombosis could not be demonstrated.

Ultrastructural evidence for adherent contact between erythrocytes and capillary endothelium was demonstrated. Endothelial cell necrosis occurred early in the development of lesions, before neuronal and glial injury. It is postulated that endothelial injury is the primary event in the development of regional lesions and secondary lesions develop as a consequence of microvascular infarction.

SAMEVATTING

Die patologie van die serebrale vorm van bosluiskoors in honde is ondersoek. Die letsels is makroskopies, histologies en elektronmikroskopies beskryf. Letsels kon makroskopies in twee groepe verdeel word: Globale letsels en gelokaliseerde letsels. Kongestiewe brein swelling, diffuse serebrale kongestie en serebrale anemie kom voor as globale letsels in serebrale babesiose. Multifokale bloeding en nekrose kom voor as gelokaliseerde letsels. Edeem was nie konsekwent teenwoordig nie, en was algemeen of verspreid.

Die meeste algemene histologiese veranderinge was in beide serebrale en kontrole gevalle teenwoordig. Gelokaliseerde letsels waarin spesifieke hisotpatologiese veranderinge voorgekom het, was kenmerkend van serebrale babesiose. Die primêre letsel is hoogs gelokaliseerde beskadiging van endoteelselle. Beskadiging van die kapillêre bloedvate ontstaan vroeg in die ontwikkeling van letsels. Verdere ontwikkeling van die letsel word gekenmerk deur peri-vaskulêre bloeding en neutrofiel infiltrasie wat aanduidend is van reperfusie beskadiging. Volontwikkelde letsels is plaaslik-ekstensief en het die voorkoms van hemoragiese infarkte. Dit is waarskynlik dat mikrovaskulêre infarksie 'n rol speel in die patogenese van die letsels, aangesien veneuse trombose nie ontstaan nie.

Noue kontak tussen rooibloedselle en kapillêre endoteel is elektronmikroskopies bevestig. Endoteelselnekrose ontstaan voordat tekens van beskadiging geidentifiseer kan word in neurone of gliaselle. Dit blyk dat kapillêre endoteelselbeskadiging die primêre letsel by die ontstaan van gelokaliseerde lesels is, en dat sekondêre lesels ontwikkel as gevolg van mikrovaskulêre infarksie.

Acknowledgments

Prof NPJ Kriek, my supervisor for this project.

Canine Babesiosis Research Group and the Dean, Faculty of Veterinary Science: Prof. Coubrough who provided the funding for the project.

The Department of Pathology, especially the "pathologists on duty" and the final year pathology clinic students who were so patient about the long and drawn-out sampling process on their cases.

The Histopathology Laboratory staff, Department of Pathology, Veterinary Faculties of UP and MEDUNSA who processed the samples for histopathology and electron microscopy, especially Marianna Rossouw.

The members of staff of the EM unit: Herklaas Els and Daleen Jocelyn.

I would also like to thank the following people for their suggestions, support and encouragement:
Piet Becker and Bruce Gummow, Alan Guthrie, Linda Jacobson, John Jardine,
Emily Lane, Banie Penzhorn, Fred Reyers, and last but not least, Stephan Vogel.

My thanks go to the many other people who contributed in so many small ways to the completion of this dissertation. I would particularly like to thank my family for their loyal support and untiring patience.

List of Abbreviations

ARDS	Acute respiratory distress syndrome
ARF	Acute renal failure
C_3	Complement 3
CNS	Central nervous system
DIC	Disseminated intravascular coagulation
F no.	File number
FDP	Fibrin degradation product
GIT	Gastro-intestinal tract
ICAM-1	Intercellular adhesion molecule – 1
ICP	Intracranial pressure
IgG	Immunoglobulin G
IgM	Immunoglobulin M
IL-1	Interleukin 1
INF-gamma	Interferon gamma
iNOS	Inducible nitric oxide synthase
Mag.	Magnification
MODS	Multiple organ dysfunction syndrome
nm	Nanometre
NO	Nitric oxide
PAF	Platelet activating factor
pcv	Packed cell volume
PM no.	Post mortem number
pRBC	Parasitised red blood cells
RCC	Red cell changes
SIRS	Systemic inflammatory response syndrome
S. no.	Histopathology sample registration number
SPA	Soluble parasite antigen
TNF	Tumour necrosis factor
VAH	Veterinary Academic Hospital
VR-space	Virchow-Robbins space
µm	Micron

List of Figures

FIGURE 5: HISTOPATHOLOGY OF REGIONAL LESIONS.

Figure 5a.
Advanced lesion with severe, multifocal to coalescing haemorrhage and malacia of the cerebral cortex.

(Mag. 40x)

Figure 5b.
An early lesion, showing a focal area of rarefaction in the neuropil (focal perivascular oedema).
(Mag. 400x)

Figure 5c.
Detail of an advanced lesion showing malacia and haemorrhage with neutrophil infiltration.
(Mag. 200x)

FIGURE 6: HISTOPATHOLOGY OF REGIONAL LESIONS

Figure 6a.
Segmental necrosis of a small vessel.
(Mag. 400x)

Figure 6b.
Area of expansion on the periphery of a severe lesion.
(Mag.200x)

Figure 6c.
Regional lesion in the white matter.

(Mag.200x)

FIGURE 7: ULTRASTRUCTURAL FEATURES OF ERYTHROCYTES

Figure 7a.
Portion of a small caliber vessel, showing the lumen containing many extensively distorted erythrocytes.
Original magnification 2600X. E854. EM1.98.

Figure 7b.
Venule with fibrin degradation products and erythrocyte fragments.
Original magnification 3400X. E848. EM1.98.

Figure 7c.
Compression of an erythrocyte within a capillary.
Original magnification 10500X. E839. EM1.98

FIGURE 8: INTERCELLULAR CONTACT POINTS

Figure 8a.
Inter-erythrocytic contact: Detail of two adjacent erythrocytes showing an amorphous granule between the two cells.
Original magnification 64 000X. E849. EM1.98.

Figure 8b.
A parasitised erythrocyte lies within a capillary. At three sites, distinct electron-dense contact points are present.
Original magnification 11500X. E905. EM4.98.

Figure 8c.
An erythrocyte ghost in contact with the endothelium at a single electron-dense site of attachment.
Original magnification 15500X. E891. EM3.98.

FIGURE 9: ULTRASTRUCTURAL FEATURES OF ERYTHRO-ENDOTHELIAL CONTACT

Figure 9a.
Erythrocyte-endothelial contact.
Original magnification 13 500X. E886. EM3.98.

Figure 9b.
Membrane stacks. Detail of contact between erythrocytes and endothelium
Original magnification 73 000X. F034. EM3.98.

FIGURE 10: ULTRASTRUCTURE - VASCULAR INTEGRITY AND COAGULATION

Figure 10a.
Fibrin thrombus.
Original magnification 2950X. E912. EM5.98.

Figure 10b.
Polymerisation of fibrin in the VR-space.
Original magnification 8900X. E743. EM27.96.

Figure 10c.
Endothelial retraction resulting in exposure of the basement membrane.
Original magnification 5800X. E879. EM6.97.

FIGURE 11: ULTRASTRUCTURE: VASCULAR INTEGRITY AND COAGULATION

Figure 11a.
Endothelial retraction resulting in exposure of the basement membrane.
Original magnification 10 000X. E928. EM6.97.

Figure 11b.
Detail of the vascular wall showing a breach in endothelial integrity.
Original magnification 4600x. E847. EM1.98.

Figure 11c.
Endothelial retraction and vasoconstriction with exposure of the basement membrane and occlusion of the vascular lumen.
Original magnification 4600x. E927. EM6.97

List of Tables

List of Appendices

Glossary of Terms

Adhesion: Flattening of parasitised erythrocytes along the vascular wall following margination.

Arterial supply territory: Volume of cerebral tissue supplied by an individual major cerebral artery.

Apoptosis: Individual cell death initiated by genetic mechanisms from within the affected cell.

Autoregulation: Compensatory vasoconstriction or dilatation of arteries and arterioles in response to physiological stimuli such as hypercapnia, hypoxia and intravascular pressure fluxes.

Border zones: Cerebral parenchyma situated on the periphery of adjacent arterial supply territories.

Cerebral flush: See congestive brain swelling.

Cerebral oedema: Increase in water content of brain tissue.

Cerebral vasomotor paralysis: Loss of cerebral vasomotor tone in arteries and arterioles. This phenomenon is a consequence of loss of autoregulation.

Compound granular corpuscles: Mononuclear phagocytic cells within the central nervous system actively engulfing necrotic debris and hence bulging with lipid vacuoles. These cells can be of microglial or adventitial origin.

Congestive brain swelling: An increase in intravascular fluid volume of the brain leading to raised intracranial pressure.

Definitive host: Host in which the parasite undergoes the sexual stage of the life cycle (in babesiosis this is the tick vector).

Delayed neuronal death: Neuronal injury that becomes morphologically appreciable by light microscopy 48 hours or more after a brief period (5 – 10 mins) of ischaemia.

Erythrocyte ghosts: Erythrocyte remnants consisting of the injured plasmalemma devoid of haemoglobin.

Fibrin degradation products: (FDP) Fragments of fibrin polymers following enzymatic breakdown of strands.

Gitter cells: See compound granular corpuscles.

Hypoxia: Oxygen deficiency as a result of various causes such as reduced concentration of oxygen in the blood (hypoxic hypoxia) or interrupted blood supply or reduced blood flow to an area (stagnant hypoxia).

Homogenizing cell change: Late stage of the ischaemic cell process in which neuronal cytoplasm stains homogeneously acidophilic with complete loss of nuclear definition.

Infarction: The process by which all cell bodies (neuronal and glial), blood vessels (arteries, veins and capillaries) and nerve fibres (myelinated and non-myelinated) in a given volume of tissue, undergo necrosis as a result of a reduction in blood flow. Ischaemic infarction occurs as a result of total obstruction of an end-arterial system. Haemorrhagic transformation of infarction occurs as a consequence of distal migration of a thrombus (embolisation deeper into area of infarction). Haemorrhagic infarcts develop as a consequence of venous obstruction.

Intermediate host: Host in which the parasite undergoes the asexual stage of the life cycle (in babesiosis this is the vertebrate host).

Ischaemic cell change: Middle stage of the ischaemic cell process in which the soma is shrunken with loss of Nissl substance and the nucleus is shrunken, dark-staining and often triangular. The cytoplasm is acidophilic, staining pink with eosin and mauve with Luxol fast blue. As neuronal injury progresses, basophilic incrustations become discernable as minute granular deposits on the plasmalemma.

Ischaemic cell process: Morphologically appreciable stages of neuronal injury commencing with microvacuolation and progressing through the stages of ischaemic cell change without incrustations, with incrustations, finally culminating in homogenising cell change after which there is disappearance of the neuron.

Karyorrhexis: Cellular necrosis characterised by nuclear fragmentation.

Karyopyknosis: Cellular necrosis characterised by nuclear shrinkage.

Margination of parasitised erythrocytes: Abnormal spatial positioning of parasitised erythrocytes against endothelium.

Microvacuolation: The earliest appreciable morphological change in neurons undergoing the ischaemic cell process (perfusion fixation). Basophilic neuronal cytoplasm contains numerous small vacuoles that cluster beneath the plasmalemma and around the nucleus.

Micro-vessel: Vessels less than 50 μm in diameter including capillaries and post-capillary venules.

Necrosis: Irreversible injury leading to cellular death within living tissue.

Perivascular space: The interstitial space around blood vessels. In normal brain, this is only a potential space, between astrocyte foot processes and the cells of the vessel wall. In microvasculature, only the basement membrane lies between the endothelium and astrocyte foot processes. Enlargement of this space may be an artifact in tissue sections, or alternatively, may represent oedema.

Pink brain: See congestive brain swelling.

Pyknosis: See karyopyknosis.

Reperfusion injury: The re-establishment of circulation after a critical period of anoxia-ischaemia which will allow a suboptimal degree of metabloic activity to occur, may be associated with a greater degree of morphologically visible tissue damage than if reperfusion did not occur.

Selective vulnerability: Site-specific neuronal response to hypoxia and other noxious stimuli. Cells showing the highest sensitivity are those of the cerebral cortex, particularly layers III,

V and VI, and large neurons such as the cerebellar Purkinje cells. Neurons in Sommer's sector of the hippocampus and in the border zones between arterial territories, are particularly sensitive to hypoxia.

Sequestration of parasites: Invasion of erythrocytes by parasites in order to escape detection by the immune system.

Sequestration of parasitised erythrocytes: Accumulation of parasitised erythrocytes in the microvasculature of organs in order to allow parasite proliferation by avoiding entrapment in the spleen. Unless otherwise specified, sequestration in the text refers to sequestration of parasitised erythrocytes.

Severe cell change: The cell body is swollen with loss of Nissl substance around a swollen nucleus. The cell margins are irregular with formation of ringlets and sometimes large vacuoles. The cell processes are stained.

Sludging (of erythrocytes): Intravascular haemagglutination of unparasitised erythrocytes in small caliber vessels. Individual erythrocytes are not necessarily discernible. Inflammatory cells and parasitised erythrocytes may be trapped in the sludge.

VR-space: Virchow-Robbins space (see perivascular space).

Wall shear stress: Force of friction acting on endothelium as a consequence of blood flow

INTRODUCTION

Cerebral babesiosis is an important, rare and rapidly fatal manifestation of *Babesia canis* infection in dogs. Numerous case studies have been published describing the disease and its pathology (5,56,63,65,66). Griffiths described cerebral babesiosis in 1922 (24) from 12 cases and van der Lugt and Jardine described 17 cases in 1994 (80). Experimental studies of canine babesiosis have failed to reproduce cerebral babesiosis as it is seen clinically (54,68). Jardine (39) investigated the ultrastructure of canine babesiosis but was unable to demonstrate morphological features of erythrocytes equivalent to those observed in cerebral malaria or bovine cerebral babesiosis (such as knobs, stellate processes or scalloping).

There are no published large-scale investigations of cerebral babesiosis in dogs, either of clinical, pathological or ultrastructural aspects of the disease. The relationship between clinical neurological signs and central nervous lesions is unknown. The role of the parasite in the development of cerebral disease is poorly understood. The causative organism is not conclusively identified, as *B. canis* has three sub-species. It is not known whether *B. canis rossi* is the only subspecies in southern Africa, and whether it expresses antigenic variability as does *Babesia bovis* (62) and *Plasmodium falciparum* (77). There is a very real possibility that cerebral babesiosis in dogs may be the best candidate for an animal model of cerebral malaria, but it has not as yet been possible to reproduce canine cerebral babesiosis experimentally. The pathogenesis is poorly understood. It is not known what influence the host's immune system has on determining survival. Immune complex deposition and activation of specific sub-populations of lymphocytes may be important factors influencing fatality. A better understanding of the pathogenesis may increase the survival rate of dogs suffering from cerebral babesiosis and in the long term, may help children suffering from cerebral malaria.

I investigated the pathology of central nervous disease in canine babesiosis. A large-scale study of gross lesions (56 cases) and histopathology (54 cases) was undertaken. Lesions were classified according to their morphology. A small ultrastructural study (7 cases) was conducted to establish whether erythrocytic changes similar to those seen in cerebral malaria and bovine cerebral babesiosis were present. The pathogenesis of cerebral babesiosis was interpreted in terms of the lesions observed.

LITERATURE REVIEW

Haemoparasitic protozoa of the genus *Babesia* are known to infect numerous host animals, including cattle, other domestic and wild ruminants, felidae, equidae, various species of rodents and man (67). In most host animals, lesions typical of a haemolytic syndrome are present and the case fatality rate is low provided treatment is instituted. Clinical findings associated with infection are highly variable and can include fever, haemolysis, anaemia, increased respiratory rate, splenomegaly, occasional hepatomegaly, swelling of lymph nodes, icterus and haemoglobinuria (30,34,45,47,67,83).

Canine babesiosis is caused by *Babesia canis*. There are three known variants of the organism, which are presumed to be distinct subspecies: *B. canis canis*, *B. canis vogeli* and *B. canis rossi* (78). The disease is widespread in the tropical and sub-tropical regions of the world (67). It has been recorded from Central and South America, the southern United States of America, Africa, southern Europe, Asia and Australia (67). It is a gradual wasting disease, not necessarily fatal, and survivors develop a carrier state (67,79). This typical form of the disease is recorded from most parts of the world and can be caused by *B. canis canis*, which is apparently more virulent than *B. canis vogeli* (73). However, in Africa in particular, a very severe, complicated and fatal form of the disease, thought to be caused by *B. canis rossi* (51,71,78), frequently develops.

Typical babesiosis may be acute, subacute or chronic (30). It may present as severe or mild disease, and can be fatal at any stage of its progression (36,54,60,67,79). The mechanisms by which babesiosis is fatal, vary with the progression of the disease (54,56). In the more acute stages, severe lung oedema, anaemia and hypoproteinaemia (56) can lead to respiratory failure (54). In protracted disease, hypovolaemic shock as a result of anaemia ultimately leads to death (54). Infection appears to be more severe in puppies and young dogs than in adult dogs (24,34,54,79). In the United States of America and Australia adult animals may become carriers and suffer recurrent relapses, but death is seldom recorded (54,67). This type of disease manifestation is associated with *B. canis vogeli* and *B. canis canis* infections (73).

In addition to the well-documented acute to subacute haemolytic form of canine babesiosis(30,54), a number of unusual manifestations (atypical forms) have been reported in France (16,56) and Africa (36,55,56,60,65,66). Moore and Williams (60) suggested that

babesiosis be categorised clinically as either uncomplicated or complicated disease. This is in contrast to the traditional *post mortem* classification of typical or atypical disease. The older terminology (typical and atypical forms) was derived from English translations of the original French (16) and is currently used as a descriptive term in the pathology of canine babesiosis. The more recent alternative terminology (uncomplicated or complicated disease) is used clinically (5,6,16,34,36,52,63,65,66,80). "Typical and atypical" will be used to refer to necropsy findings and "complicated and uncomplicated" will be used to refer to clinical findings.

It must be stressed that not all complicated/atypical forms are always present in all cases. Usually there is involvement of more than one organ, the exact combinations being highly variable from case to case (24,54,55,56,67,68). In complicated cases, failure of a single organ or organ system may predominate, while in others, multiple organ failure is present (36,56,60). In the majority of cases suffering from uncomplicated disease, the spleen, lymph nodes, liver and kidneys are affected to a greater or lesser extent (30). Failure of organs such as the liver, lungs, kidneys, heart, musculature, pancreas, gastro-intestinal tract, central nervous system or combinations thereof lead to the development of complicated or atypical disease. Disturbances in the circulatory system are thought to cause the haemoconcentration form of the disease, or the oedema form (36,56,60). Abnormalities of coagulation and immune mediated haemolytic anaemia have also been reported (36).

In the first quarter of this century, clinical neurological signs associated with canine babesiosis (then termed piroplasmosis) were observed by researchers from France (16) and Africa (24). Reports from Africa included both central (5,6,16,24,36,60,63,65,66,36) and peripheral (55,56,60,68,80) nervous disorders of canine babesiosis. Griffiths categorised canine babesiosis into five different groups, one of which was "pseudo-rabies" or cerebral babesiosis (24). In 1947, Purchase (66) published observations of high cerebral parasitaemias in sections from dogs dying of suspected rabies. Purchase termed this form of disease cerebral babesiosis.

Basson and Pienaar (5) described the lesions of canine cerebral babesiosis from two cases. Piercy (65) described bilaterally symmetrical haemorrhages in the cerebrum of a dog that died peracutely of babesiosis. Cerebral ecchymoses were not reported by Purchase (66), Malherbe and Parkin (56) or Okoh (63).

The two primary microscopic changes associated with canine cerebral babesiosis include accumulation of parasitised erythrocytes in cerebral capillaries (5,63,65,66) and malacia with haemorrhage ranging in size from petechiae (5,65,66,80) through ecchymoses to suggillations (5,60). Peripheral parasitaemia may be high or low in canine cerebral babesiosis (65,66).

Canine cerebral babesiosis was defined in 1965 as *an atypical manifestation of babesiosis that is characterised by the following: nervous symptoms, sludging of parasitised erythrocytes in the smaller vessels and capillaries of the brain, and referable lesions* (5). The presence of bilaterally symmetrical haemorrhage and malacia in the cerebral cortex is considered to be the hallmark of cerebral babesiosis (5). Purchase (66) was the first to publish a description of canine cerebral babesiosis. He made three important histopathological observations:

1). Vessels were packed with parasitised erythrocytes;
2). An uneven distribution of capillary filling was present;
3). There was no localised cellular reaction to the parasites by the host.

Purchase made no mention of haemorrhage, and it must be assumed that this was not present in the sections he examined.

Basson and Pienaar (5) described the macroscopic lesions of canine cerebral babesiosis from two cases. The cerebral lesions of both cases were similar, and included severe congestion, mild oedema, and roughly bilaterally symmetrical haemorrhages in the cerebral cortex, dentate nucleus and caudate nucleus. Piercy (65) described bilaterally symmetrical haemorrhages in the cerebrum of a dog that died peracutely of babesiosis. Thrombosis of small arteries, causing areas of necrosis, was observed in a case report by Botha (6), who also observed liquefactive necrosis and extensive haemorrhages in the cerebral substance. The lesions observed by Botha may have been a consequence of diamidine toxicity (61). In contrast, cerebral ecchymoses were not reported by Purchase (66), Malherbe and Parkin (56) or Okoh (63).

Microscopic lesions reported in canine cerebral babesiosis are variable. In the majority of cases sludging of parasitised erythrocytes in the smaller vessels of the brain is considered a significant finding (5,54,63,65,66) and is also reported from *B. bovis* infection in cattle (14,17). Petechial haemorrhage is frequently observed (5,65,66,80) and perivascular haemorrhages are particularly noted in the cerebral cortex (5,80). Larger haemorrhagic

lesions have a tendency to be bilateral and symmetrical (5,65), involving the cerebral cortex (5,60) cerebellum and occipital lobes (60). Fibrin thrombi were reported by Moore and Williams (60). Margination of parasitised erythrocytes (pRBCs) in larger veins was observed by Basson and Pienaar (5) and layering of pRBCs along the endothelium of blood vessels was reported by Maegraith *et al.* (54).

Basson and Pienaar (5) also reported: Severe, diffuse, cerebral congestion and oedema; homogeneous, eosinophilic material in the Virchow-Robbins (VR) spaces; infiltration of the perivascular spaces by neutrophils or mononuclear cells; degenerative and necrotic changes in the neuropil; *Babesia* parasites free in the lumen of capillaries or in tissues; glial cells showing increased cytoplasmic volume and protein droplets in the VR-spaces or in vessel walls.

Sludging of parasitised erythrocytes in the smaller vessels of the brain has been reported in the absence of neurological signs in babesiosis (5,54,63). It has been suggested that microvascular obstruction may result from parasitic emboli (11) , in keeping with theories of the pathogenesis of cerebral malaria (18).

The pathogenesis of cerebral babesiosis is poorly understood. Factors that may play a role in the development of lesions include hypoxia (5,54), increased vascular permeability (54,55,56,68) microvascular obstruction (11,60) and infarction (5,60).

Maegraith *et al.* (54) demonstrated that even in the presence of severe anaemia in babesiosis, the blood was still capable of delivering an adequate supply of oxygen to the brain, and brain hypoxia was not demonstrable in their cases. In the presence of anaemia the oxygen carrying capacity of the blood is still sufficient to sustain life (23,54). An additional factor such as pulmonary insufficiency (hypoxic hypoxia) is required, for cerebral hypoxia to develop (23). Changes in pH and other physiological disturbances associated with inflammation may adversely influence the ability of haemoglobin to release oxygen in babesiosis infections (50).

Selective vulnerability of neurons is used to explain the distribution of neuronal ischaemic cell change following cerebral hypoxia (23). It is well documented in numerous species: rat (10), Rhesus monkey (7) and other mammalian species (42). The causes of ischaemic cell change are multiple, including various mechanisms of hypoxia, hypoglycaemia, cytotoxicity

and intoxication (8). Selectively vulnerable sites in the brain include Sommer's sector and the end folium of the hippocampus, the putamen and amygdala, laminae III, V and VI of the cerebral cortex, cerebellar Purkinje cells and basket cells of the cortex, and the border zones of arterial territories. Ischaemic cell change occurs more rapidly in the floors and sides of sulci than in the crests of gyri (23).

Selective vulnerability of neurons is explained by several mechanisms. Some sites are vulnerable to hypoxic injury during hypotension (border zones), while other sites develop injury as a result of a proposed biochemical vulnerability to hypoxia (Purkinje cells, basket cells) (23).

It is thought that laminar cortical necrosis and total cortical necrosis develop as a consequence of microvascular injury (44). The capillaries supplying layers V and VI are thought to be highly susceptible to hypoxic injury, while layer IV, which is more resistant, has a much higher capillary density (44). Capillaries in the depths of sulci are the first sites to show impaired filling in experimentally-induced cerebral infarction in the cat (44).

In babesiosis of cattle, hypotension has been suggested as an important predisposing factor leading to erythrostasis of pRBC (14,72). A sudden significant drop in blood pressure has been shown to cause hypoxic injury to neurons in the border zones of arterial territories in some species (23). This suggests that hypotension in canine babesiosis, albeit insufficient in the majority of cases to induce cerebral hypoxia, may predispose to margination and stasis of pRBC, allowing a nidus of microvascular obstruction to develop more readily in border zones than in other regions of the brain.

It is extremely difficult to produce cerebral infarction in dogs, because of the tremendous efficiency of the collateral blood supply (22,46,76,85). Simultaneous surgical occlusion of the internal carotid artery, the middle and rostral cerebral arteries and the posterior communicating artery on the right side, allows consistently reproducible unilateral infarction in the thalamus. At least six arteries on one side of the circle of Willis have to be occluded to induce unilateral cerebral mantle infarction in the dog (76). This suggests that significant cerebral infarction in babesiosis would have to occur in large arteries in order to produce the extensive lesions observed in the majority of cases. Alternatively, venous infarction may play a role in lesion development (23).

Cerebral infarction is defined as a volume of tissue within which all cell bodies (neuronal and glial), blood vessels (arteries, veins and capillaries) and nerve fibres (myelinated and non-myelinated) have undergone necrosis as a result of a reduction in blood flow (23). Infarction may occur as a consequence of arterial or venous obstruction, or following a critical reduction in blood flow. Ischaemic infarction occurs as a consequence of arterial obstruction (23). Haemorrhagic infarction may occur in three ways: by reperfusion following migration of an arterial embolus (haemorrhagic transformation of infarction), by partial intermittent arterial occlusion, and by venous occlusion (44,49).

Histologically, cerebral infarction is recognisable within the first 4 – 6 hours following occlusion, and is characterised by coagulative necrosis of all tissue elements. Dead neurons have intensely eosinophilic vacuolated cytoplasm and their nuclei stain poorly with haematoxylin. With increasing time, cellular staining deteriorates and neuronal ghost cells are barely discernable. No selective vulnerability of neurons is noted, and the process of neuronal necrosis is thought to be distinct from the ischaemic cell process. In the capillary bed there is ultrastructural evidence of early necrosis and swelling of endothelial cells, and after 2 days the capillary bed can no longer be identified. Larger vessels may be identifiable several weeks after infarction. Pale myelin staining and swelling of axons and myelin sheaths develop between 16 and 24 hours following infarction (23).

Ischaemic infarction in the canine brain has been induced experimentally (85). The four-artery occlusion model has been used in the dog to induce ischaemic thalamic infarction (46). Haemorrhagic infarction secondary to ischaemic infarction following reperfusion into an area where neuronal injury is already apparent (49), is termed haemorrhagic transformation of infarction.

A critical period of 3 to 12 hours of vascular occlusion followed by reperfusion, is necessary for the occurrence of haemorrhagic transformation of infarction in the dog (46). With less than 3 hours of occlusion, vascular injury is insufficient to allow extravasation of erythrocytes, so haemorrhagic transformation does not occur in under 3 hours of infarction. Haemorrhagic transformation of infarction is less likely to occur after prolonged ischaemia in excess of 12-24 hours, as necrotic debris and neutrophils obstruct the vessels in the ischaemic site, and blood is unable to enter the damaged area (46). After 3 to 6 hours of total arterial obstruction, ultrastructural features of endothelial injury progress from swelling of endothelial cells and pericytes in the early stages, to destruction of the tight junction at 6

hours. After 12 hours of occlusion, erythrocytes can be observed in the gaps between widened tight junctions. A rapid rise in regional cerebral blood flow following the end of the period of occlusion suggests that haemorrhagic transformation occurs in the first half hour following reperfusion (46). Haemorrhagic infarction was not induced experimentally unless the duration of vascular occlusion was at least 3 hours. This correlates well with findings suggesting that impairment of vascular function during ischaemia only develops after at least 3 hours and is more pronounced after 6 hours (44). Three hours is the approximate duration of ischaemia required to induce microvascular injury with increased vascular permeability (35) or reduced vascular filling (44). The most vulnerable vessels are the capillaries in the depths of sulci in the cerebral cortex, which show homogeneous loss of filling by 6 hours (44). However, morphological endothelial injury is not demonstrable at the ultrastrucural level even after 6 hours of ischaemia (82) although total loss of capillaries is present at 48 hours (23). The first morphological signs of neuronal injury, namely microvacuolation of neuronal cytoplasm, can be demonstrated 15 to 30 minutes after the onset of ischaemia if tissue is fixed by perfusion (7,8,10). Ischaemic cell change can develop very rapidly. It is appreciable in rodent tissue after as little as 15 – 30 minutes of survival time following an ischaemic insult (9). After 4 -12 hours of ischaemia, ischaemic cell change with and without incrustations and early homogenising change can be observed in sections (23). Ischaemic cell change with incrustations can be seen as early as 30 minutes of survival time following an ischaemic insult in the rat, and 90 minutes in non-human primates (9). This type of change can persist in large neurones of the rat up to 24 hours and up to 48 hours in the monkey (9). Homogenising cell change has been observed after only 4 hours of survival in the rat, and can persist up to 21 days following hypoxia in this species. The same change fades more rapidly following infarction (7 – 10 days) (9). In the non-human primate, homogenising cell change persists for about 10 days (9).

Koshu et al.(46) showed that haemorrhagic transformation of infarction is dependent on a post-ischaemic rise in cerebral blood flow following reperfusion. A no-reflow phenomenon did not occur in those dogs whose regional cerebral blood flow was monitored in his study. In venous infarction, venous flow is halted, and back-damming of blood occurs in the region drained by the obstructed vein (23). This type of lesion gives rise to severe, locally-extensive haemorrhage in the injured neuropil.

Occlusion of superficial cortical veins induces unilateral lesions involving the cortex and subcortical structures. Occlusion of internal cerebral veins cause infarcts that are deep-

seated, bilateral and close to the midline. Occlusion of the superior saggital sinus is accompanied by extensive bilateral subcortical haemorrhage and malacia of the frontal and parietal lobes in particular. In adults, perivenous ring haemorrhages are present histologically, while in infants and young children, confluent myelin breakdown and even liquifaction of white matter, is seen with sparing of cortical tissue and basal ganglia. Infections and dehydration have been identified as predisposing factors for intracranial venous infarction, but causative associations between thrombosis and the presumptive risk factors have rarely been demonstrated (21).

In cats, permanent occlusion of the middle cerebral artery resulted in lesions in cortical capillaries only. Temporary occlusion of the artery resulted in 6 animals (60%) showing capillary injury in the white matter, 2 of which had lesions restricted to white matter. Additionally, capillaries in certain cortical sites may be more vulnerable to fluctuations in blood flow, than subcortical capillaries, paricularly with respect to grey and white matter. Flow rates in grey matter are higher than in white matter (44).

The pathogenesis of the lesions seen in atypical forms of babesiosis is uncertain. It has been suggested that the pathogenic mechanisms involved in malaria and babesiosis may be similar (12,36,47,54). Ultrastructural studies of cerebral malaria and bovine babesiosis have demonstrated changes in the structure of the erythrocyte membranes, and the endothelial surfaces, which may be responsible for the sequestering behaviour of parasitised erythrocytes in these diseases. A single ultrastructural case report of *Babesia canis* infection (wild dog - *Lycaon pictus)* has been published (13). Erythrocyte plasmalemmal abberances such as knobs or stellate projections (2) were not observed.

Microvascular obstruction has long been thought to be an important pathogenic factor in babesiosis. Brumpt (11) suggested that sludging of parasitised erythrocytes in microvessels was the primary factor influencing the development of cerebral babesiosis. Moore and Williams suggested that disseminated intravascular coagulation (DIC) gave rise to complications in babesiosis, including cerebral lesions (60).

Jacobson and Clarke (36) discussed the pathogenesis of complicated canine babesiosis, drawing attention to the systemic inflammatory response syndrome (SIRS), multiple organ dysfunction syndrome (MODS), and the possible role of tumour necrosis factor (TNF) and nitric oxide (NO) in the development of disease. In particular, raised levels of cerebral nitric

oxide were suggested as a possible cause of reversible coma without residual effects in cerebral babesiosis (12).

Canine cerebral babesiosis has some clinical and morphological similarities to human cerebral malaria (36,54,55,66), *Plasmodium berghei yoelii* infection in mice (4), *Plasmodium knowlesi* malaria in Rhesus monkeys (*Macaca mulatta*) (32) and cerebral babesiosis in cattle. It has been suggested that the pathogenic mechanisms involved in malaria and babesiosis may be similar (12,36,54,63). Electron microscopic studies of brain sections of malaria and bovine babesiosis cases have demonstrated changes in the structure of the erythrocyte membranes, and the endothelial surfaces, which may be responsible for the behaviour of parasitised erythrocytes in these diseases. An ultrastructural study of the pulmonary vasculature in mice infected with the WA1 strain of *Babesia* showed endothelial cell hyperplasia with intact tight junctions (28).

Adherence of parasitised erythrocytes to one-another, to unparasitised erythrocytes and to endothelium, has been observed in cattle infected with *Babesia bovis* (3,64,84), Rhesus monkeys infected with *Plasmodium knowlesi* (32) and humans infected with *Plasmodium falciparum* (1,53,64). The interaction between parasitised erythrocytes (pRBCs) and endothelium is termed sequestration and refers to the sequestration of pRBCs in capillaries and small caliber vessels within organs. Long, slender connecting strands between adjacent parasitised erythrocytes have been described from ultrastructural studies of bovine babesiosis (84). Stellate projections on the surface of erythrocytes (elliptical protrusions) were observed to effect adhesion between parasitised erythrocytes and endothelium in cerebral babesiosis of cattle (3). Aikawa *et al.* (1) described knobs on the membranes of erythrocytes infected with *P. falciparum*, which act as focal junctions of attachment to the endothelium.

Attachment of erythrocytes to endothelial cells and erythrocyte agglutination, are not confined to the brain in malaria and babesiosis. Gutierrez *et al.* (25) demonstrated adhesion of parasitised erythrocytes to the endothelium of the lungs of *Aotus* monkeys experimentally infected with *Plasmodium falciparum*. Colly and Nesbit (13) demonstrated intravascular agglutination of *B. canis*-infected erythrocytes in pulmonary blood vessels of a captive-bred wild dog (*Lycaon pictus*).

In addition to binding with other cells, erythrocytes undergo certain morphological changes in bovine babesiosis and cerebral malaria. Lipid peroxidation of erythrocyte membranes may influence rigidity and deformability of the red cell. Lipid peroxidation is induced by free radicals and has been implicated in causing the microvascular stasis characteristic of *B. bovis* infection (14). Decreased vitamin E levels could result in increased erythrocyte membrane lipid peroxidation, leading to loss of deformability of the erythrocyte, with consequent capillary pooling (86). Oxidative reactions following release of TNF in malaria and babesiosis could cause lipid peroxidation of erythrocyte membranes (12). Ultrastructurally visible projections of the plasmalemma of endothelial cells (endothelial pseudopodia), which extend into the vascular lumen as long, slender projections, have been observed in cases of falciparum malaria in man (53). Similar endothelial pseudopodia have been described in the cerebellum of chickens fed a diet high in linoleic acid and low in vitamin E (86), and in Rhesus monkeys infected with *Plasmodium knowlesi* (32).

It has been shown that adherence of erythrocytes to one another and to the endothelium can occur in response to a decrease in circulatory flow rate (14). Increased membrane-bound haemoglobin, hypotension of acute infection, and altered plasma components are thought to contribute to decreased circulatory flow rate. The plasma components most likely to influence this, are fibrin and cryoglobulins (14). A decrease in circulatory flow rate would decrease oxygen delivery to the tissue, increasing the risk of capillary endothelial hypoxia and conversion of xanthene dehydrogenase to xanthene oxygenase (33). Xanthene oxygenase converts available oxygen to superoxide which, under normal conditions, would be neutralised by vitamin E and other radical scavengers (20,33). Injury to tissue as a consequence of ischaemia, is thought to occur following reperfusion, and is mediated by oxygen free radicals such as superoxide, but also hydroxyl radicals (20). Although lipid peroxidation is a prominent manifestation of oxidative cell injury, iron-dependent nonperoxidative mechanisms of oxidative cell injury have been described (19). Mitochondrial damage is the biochemical basis of the nonperoxidative mechanism of oxidative cell injury, in which irreversible cell injury develops in the absence of detectable lipid peroxidation (19). Iron-dependent nonperoxidative mechanisms of oxidative injury are thought to occur as a consequence of loss of mitochondrial energization such as ischaemia, while peroxidative mechanisms function in reperfusion injury (19). Other effects of free radical reactions include dyserythropoiesis, intravascular haemolysis and intravascular fibrin precipitation (14). Rapid and progressive decline in thrombocyte levels has been associated with endotoxin administration (17).

The possibility that canine cerebral babesiosis could be used as an experimental model for human cerebral malaria, has been the primary driving force behind research in the former disease (54,68). Before this possibility can be realized, much work will be required to gain an understanding of the mechanisms of canine cerebral babesiosis. It is only when critical aspects of the pathogenesis are fully understood, that it will be possible to develop an experimentally repeatable canine model of cerebral babesiosis for cerebral malaria. Determining which aspects are critical will form the framework for future research in babesiosis, and at the present level of understanding it is not possible to predict which, if any, of the factors influencing the pathogenesis of cerebral babesiosis, are critical to the development of cerebral disease.

A good fundamental understanding of pathogenic mechanisms in babesiosis will lead to improved therapeutic and prophylactic approaches to the disease. Research in the canine host may also have some useful applications in the bovine host.

Research objectives

The aims of this study were:

1). To describe the cerebral lesions of canine babesiosis at the macroscopic and light-microscopic level.

2). To determine what ultrastructural pathology is present in canine cerebral babesiosis, and whether changes are comparable or not to those seen in either bovine cerebral babesiosis or cerebral malaria in man.

3). To improve current understanding of the pathogenesis of cerebral babesiosis

MATERIALS AND METHODS

For the purposes of this study, any case positively confirmed as suffering from babesiosis with concurrent central nervous signs, cerebral lesions at necropsy, or both, was classified as cerebral babesiosis. Cases were excluded if other possible causes for neurological signs or cerebral lesions were present. Babesiosis cases lacking central nervous involvement were classified as controls.

GROSS AND HISTOPATHOLOGY

Case selection

Sequential clinical cases of babesiosis that died and were registered for necropsy at the Department of Pathology, Faculty of Veterinary Science, were initially included in the study. Case submissions from 1996, 1997 and 1998 were sampled. The original sample was then divided into two groups. The first group included all cases that could be classified as babesiosis with central nervous involvement (cerebral babesiosis): babesiosis cases with a history of neurological signs and/or lesions of the CNS. Cases of babesiosis that could not be classified as cerebral were assigned to the control group (non-cerebral babesiosis).

Various complicating factors made it necessary to exclude certain cases from the study following initial selection. Cases were excluded if they were suffering from intercurrent disease, if parasitaemia could not be verified, if CNS lesions could be attributed to a cause other than infection with *Babesia canis* or if neurological signs could be attributed to a cause other than infection with *B. canis*.

Study design

A cross-sectional study was done, using sequential cases admitted for necropsy. A single blind study was conducted. The main identification number for each case was a PM number issued at necropsy. In order to refer back to the necropsy findings after histological examination, an S number was attached to the PM number by the laboratory, at registration. The history form submitted with the case at necropsy examination, had an F number for reference back to the clinical history.

In this manner, all relevant information could be kept apart until the histological examination of all cases had been completed, and reliably brought together again for the final analysis of all cases at the end of the study. Many of the exclusion criteria were based on histological findings, and the majority of cases were only excluded at the end of the study.

Experimental procedure

A full necropsy was performed on each case. A routine peripheral blood smear was made from the ear, to establish whether parasites were present. The whole brain was removed from the cranium and a cerebral smear was made from the central region of the marginal gyrus. The two halves of the cerebrum were gently separated at the saggital sinus, and an incision was made through the corpus callosum into the median area of the lateral ventricles. The whole brain was then immersed in 10% buffered formalin. The incision allowed formalin to penetrate the lateral ventricles and accelerated the rate of fixation, without unduly distorting the cerebral morphology. Duration of fixation was approximately 7 days, depending on the size of the brain. Some brains had to be sectioned after 48 hours, for diagnostic purposes, and the remaining sections were then returned to the formalin for an additional period of fixation.

The fixed brain was removed from the formalin, and sites of lesions were recorded on a diagram sheet (Appendix A). Lesions were photographed, if present, and the brain was then sectioned and examined for internal lesions. Internal lesions were also recorded on a diagram sheet (Appendix A) and then photographed. Additional comments pertaining to unusual features of the lesions, were made on the diagram sheets.

Sectioning

Brain samples

A transverse section was made at the parieto-occipital junction, immediately rostral to the cerebellum. The cerebellum was sectioned longitudinally with an initial medial cut, and then lateral cuts were made at 2-4 mm intervals to left and right of the midline. The two parts of the occipital lobe were sectioned transversely, as were the remainder of the cerebrum and mid-brain. The sections were laid out in columns from left to right, the most rostral part of the frontal lobe situated in the top left corner, and the most caudal part of the occipital lobe in the bottom right corner. The cerebellum was positioned below the other sections, as a bottom row. In all cases, true left was on the left, and true right was on the right. The sections were therefore viewed "from behind".

The following sections were made from all brains sampled for histopathology:

1. median cerebellum and brain stem
2. mid-occipital lobe left
3. mid-occipital lobe right
4. rostral colliculus and caudal hippocampus left
5. rostral colliculus and caudal hippocampus right
6. parieto-temporal cortex, thalamus and rostral hippocampus left
7. parieto-temporal cortex, thalamus and rostral hippocampus right
8. fronto-parietal cortex, thalamus and caudate nucleus left
9. fronto-parietal cortex, thalamus and caudate nucleus right
10. mid-frontal cortex left
11. mid-frontal cortex right
12. olfactory bulbs
13. lesions at sites in addition to those routinely sampled

Spinal cord samples

The spinal cord was removed from the carcass, suspended in a 2-litre measuring-cylinder and fixed in 10% buffered formalin. After fixation, the spinal cords were sectioned transversely at 2-4 mm intervals. In the cranial intumescence, mid-thoracic and mid-lumbar areas, 2-4 mm wide longitudinal sections (length:10mm) were cut.

Routine samples from the spinal cord were blocked as follows:

A. mid-cervical and cranial intumescence.
B. mid-thoracic
C. mid-lumbar
D. caudal intumescence and cauda equina.

Lesions, when present, were blocked according to the appropriate region of the spinal cord.

Laboratory processing of samples

All samples were routinely embedded in paraffin wax and sectioned at 6μm thickness using an HM 400R Microm sliding microtome. The sections were mounted on glass slides and stained with haematoxylin and eosin (Appendix B). Additional selected sections were stained with Giemsa (Appendix B).

Samples for serial sectioning were selected from cases with severe lesions. Six lesions were selected (5 cases). The wax blocks were serially sectioned, every 15th section being mounted on a glass slide.

Clinical history

A full clinical history was obtained either from the clinicians involved with the cases and/or from hospital records. Cases that were submitted for necropsy directly by the owner (mostly cases that were found dead or had died without a clinical examination) were classified in a third group: clinical signs unknown. These last formed a very important subgroup of untreated cases. This subgroup also contained those few cases that had died during the clinical examination before treatment was given, for which clinical neurological signs were documented.

Data analysis

Gross lesions were categorised in terms of lesion type (diffuse or multifocal). A detailed examination of haemorrhagic and malacic lesions was made in order to detect distribution patterns (Appendix C). Distribution of lesions was classified in terms of the lobes of the brain affected, the sulci and gyri involved, and the arterial supply field involved. (See Appendix D for the regions of the brain supplied by the cerebral arteries.)

The histopathology of the brain was described and compared in both cerebral and control cases. The control group comprised all cases that could not be classified as cerebral babesiosis on the basis of either lesions or clinical neurological signs.

ULTRASTRUCTURE

Sampling procedure

The ultrastructure of seven babesiosis cases was examined.

Fresh cases (2)

These cases were selected because they had a history of severe acute babesiosis, and could be sampled rapidly after death. The brain was removed from the cranium within 20 minutes of death and examined for gross lesions. Samples were taken in and around sites of macroscopically visible haemorrhage present in one case. Similar samples were taken from the thalamus, cortex and cerebellum in the second case, which had no cerebral lesions

(control). The tissue was cut into 1mm cubes and fixed in 2,5% glutaraldehyde in 4% of 0.1M Millonig's buffer, within 30 minutes of death.

Archival cases (5)

After histological examination, cases were selected for electron microscopic examination. Four cases with a range of histopathological changes and one case with overt margination were selected. The tissue was retrieved from the paraffin-wax blocks and reprocessed for electron microscopy. Case 5 was retrieved directly from formalin-fixed material prior to processing for histopathology.

Processing of samples

Retrieval of formalin fixed tissue

Selected samples were cut down to 1mm cubes and placed in 4% Millonigs phosphate buffer for 15 minutes. The samples were then placed in fresh Millonigs phosphate buffer for a further 15 minutes. Samples were then transferred into glutaraldehyde.

Retrieval of paraffin wax embedded tissue

The wax block was melted at low temperature and the tissue retrieved. Selected sites were cut into 1mm cubes and placed into a small casette. The casettes were stored in Xylene (Xylol) overnight. The tissue samples were then processed in decreasing concentrations of acetone, from 100%, 96%, 70%, 50% down to 25%, stirring slowly. Exposure to each concentration was for 15 minutes. The samples were then placed in a 4% solution of Millonigs phosphate buffer at pH7,3 for 5 minutes, after which they were placed in glutaraldehyde.

Processing of tissue samples fixed in 2,5% glutaraldehyde in buffer

The tissue blocks were washed twice, for 10 minutes, in Millonig's phosphate buffer (pH7,3) and post-fixed in osmium tetroxide for 1 – 2 hours. They were then rinsed in buffer and distilled water, after which they were passed through a series of increasing concentrations of acetone for dehydration (25%, 50%, 70%, 80%, 90%, 95%, 100% - for 15 minutes each). The last step was repeated. Impregnation in resin was done in three stages, increasing the resin to acetone ratio from 1:3 (1h), 1:1 (1h), 3:1 (overnight) to 100% (1h). The samples were then embedded, and polymerised at 45°C for 5 hours, and then at 60°C overnight. All samples were examined under the Phillips CM10 transmission electron microscope at the Department of Anatomy (Veterinary Faculty).

RESULTS

Of 145 cases sampled at *post mortem*, 43 cases (29,7%) were excluded (Appendix E). Of the remaining 102 cases, 56 (55%) had involvement of the central nervous system. Grossly visible regional lesions were present in 31 of the 56 cases with cerebral involvement (55%), while 16 (28,5%) had global lesions. There were 4 cases that had congestive brain swelling (increased intravascular fluid volume of the brain, leading to raised intracranial pressure), 8 that had cerebral pallor and 4 had moderate to severe congestion but not congestive brain swelling (Table 1). There were 18 cases (32%) with grossly appreciable oedema. Thirty seven (37) cases had a history of neurological clinical signs of which 9 (24%) had no significant gross cerebral lesions suggestive of cerebral babesiosis. Ninety-one (91) cases were examined histologically, of which 37 (40%) were excluded (Appendix C). Of the remaining 54 cases, 32 (59%) had significant histological changes suggestive of cerebral babesiosis and 22 cases (41%) were classified as controls (non-cerebral babesiosis).

The age range for the study sample was 3 weeks to 17 years, with 52,5% of cases under the age of 2 years. The ratio of male to female cases was 1,2:1 for the whole sample, which consisted of 26 different breeds. The breeds with the highest frequency in the sample population were Staffordshire bull terriers (12), Maltese terriers (7), German shepherd dogs (6), Rottweilers (6) and boerboels (6).

Changes in the brain could be divided into two broad categories at the histological level: those present in both control and cerebral cases and those restricted to cerebral cases. Changes common to control and cerebral cases were considered a reflection of systemic inflammation in fatal babesiosis. Lesions considered distinctive for cerebral babesiosis included congestive brain swelling and multifocal haemorrhage and malacia of the grey matter. Cases with microscopic vascular-associated lesions only, were classified as pre-cerebral in the cerebral group. Cases with cerebral lesions did not necessarily have a history of clinical neurological signs. Cases with clinical neurological signs that could not be attributed to other causes, and which showed cerebral changes present in controls, were classified as cerebral babesiosis on the basis of their history.

Table 1. Lesions observed in the canine brain in cerebral babesiosis (n=56).

LESION	FREQUENCY (%)
GLOBAL LESIONS	**16 (28,5)**
Diffuse pallor	8
Mild to moderate congestion	4
Congestive brain swelling	4
REGIONAL LESIONS	**34 (61)**
Haemorrhage and malacia	31
Congestive brain swelling with haemorrhage and malacia	2
Malacia only	1
OEDEMA	**18 (32)**
Mild to moderate oedema	13
Severe oedema	5
NO GROSS LESIONS	**9 (16)**
Histological lesions only	6
No morphological changes	3

LESIONS

The gross cerebral lesions observed in dogs suffering from babesiosis were classified as either global or regional (Table 1). Global lesions affected the brain tissue diffusely. Two types of global lesion were observed: congestive and anaemic. (Figures 1a & 1b). Congestive lesions were divided into two categories: mild to severe diffuse cerebral congestion (which could not, on its own be used as a criterion for classifying a case as cerebral babesiosis) and congestive brain swelling (which was classified as a lesion indicative of cerebral babesiosis). Anaemic lesions were classified as diffuse cerebral pallor

FIGURE 1: GLOBAL CHANGES IN CEREBRAL BABESIOSIS.

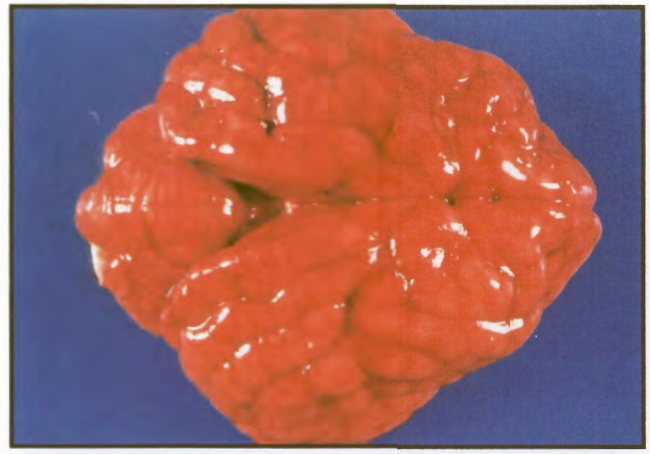

Figure 1a. (Top)
Congestive brain swelling. Severe, diffuse congestion of the brain is present. The tissues have a moist, glistening appearance, due to severe oedema.

Figure 1b. (Middle)
Diffuse pallor of the brain. The arrowhead indicates the site from which the brain smear was sampled. The arrow indicates the site where a transverse incision was made through the brain.

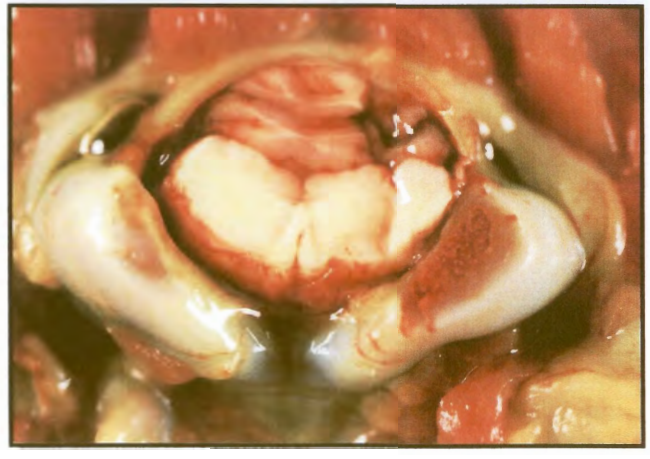

Figure 1c. (Bottom)
Cerebellar prolapse through the foramen magnum due to severe diffuse cerebral oedema. The caudal part of the cerebellar vermis has undergone forceful distortion through the foramen magnum, resulting in compression of the medulla oblongata.

to avoid suggesting a pathogenesis for the changes observed. The presence of diffuse cerebral pallor alone could also not be used as a criterion for classifying a case as cerebral babesiosis. Regional lesions were characterised by multifocal haemorrhage and malacia, and cases with regional lesions were always classified as cerebral babesiosis. Cerebral oedema was associated with lesions in 32% of cases, and could be distributed either globally (Figure 1c) or regionally.

GLOBAL LESIONS

CONGESTIVE BRAIN SWELLING

Congestive brain swelling is a process by which intracranial pressure is raised as a consequence of a critical increase in the intravascular fluid volume within the cranium. It is thought to be a consequence of failure of autoregulation leading to non-responsive vasodilation (58). It was observed in 4 cases (Table 1). There was severe diffuse congestion of the entire brain with associated oedema (Figure 1a). The severe congestion of the microvasculature imparted a homogeneous bright pink colour to the cerebral and cerebellar cortex macroscopically ("pink brain" or "cerebral flush"). The larger vessels draining the cortex were engorged with blood. The congestion of the medium caliber vessels imparted an injected appearance to the cortical surface. The cerebellar cortex was similarly congested. Regional lesions were present in 2 of the 4 cases.

Histologically, these cases showed severe diffuse congestion of the cortical microvasculature. The degree of oedema was variable, with severe lesions in the white matter tracts and multifocal rarefaction of the cortical neuropil in one case. A second case had less severe oedema histologically. The density of parasitised erythrocytes was variable, being high in some cases and low in others. Sludging of erythrocytes irrespective of parasitaemia was a common finding in the majority of microvessels in these cases. In one case, widespread sites of petechial haemorrhage were particularly common in the molecular layer (with extension into the underlying layers), in the crests of gyri and floors of sulci. This case also showed severe diffuse sludging of erythrocytes within the microvasculature. Thrombosis was not demonstrated, hypoxic neuronal changes were rare, and neutrophils were not observed. Parasites were absent. A striking feature of a case with associated regional lesions was severe congestion of the arterial tree in addition to the more distal vasculature.

DIFFUSE CEREBRAL PALLOR

The brain parenchyma was diffusely pale in affected cases (Figure 1b) although some degree of vascular filling of larger vessels (arteries and veins) was usually present. In 7 of the 8 cases with cerebral pallor (Table 1), clinical neurological signs were recorded. Table 2 gives the clinical signs, packed cell volume and antibabesial treatment, where known, of these cases.

Table 2. Cases with a history of clinical neurological signs in which the only apparent lesion was severe pallor of the brain. Haemorrhage and malacia were not found in these cases. Packed cell volume (PCV) is given where available (n = 7).

S. NUMBER	PCV	CLINICAL NEUROLOGICAL SIGNS	ANTIBABESIAL TREATMENT
1148.96	6	Positive neurological signs (unspecified)	untreated
205.97	Not measured	Seizures	untreated
231.97	24	Semi-coma	Trypan blue
268.97	8	Opisthotonus, extensor rigidity	untreated
70.98	25	Coma	Diminazene aceturate
105.98	21	Opisthotonus, trembling, collapse.	Diminazene aceturate
475.98	11	Focal seizures, blindness	Diminazene aceturate

Diffuse pallor in association with neurological signs was classified as cerebral babesiosis if no other cause for the neurological signs could be identified other than infection with *B. canis*. Internal regional lesions were not found, the brain being diffusely pale in all of these cases. Macroscopically visible oedema was not necessarily present. Anaemia (Table 2) was demonstrable in only 3 cases.

Histological features were found to be similar to fatal non-cerebral babesiosis in 7 of the 8 cases. The microscopic features of fatal non-cerebral babesiosis included distinctive erythrocytic changes, non-specific inflammatory reactions and diffuse endothelial changes. The eighth case had pre-cerebral lesions as described in the section on regional lesions.

HISTOLOGICAL FEATURES COMMON TO CONTROL AND CEREBRAL CASES

Several morphological features of the brain in fatal babesiosis were observed in both control cases and cases with central nervous involvement. These histopathological changes of the brain could not be attributed to cerebral babesiosis as they were commonly observed in control cases. Table 3 gives the histopathological features of cerebral changes in fatal babesiosis. Features distinctive for cerebral babesiosis lesions will be discussed under the section on regional lesions.

Changes in erythrocyte morphology and behaviour, parasitaemia, mild to moderate congestion, uneven vascular filling, monocytic leukostasis, endothelial nuclear swelling, intravascular fibrin polymerisation and microhaemorrhages were common findings in both cerebral and control cases. Red cell changes (RCC) included anisocytosis, haemoglobin leaching with erythrocyte ghost formation, erythrocyte squaring in small caliber vessels, sludging and parasite invasion. Anisocytosis appeared to be due to both enlargement of some erythrocytes and fragmentation of others. Parasitised erythrocytes tended to be increased in size and showed an associated loss in haemoglobin staining (haemoglobin leaching). Some erythrocytes were so pale due to haemoglobin loss, the cytoplasm was barely discernable within the cell membrane. Such erythrocytes are termed ghost cells. Erythrocytes sometimes assumed a square shape within microvessels as if the red cell's plasmalemma were fused to the endothelium on opposite sides (erythrocyte squaring – should not be confused with compression of erythrocytes in capillaries). Apparent fusion of the erythrocyte membranes to one-another within vessels gave the appearance of sludging within the vasculature. Erythrocyte sludge was most commonly observed between unparasitised cells, but parasitised erythrocytes could also be trapped within sludge, as were monocytes. Monocytic leukostasis was often associated with sludging of erythrocytes in small veins draining the cortex.

Table 3: Frequency of histopathological changes in the brain in fatal canine babesiosis. Frequencies are given as a percentage of control cases in column 2, as a percentage of cases with cerebral involvement in column 3 and as a combined percentage of the total number of cases examined in column 4. (N = 54)

	CONTROL CASES (%)	CASES WITH CEREBRAL INVOLVEMENT (%)	TOTAL (%)
TOTAL CASES	22	32	54
RED CELL CHANGES	20 (91)	22 (69)	42 (78)
MARGINATION ONLY	4 (18)	9 (28)	13 (24)
MARGINATION AND ADHESION	10 (45)	5 (15.5)	15 (28)
PARASITES	17 (77)	28 (87.5)	45 (83)
MULTIPLE PARASITES PER CELL	4 (18)	1 (3)	5 (9)
MONOCYTIC LEUKOSTASIS (AGGREGATES)	17 (77)	24 (75)	41 (76)
MONOCYTOSIS WITHOUT MONOCYTIC LEUKOSTASIS	2 (9)	0	2 (4)
FOAMY PERICYTES	7 (32)	9 (28)	16 (29.5)
NEUTROPHILS	7 (32)	27 (84)	34 (63)
LYMPHOCYTES	7 (32)	4 (12.5)	11 (20)
PLASMA CELLS	2 (9)	0	2 (3.7)
PERIVASCULAR CUFFING	2 (9)	7 (22)	9 (16.5)
ROD CELL PROLIFERATION	1 (4.5)	2 (6)	3 (5.5)
COMPOUND GRANULAR CORPUSCLES	1 (4.5)	1 (3)	2 (4)
GEMISTOCYTES	0	2 (6)	2 (4)
TYPE 2 ALZHEIMER CELLS	0	10 (31)	10 (18.5)
ISCHAEMIC CELL CHANGE	1 (4.5)	22 (69)	23 (42.5)
NEURONAL NECROSIS OR HOMOGENISING CHANGE	1 (4.5)	12 (37.5)	13 (24)
CONGESTION	7 (32)	15 (47)	22 (40.5)
ENDOTHELIAL NUCLEAR SWELLING	15 (68)	21 (65.5')	36 (66.5)

	CONTROL CASES (%)	CASES WITH CEREBRAL INVOLVEMENT (%)	TOTAL (%)
SEGMENTAL MICRO-VASCULAR NECROSIS	1 (4.5)	22 (69)	23 (42.5)
VASCULITIS	0	11 (34)	11 (20)
UNEVEN VASCULAR FILLING	10 (45)	9 (28)	19 (35)
OEDEMA OF CORTEX AND/OR SUB-CORTICAL GREY MATTER	3 (13.5)	24 (75)	27 (50)
OEDEMA OF SUBCORTEX	5 (23)	15 (47)	20 (37)
SPINAL CORD INVOLVEMENT	3 (13.5)	6 (19)	9 (16.5)
WHITE MATTER INVOLVEMENT	7 (32)	17 (53)	24 (44)
VASOGENIC OEDEMA	7 (32)	15 (47)	22 (40.5)
WHITE MATTER RING HAEMORRHAGES	0	2 (6)	2 (3.5)
HAEMORRHAGE	13 (59)	32 (100)	45 (83)
MICRO-HAEMORRHAGE	11 (50)	14 (43)	25 (46)
PETECHIAL HAEMORRAHGE	2 (9)	22 (69)	24 (44)
PERIVASCULAR OR RING HAEMORRHAGES	3 (13.5)	10 (31)	13 (24)
ECCHYMOTIC OR LARGER HAEMORRHAGE	0	23 (72)	23 (42.5)
EXTRA-VASCULAR FIBRIN POLYMERISATION	0	9 (28)	9 (16.5)
EARLY LESIONS ONLY	0	5 (15.5)	5 (9)
INTERMEDIATE LESIONS BUT NO ADVANCED LESIONS	0	4 (12.5)	4 (7)
ADVANCED LESIONS	0	19 (59)	19 (35)
NO REGIONAL LESIONS BUT NERVOUS SIGNS CLINICALLY	0	4 (12.5)	4 (7)
CONGESTIVE BRAIN SWELLING	0	1 (3)	1 (2)
INTRA-VASCULAR FIBRIN POLYMERISATION	10 (45)	9 (28)	19 (35)
AUTOLYSIS	12 (54.5)	12 (37.5)	24 (44)
MILD AUTOLYSIS	5 (23)	3 (9)	8 (15)
MODERATE AUTOLYSIS	6 (27)	7 (22)	13 (24)
SEVERE AUTOLYSIS	1 (4.5)	2 (6)	3 (5.5)

Parasites were present in the cerebral vasculature in 17 control and 28 cerebral cases. A total of 83 % of cases were still positive for parasites at necropsy. Parasites were always present in untreated cases and were rarely observed in treated cases. The degree of parasitaemia in cerebral microvasculature varied between cases, between sections from the same case, and from site to site within individual sections. A striking observation was the presence of overwhelming numbers of capillaries densely packed with parasitised erythrocytes in odd cases that did not develop any lesions considered suggestive of cerebral babesiosis, and did not have any history of clinical neurological signs.

Capillaries containing a very high percentage of parasitised erythrocytes (pRBC) were randomly scattered throughout the cortex in cases with high parasitaemia. Parasitised erythrocytes were not consistently associated with lesions, even in untreated cases. The density of pRBC within vessels was variable to the extent that, it was sometimes possible to examine the majority of sections from a single brain without being able to demonstrate any parasites. From such a case, only a single section or a few sections would yield variable numbers of parasites in a restricted area. Parasite distribution could be restricted to certain areas, such as focally in the sulcal floors of the cortex or in particular lobes. For example: the parasite density could be far higher in the frontal lobes than in other parts of the cortex or the cerebellum. Multiple parasites per cell were occasionally observed in cases with high parasitaemias (9% of all cases). Eighteen percent of all control cases and 3% of cerebral cases had multiple parasites per cell. Up to 16 organisms per cell, were visible in individual erythrocytes.

High densities of pRBC could not be considered the cause of cerebral babesiosis as they were present to varying degrees in the majority of fatal cases of babesiosis. They reflect the inflammation consequent upon systemic haemoparasitic infection. The majority of changes were observed in erythrocytes, or were associated with the vasculature. An inflammatory response directed at the parasite or present within the cerebral tissue, was not observed in the absence of endothelial injury.

Erythrocytes showed certain consistent morphological changes (RCC, Table 3) which were independent of the presence of parasites within them. The most common changes observed were loss of the biconcave shape of the cell, increased cell size and loss of eosinophilia (haemoglobin loss). Some erythrocytes appeared to be square rather than spherical or biconcave, assuming this shape only in microvessels. Some erythrocytes were observed to

have a normal size and shape, contained a pair of well-defined pear-shaped parasites, and had a normal, dark-staining (red) haemoglobin content. In cases that received blood transfusion therapy, the majority of erythrocytes showed normal morphology.

Two broad categories of abnormal erythrocyte behaviour were observed: sludging and margination/adhesion. Intravascular precipitation of erythocytes with apparent agglutination was referred to as sludging. Approximation of pRBCs to the vascular wall was termed margination. Flattening of marginated pRBCs along the vessel wall, with extended membrane approximation, was termed adhesion.

A common occurrence in babesiosis is the apparent precipitation of erythrocytes within smaller blood vessels (post capillary venules and the venules draining the cerebral cortex). Sludge was composed of a mosaic-like mass of parasitised and unparasitised erythrocytes, the appearance being enhanced by variable stainability of the erythrocyte plasma, the presence of erythrocyte ghosts and trapped inflammatory cells. In 76% of cases, monocytic leukostasis within the vasculature was observed as a consequence of trapping of these cells in sludge. Occasionally, other leukocytes such as neutrophils were also present (32% of controls). Fibrin strands were observed forming a network between erythrocytes in 35% of cases. The frequency of intravascular fibrin polymerisation was higher in control (45%) than in cerebral cases (28%) (Table 3). Thrombocytes were not observed.

Margination was observed in arteries, arterioles and venules. It may have occurred in capillaries but this could not be appreciated in vessels with a diameter only fractionally greater than that of erythrocytes. It was frequently observed in small caliber venules. Margination was present in the absence of apparent adhesion in 24% of all cases. It was observed in the majority of sections of a given case, but showed a patchy distribution. Margination and adhesion were observed in 45% of control cases, and 15.5% of cerebral cases (Table 3).

Adherence of pRBC was characterised by flattening of the erythrocyte membrane along the endothelium (28%). This caused marked distortion of the erythrocyte shape. Adherent cells in small vessels attached to the endothelium on one side only were limpet- or lozenge-shaped. Adherent pRBC in microvessels were frequently square or rectangular in sections as a result of attachment to opposite sides of the vessel lumen. Unparasitised erythrocytes were also observed to attach to vessel walls.

Congestion of small vessels, particularly the capillaries, post-capillary venules and smaller veins draining the cortex was seen in 32% of control cases and 47% of cerebral cases. Uneven vascular filling in which some micro-vessels were filled with erythrocytes, while adjacent vessels were empty, was present in 45% of control cases and 28% of cerebral cases (Table 3).

The nuclei of endothelial cells in the microvasculature were swollen and dark in 68% of control cases and 65% of cerebral cases. They projected into the vascular lumen and, in capillaries, these enormously enlarged and active nuclei sometimes appeared to obstruct the lumen. Endothelial proliferation was rarely observed.

Monocytic leukostasis was characterised by intravascular aggregates of apparently adherent monocytes. Aggregates frequently contained monocytes interspersed with erythrocytes, the cell masses appearing to fill the vascular lumen and adhere to the vessel wall. Monocytic leukostasis was common to both cerebral and control cases (76%, Table 3). Monocytosis without monocytic leukostasis was characterised by increased numbers of free monocytes within the vasculature. This was observed in 2 control cases. In 13% of cases, severe neutrophilia was present instead of monocytosis. Lymphocytes (seen in 20% of cases) and plasma cells (seen in 4% of cases) were observed far less frequently than monocytes. Lymphocytosis was seen in 32% of control cases and in 12% of cerebral cases.

In many cases, pericytes associated with the post capillary venules and slightly larger venules, developed a foamy appearance (29.5% of cases). The greatly expanded cytoplasm of these cells was tinged pale yellow-brown. The nuclei appeared small and dense, suggestive of pyknosis. This pericytic reaction was also observed in association with splenic microvasculature. It was readily demonstrated in brain smears and was present in both cerebral (28%) and control (32%) cases. Rare cellular reactions in babesiosis include microglial rod cell reactivity (5%) and development of compound granular corpuscles (4%) (Table 3).

Micro-haemorrhages were observed in 50% of control cases and 43% of cerebral cases (Table 3). They were not associated with rarefaction of the neuropil surrounding affected vessels, vessel injury, or the presence of inflammatory cells.

Intravenous fibrin polymerisation was seen in 45% of control cases and 28% of cerebral cases (Table 3). Intravenous fibrin polymerisation was associated with early *post mortem* changes. Homogenising change in neurons with haloes was an indication of advanced *post mortem* change.

OEDEMA

Oedema of the brain was found in conjunction with both global (Figures 1a & 1c) and regional (Figure 4a) lesions and was grossly appreciable in 18 cases (Table 1). Fluid accumulation was diffuse within the tissue, imparting a flattened appearance to the contours of the sulci and gyri (Figure 4a). The texture of the tissue was softened. Mild dilatation of the ventricles was observed in 5 cases (Appendix C). Oedema was present in most cases (6/8) showing diffuse pallor (Appendix C). Severe diffuse oedema did occasionally occur, particularly in association with the haemoconcentration form of the disease in which generalised oedema was sometimes observed and in cases with congestive brain swelling. Distortion of the cerebellar profile was observed in 3 cases (Figure 3b). Prolapse of the caudal lobe of the cerebellar vermis through the foramen magnum was observed in one case (Figure 1c).

A fairly common histological observation was the presence of oedema in the white matter (40,5%). This lesion appeared to be consistent with vasogenic oedema. Although diffuse oedema was rarely observed macroscopically, it was a common microscopic observation. It was seen in 47% of cerebral cases and 32 % of controls (Table 3). Localised oedema of the grey matter was consistently associated with regional lesions and is discussed in the appropriate section.

FIGURE 2: REGIONAL LESIONS ON THE CEREBRAL SURFACE.

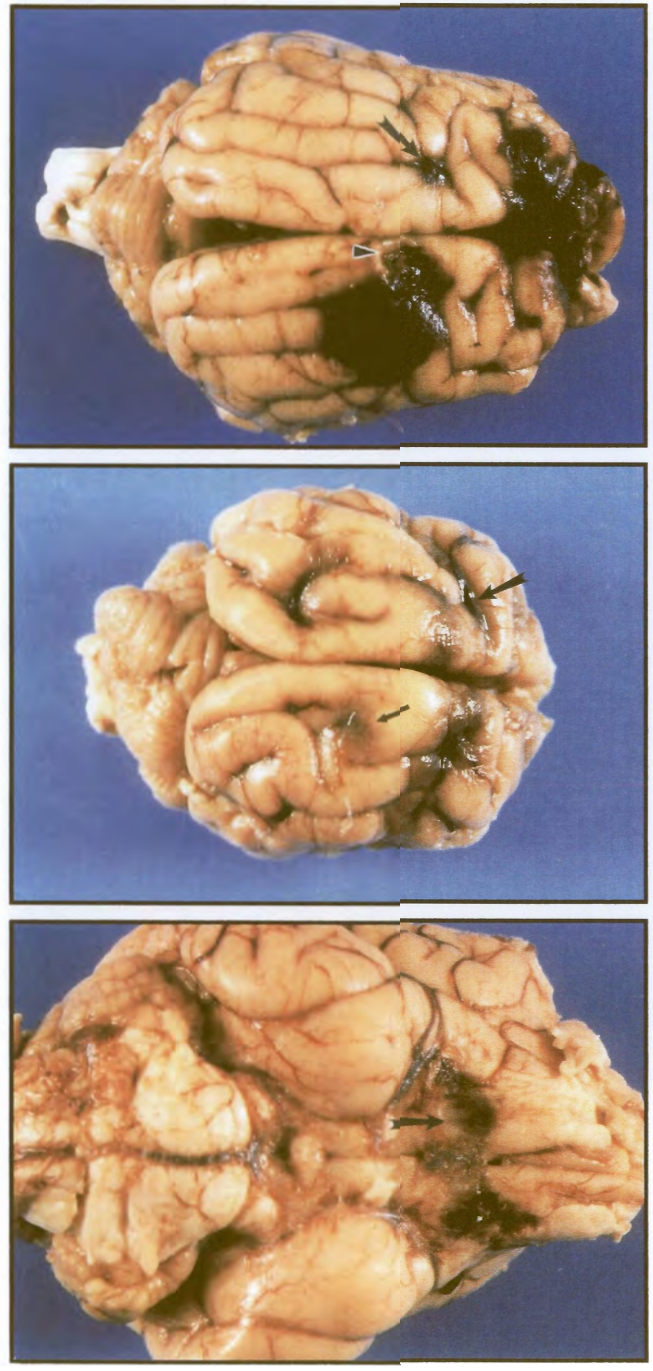

Figure 2a. (Top)
Severe multifocal cerebral cortical haemorrhage and malacia. The lesions are bilateral but not strictly symmetrical in this case. Lesions are predominantly situated in the rostral half of the cerebrum. Severe malacia is present within the haemorrhagic sites (arrowhead). The small lesions are closely associated with sulci (arrow).

Figure 2b. (Middle)
Bilateral, multifocal cerebral cortical haemorrhage and malacia. The haemorrhagic site is dull. Both the dullness and the sunken nature of the lesions (small arrow) suggest the presence of malacia. The sulcal veins are very dilated due to engorgement with blood (large arrow) indicating severe congestion.

Figure 2c. (Bottom)
Bilaterally symmetrical haemorrhage and malacia of the olfactory tubercle. The sunken area of grey discoloration is indicative of necrosis (arrow). The large superficial veins are severely congested.

FIGURE 3: GROSS FEATURES OF REGIONAL LESIONS ON THE CUT SURFACE

Figure 3a. (Top)
Severe multifocal haemorrhage and malacia of the brain. Lesions involving the cortex are distributed through the entire length of the brain, primarily involving the dorsal regions of both hemispheres and predominating in the rostral quadrants. The right frontal lobe shows severe focal malacia (white-edged arrowhead). The white matter of the cortex acts as a barrier to the haemorrhage, and is generally spared. The floors and sides of the cingulate sulci have characteristic deep lesions (white-edged arrow). The caudate nucleus shows bilateral haemorrhage, with a more severe lesion on the left (black arrow). The frontal lobe of the cerebellum shows focal cortical ecchymosis of the ventral lingula (white arrowhead). The caudal colliculi have bilateral focal ecchymoses (white arrows).

Figure 3b. (Middle)
Severe locally extensive haemorrhage and malacia of the dorsal cortex with multifocal ecchymoses and petechiae. There is extensive liquefactive necrosis of the cortex of the right frontal lobe with malacia and ecchymosis of the right thalamus (black arrow). There are multiple sites of deep sulcal haemorrhage and malacia. Numerous petechiae are present in the medulla oblongata and other sites, including single points of haemorrhage in the white matter tracts. Multiple ecchymoses are present in the caudal colliculus and caudate nucleus, and there is compression of the cerebellum with associated haemorrhage. The cerebellar cortex is preferentially affected with sparing of the subcortex. There is compression of the nodulus and uvula of the vermis (white-edged arrowhead).

Figure 3c. (Bottom)
Severe, multifocal to coalescing haemorrhage and malacia of the cerebral cortex and sub-cortical grey matter. The lesions are confined to the cortex and subcortical grey matter of the caudal colliculus (arrows). The right frontal lobe shows locally extensive malacia with separation of the necrotic tissue (white-edged arrowhead). The floors of the sulci are particularly affected in this case (white arrowheads) with few lesions extending to the external surface. Although the cortical lesions are bilateral, they are not symmetrical, in contrast to the collicular lesion. The majority of lesions occur in the rostro-dorsal quadrant of both hemispheres.

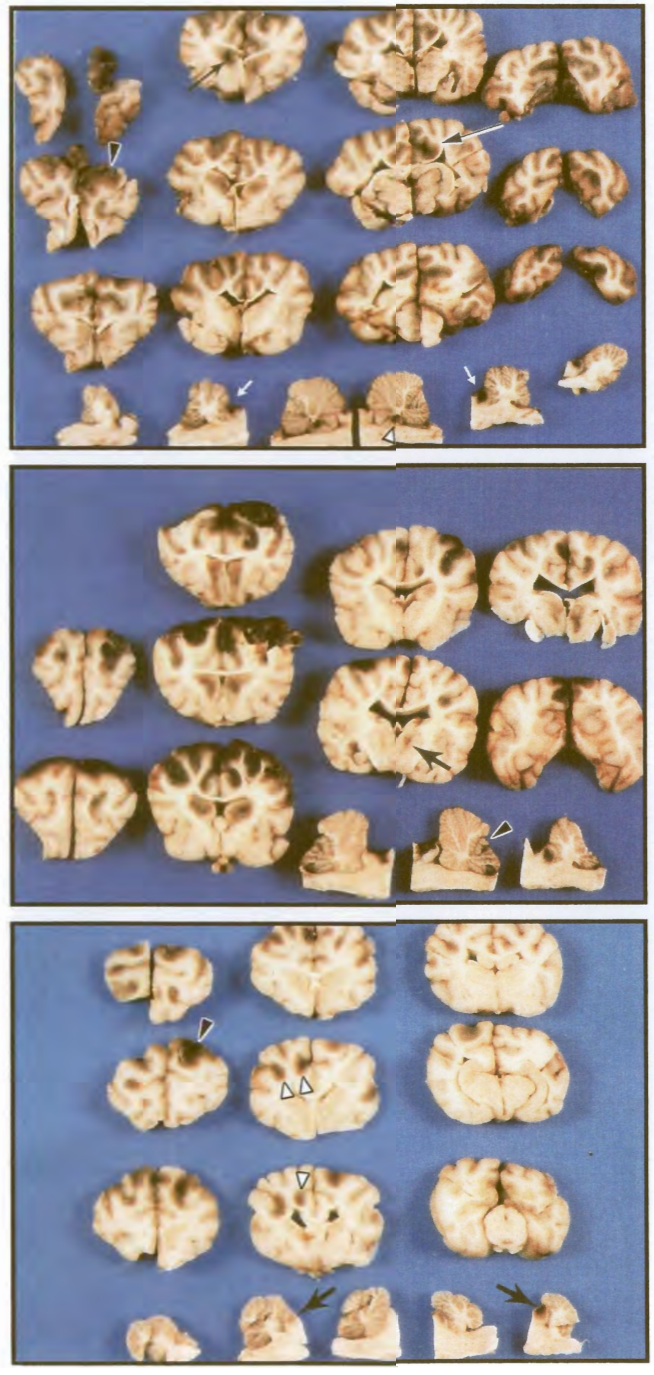

FIGURE 4: DETAIL OF GROSS FEATURES OF REGIONAL LESIONS IN CEREBRAL BABESIOSIS.

Figure 4a. (Top)
Severe haemorrhage and malacia of the cerebral cortex. The majority of lesions occur on the floors of sulci and extend along the sides to the surface (white edged arrow) The white matter forms a barrier to the expansion of the lesion (broad black arrow). Oedema with resultant flattening of the gyri is well demonstrated on the left (arrowheads). The lesion is bilaterally symmetrical, with involvement of both *corpora* of the caudate nuclei and petechiae in the lenticular nuclei (slender black arrow). There is haemorrhage and multifocal necrosis of the adenohypophysis.

Figure 4b. (Middle)
Severe haemorrhage and malacia of the cerebellar vermis. The rostral lesion has a deep sulcal distribution (black arrow), in contrast to the more superficial distribution of the caudal lesion (white-edged arrow). The roughly square shape of the cerebellum suggests that the structure may have undergone compression as a result of oedema.

Figure 4c. (Bottom)
Global haemorrhage of the hypophysis. The hypophysis is uniformly dark red to black (arrowhead). The lesion is similar in appearance to infarction, although no actual thrombosis could be demonstrated. There is severe congestion of the surrounding veins.

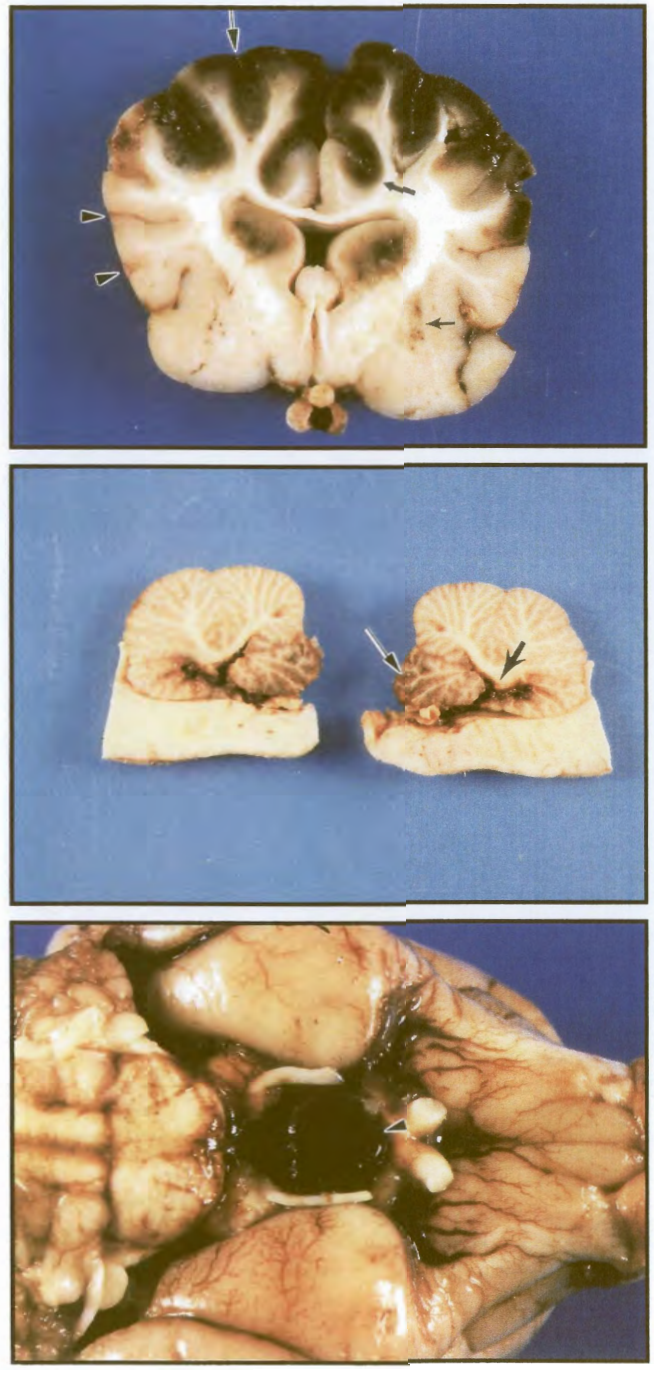

GROSS FEATURES OF REGIONAL LESIONS

Multifocal cerebral haemorrhage and malacia (Figures 2, 3 & 4) were the most common types of lesion present in cerebral babesiosis (61%). The frequency of distribution of such lesions is shown in Table 4 (26 cases).

Table 4: Distribution of macroscopically visible haemorrhage and malacia in the CNS. (n = 26).

SITE	FREQUENCY (%)
CEREBRAL CORTEX Gyral crests Deep sulcal cortex	19 (73) 15 17
CAUDATE NUCLEUS	15 (58)
COLLICULUS Rostral colliculus Caudal colliculus	10 (38) 4 9
LATERAL GENICULATE BODY	3 (11,5)
THALAMUS	9 (34)
HYPOPHYSIS	2 (8)
PIRIFORM LOBES	3 (11,5)
OLFACTORY TRACT	7 (27)
CEREBELLUM	13 (50)
MEDULLA OBLONGATA	3 (11,5)
SPINAL CORD	2 (8)

Macroscopically visible haemorrhagic/malacic sites in the brain were seen in all of these cases, ranging in size from petechiae to suggillation. The cerebral cortex was more often affected than other sites, with rare involvement of the white matter. Haemorrhage was also seen in the cerebellar cortex, brain stem, cerebral nuclei, thalamus, olfactory tract, hypophysis and spinal cord.

Although large haemorrhagic lesions were frequently bilateral, they were seldom symmetrical. Unilateral lesions, and lesions that predominated on one side of the brain, were also seen. In one case, disseminated petechiae and ecchymoses were distributed widely through the cerebral cortex.

Macroscopically appreciable malacia was consistently associated with severe haemorrhage. It was most commonly observed in cases with locally extensive haemorrhagic lesions (Figures 2-4). In these cases, necrotic sites were located within the areas of haemorrhage. Severe malacia was most often observed in the cerebral cortex in the crests of extensively haemorrhagic gyri (Figures 2a, 3a, 3b & 4a). Malacia in the absence of haemorrhage was observed in one case although several cases with haemorrhagic lesions also had foci of malacia lacking haemorrhage.

Pale areas of malacia were observed on the periphery of zones of haemorrhage (Figures 2a & 2c). Areas of malacia ranged in size from a few millimeters to as much as a centimeter in diameter. In larger lesions, cystic spaces were sometimes formed (Figure 3b). Necrosis of the hypophysis (Figure 4a) was present in 2 cases (Table 4).

DISTRIBUTION OF REGIONAL LESIONS

The distribution of regional lesions was classified in terms of the anatomical sites of the brain that were affected (Table 4), the frequency with which the arterial territories of the respective cerebral arteries were affected (Table 5), and the frequency with which different lobes were affected (Table 6).

Table 4 gives the distribution of haemorrhagic/malacic lesions in the central nervous system in canine babesiosis. The cerebral cortex was the primary site for lesions (73%). The floors and sides of sulci were always affected in lesions involving the cortex. The superficial cortex tended to be affected in cases with more extensive lesions, in which cases the crests of gyri were involved (Figure 3).

Petechiae in the absence of ecchymoses or larger haemorrhagic lesions were present in the thalamus of a single case with congestive brain swelling. Petechiae were more likely to be observed in the thalamus, lateral geniculate nuclei, pyriform lobes, brain stem and spinal cord than in the cerebral cortices. They were common in the cortex and subcortex of the cerebellum. A single case showed disseminated cerebral petechiation (and small ecchymoses of 1mm diameter) over the cortical surface.

Ecchymoses were often observed as crescent-shaped or circular lesions confined to the depths of sulci (Figure 3). Larger haemorrhages extended to the superficial cortical tissue (Figures 3 & 4a). The caudate nucleus, caudal colliculus and olfactory tracts were more likely to develop ecchymoses than petechiae. Coalescent areas of ecchymosis were primarily seen in the cortical tissue, and often formed haematomas that were associated with malacia (Figures 2a, 3a & 3b).

The cerebellar cortex was affected in 50% of cases with regional lesions (Table 4, Figures 3a, 3b & 4b). The caudal cerebellar lobe was more frequently involved than the rostral lobe with 77% of cerebellar regional lesions involving the vermis. The ventral aspect of the cerebellum was more likely to show haemorrhage than the dorsal aspect. Haemorrhage was predominantly observed in the cortex, rarely extending into the white matter. The *nucleus interpositus* was affected in one case. Malacia was frequently associated with larger haemorrhagic sites (Figure 4b). In PM1.98, ecchymosis (and malacia) was present in the border zone between the rostral and caudal cerebellar arteries. Severe malacia of the grey-white junction was present in PM50.98.

Of the basal nuclei, the caudate nucleus was most frequently involved (58% of cases, Table 4). The rostral part of the caudate nucleus (*caput* and *corpus*) was more commonly affected than the *cauda* (Table 4). Figures 3a, 3b & 4a show bilaterally symmetrical lesions of the caudate nucleus. In some instances the lesion was unilateral or bilateral and asymmetrical. This site was affected in 6 cases (23%) in which superficial lesions were not present in the cerebral cortex.

Regional lesions were present in the caudal colliculus in 9 of 10 cases with collicular involvement. The rostral colliculus was affected in 4 cases, only one of which did not have lesions in the caudal colliculus. The lesions in the caudal colliculus tended to be spherical, 3

to 5mm in diameter and exclusively haemorrhagic (malacia was not obvious macroscopically). In most instances this lesion was bilateral (Figure 3), but unilateral lesions were also observed.

Table 5: Distribution of haemorrhage and malacia in the brain: arterial supply territory affected. Figures in square brackets denote frequencies for involvement restricted to the respective vessel. (n = 26).

ARTERIAL TERRITORY	FREQUENCY (%)
CEREBRAL HEMISPHERES	
Rostral cerebral artery	16 [1] (61.5)
Middle cerebral artery	22 [6] (85)
Caudal cerebral artery	11 [0] (42)
CEREBELLUM	
Rostral cerebellar artery	6 [4] (23)
Caudal cerebellar artery	8 [6] (31)
MEDULLA OBLONGATA	
Vertebral artery	2 [0] (8)
BORDER ZONES	(54)
CEREBRAL ARTERIES	
Rostral-middle	10
Rostal-caudal	7
Middle-caudal	1
CEREBELLAR ARTERIES	
Rostral -caudal	1

The lateral geniculate body and piriform lobes had lesions in 11,5% of cases with regional lesions (Table 4). These sites were more likely to develop petechial haemorrhages than ecchymoses.

Haemorrhage in the thalamus was seen in 9 cases (Table 4). Lesions tended to be bilateral and symmetrical in this site. Under most circumstances, petechiae were present and malacia

was rarely seen. Unilateral malacia was present in one case in which ecchymosis was also observed (Figure 3b). Petechiae were noted in the lenticular nuclei.

The hypophysis was affected in two cases. The first case showed severe congestion with associated ecchymosis. The second case had multifocal necrosis of the adenohypophysis in addition to congestion and haemorrhage. Figure 4c shows total haemorrhagic infarction of the hypophysis.

Seven cases showed lesions in the olfactory tract. No lesions were observed in the olfactory bulb in the cases examined. There were 6 cases in which ecchymoses were observed in the olfactory tubercle. The olfactory peduncle was involved in 3 cases. Two of the cases showed lesions in both the tubercle and the peduncle. Figure 2c shows a bilaterally symmetrical haemorrhagic lesion of the olfactory tubercle. The underlying cortex was not affected. Lesions in the olfactory tract were rare by comparison with other sites, and appeared to be restricted in size to that of ecchymoses or smaller.

Regional involvement of the white matter in cerebral babesiosis was rare. Haemorrhage did not tend to expand into the white matter unless cortical lesions were very severe. In affected cases, coalescent areas of haemorrhage were present, forming sites of suggillation within the white matter tracts. Petechiae and small ecchymoses were often situated on the periphery of such lesions.

Isolated petechiae and small ecchymoses were rarely observed in the white matter. Individual small sites of haemorrhage, 0.5 to 2mm in diameter, or tiny clusters of minute petechiae involving an area less than 1mm in diameter were occasionally observed in white matter tracts of the cerebrum, cerebellum, brain stem and spinal cord. Regional lesions in the white matter occurred by extension from severely affected grey matter.

Regional lesions occurred in the cortical tissues supplied by the middle cerebral artery in 85% of cases, whereas the frequency of lesions in cortical tissue supplied by the rostral or caudal cerebral arteries was 61% and 42% respectively (Table 5). Lesions were present in the border zones of arterial territories in 54% of cases. Lesions were observed in the border zones of the rostral cerebral artery in 17 cases of which 10 were peripheral to the middle cerebral artery and 7 to the caudal cerebral artery. Lesions confined to border zones were rare. Usually they were present in one or more arterial territories adjoining the border area.

Table 6: Distribution of multifocal malacic and haemorrhagic lesions in the brain (n = 26).

Table 6A.

Frequency of haemorrhage and malacia observed in sulci.

SULCUS	FREQUENCY
Post-cruciate sulcus	7 (32)
Coronal sulcus	9 (41)
Ansate sulcus	9 (41)
Marginal sulcus	5 (23)
Suprasylvian sulcus	4 (18)
Ectosylvian sulcus	3 (13,6)
Endomarginal sulcus	2 (9)
Ectomarginal sulcus	1 (4,5)
Splenial sulcus	2 (9)

Table 6B.

Frequency of haemorrhage and malacia observed in gyri.

GYRUS	FREQUENCY
Sylvian gyrus	1 (4,5)
Suprasylvian gyrus	7 (32)
Endomarginal gyrus	8 (36)
Marginal gyrus	6 (27)
Ectosylvian gyrus	8 (36)
Ectomarginal gyrus	2 (9)
Occipital gyrus	1 (4,5)
Splenial gyrus	1 (4,5)

Table 6C. Frequency of haemorrhage in different lobes of the cerebral cortex.

LOBE	CASE FREQUENCY (%)	ASSOCIATED SULCI	ASSOCIATED GYRI
Frontal	16 (57)	34	29
Parietal	14 (50)	38	29
Temporal	9 (32)	7	8
Occipital	11 (39)	17	12

In the cerebellum, the area supplied by the caudal cerebellar artery (31%) was more frequently affected than that of the rostral cerebellar artery (23%). The cerebellar border zone was not affected in any of the cases examined.

The distribution of regional lesions in the cerebral cortex is given in Table 6. Tables 6A and 6B give the frequency of lesions around sulci and in gyri respectively. In Table 6C the frequency of affected lobes of the cerebrum is given. Regional lesions of the sulci were most frequently observed in the frontal (57%) and parietal (50%) lobes, with the highest frequencies in the coronal and ansate sulci (41%). The ectomarginal sulcus of the temporal lobe was least frequently affected (4,5%). Peri-sulcal lesions on the surface tended to be restricted to sites where the sulci ended, such as the tip of the cruciate sulcus. The sulci could act as a barrier to the expansion of lesions, with the crest of one gyrus being affected on one side and the opposite gyrus apparently unaffected (Figures 3b & 3c).

Regional lesions were most frequently observed in the endomarginal and ectosylvian gyri (36%), and in the parieto-frontal cortex supplied by the middle cerebral artery. The sylvian, occipital and splenial gyri were least frequently affected (4,5%). Haemorrhage and malacia of the temporal lobe were usually restricted to multifocal ecchymoses, while the frontal lobe often showed locally extensive full-thickness cortical haemorrhage involving the depths and sides of sulci as well as the gyral crests. Petechial and ecchymotic haemorrhages of small extent were usually confined to the floors of sulci. Ecchymoses were also observed in the crests of gyri in more severe cases.

Haemorrhage in the cerebrum occurred more frequently in the frontal (57%) and parietal (50%) lobes than in the occipital lobe. These three lobes frequently had severe lesions with extension to the surface. The temporal lobe was least frequently affected (32%). Haemorrhage occurred more frequently in the rostral and dorsal halves of the brain, with ventral and medial lesions involving the cerebral cortex occurring rarely. Ventral lesions were most likely to occur along the midline, commonly associated with the olfactory tract, hypophysis, piriform lobes and cerebellar vermis. Lesions in the temporal lobes tended to be less extensive than those in other lobes.

THE HISTOLOGICAL FEATURES OF REGIONAL LESIONS

Haemorrhage in canine cerebral babesiosis shows a close association with the vasculature, erythrocytes tending to remain within the VR-space, or as a narrow zone around vessels (perivascular haemorrhage). In pre-cerebral cases (in which lesions were only discernable histologically) haemorrhages remained largely restricted to the VR-spaces. In early lesions, haemorrhage was observed in the VR-spaces or in the neuropil surrounding vessels. Erythrocytes were observed to collect around vessels, often with a regular zone of erythrocyte-free neuropil immediately surrounding a central capillary or venule (Figure 6a and 6c). In intermediate to advanced lesions, haemorrhage ranged in size from microscopic pericapillary extravasations of erythrocytes, to locally extensive suggillation in the neuropil (Figure 5). The lesions show a transition from a subtle, early, localised perivascular change, in which oedema predominates (Figure 5b), to an advanced, locally extensive change in which haemorrhage and malacia predominate (Figure 5a & 5c). In six cases, histological changes suggestive of cerebral babesiosis were observed in the absence of macroscopically visible regional lesions.

EARLY LESIONS (15,5%, Table 3; Figure 5b)

The subtlest lesions observed in cerebral babesiosis consisted of minute zones of rarefied neuropil in the grey matter, which were readily observed as pale, circular areas while scanning under 100x magnification. Closer examination of such sites (400x magnification) showed that rarefaction was centered around individual microvessels, or in slightly larger lesions, around a cluster of microvessels. These sites represented localised areas of perivascular oedema.

In addition, a homogeneous eosinophilic change in staining properties was observed in individual capillaries, post capillary venules and/or small caliber venules within the rarefied areas. This finding was interpreted as segmental necrosis of the micro-vasculature. It was characterised by partial loss of cellular detail of the vessel giving it a smudged appearance, and loss of vessel wall detail (Figures 5b). Extravasation of erythrocytes associated with injured capillaries, as well as areas of rarefaction, were convenient methods for detecting segmental necrosis in apparently normal neuropil.

Early lesions were not always associated with segmental micro-vascular necrosis. Combinations of oedema, micro-vascular necrosis and microhaemorrhages were usually necessary to detect early lesions. Associated neurons always appeared

FIGURE 5: HISTOPATHOLOGY OF REGIONAL LESIONS.

Figure 5a. (Top)
Advanced lesion with severe, multifocal to coalescing haemorrhage and malacia of the cerebral cortex. The moth-eaten appearance of the haemorrhagic area is due to the multiple sites at which haemorrhage arises within the affected zone. The sulcus acts as a barrier to the expansion of the haemorrhage. (Mag. 40x)

Figure 5b. (Middle)
An early lesion, showing a focal area of rarefaction in the neuropil (focal perivascular oedema). A portion of a post-capillary venule has undergone segmental necrosis (arrow). There is no apparent haemorrhage in the site, and the neurons in the surrounding neuropil appear normal (white arrows). Neutrophil infiltration is absent and no glial response is present. (Mag. 400x)

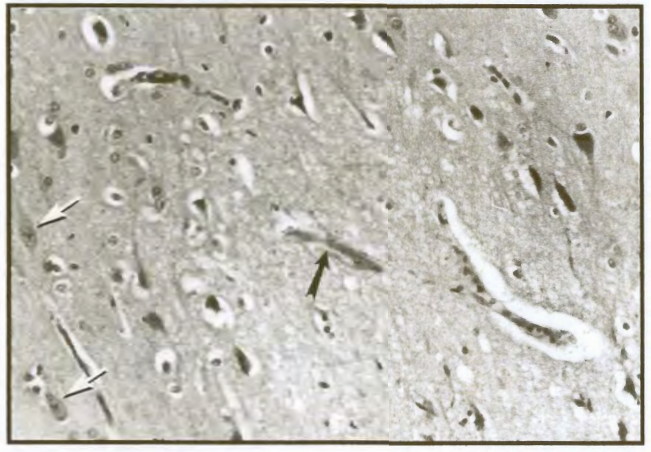

Figure 5c. (Bottom)
Detail of an advanced lesion showing malacia and haemorrhage with neutrophil infiltration. There is multifocal vacuolation of the neuropil, particularly in association with small blood vessels. Many of the neurons show ischaemic cell change and homogenising change. Their nuclei are indistinct and have a smudgy appearance (arrowheads). Segmental necrosis of a portion of a capillary is accentuated by the presence of polymerised fibrin in the VR-space (broad arrow).
(Mag. 200x)

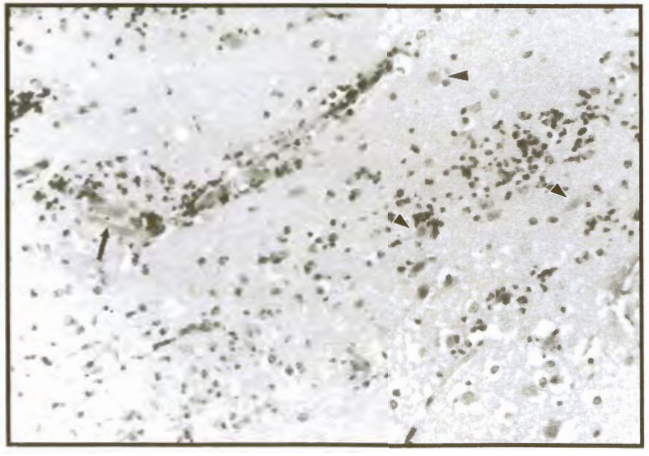

morphologically normal. Neutrophil infiltration was not observed. On the periphery of advanced lesions, multiple foci of injury characteristic of early lesions were observed, with the distinguishing feature that these sites were infiltrated with neutrophils (Figure 6b).

INTERMEDIATE LESIONS (12,5%, Table 3.)

Intermediate lesions were characterised by mild to moderate petechial haemorrhage, vascular injury and minimal neutrophil infiltration without demonstrable neuronal injury. These lesions were very rare. Haemorrhage was readily discernable in intermediate lesions, with a very distinctive perivascular distribution. Within a confined site of dense micro-vascular injury, coalescence of numerous adjacent perivascular haemorrhages formed areas of haemorrhage that were macroscopically visible.

Multifocal segmental necrosis of capillaries and small caliber arterioles and venules were fairly consistently demonstrable in sites of haemorrhage. Congested capillaries packed with parasitised erythrocytes were frequently associated with lesions, but were not necessarily present. In treated cases, parasitised erythrocytes were often absent. In lesions in which erythrocytes escaped the VR-space and penetrated the neuropil, morphologically unaltered neuronal cell bodies could be appreciated. In these lesions, neutrophils were rarely seen.

ADVANCED LESIONS (Figures 5a & 5c)

Advanced lesions were characterised by multifocal haemorrhage, neuronal necrosis, severe segmental vascular necrosis and neutrophil infiltration organised into a distinctive pattern of arrangement around blood vessels. Astrogliosis (Type 2 Alzheimer cells) and microglial reactivity were observed in lesions of longer standing (Figure 5c).

Coalescence of numerous localised perivascular haemorrhages, with extensive haemorrhage into the adjacent neuropil was the most obvious feature of advanced lesions. Associated with the haemorrhage, was moderate neutrophil infiltration into the injured area. The degree of neutrophil infiltration tended to be moderate rather than severe, and could be observed within haemorrhagic sites, but also in surrounding sites of apparently unaffected tissue (Figure 5a).

Margination of neutrophils within the vasculature was an infrequent observation (28%) as was perivascular neutrophilic cuffing (22%, Table 3). Occasionally,

trapped neutrophils were observed in erythrocytic sludge in post capillary, and slightly larger caliber venules. Monocytic trapping in sludge was common (75%). Neutrophil invasion of the tissue was associated with neuronal necrosis. All later stages of the ischaemic cell process were observed, including ischaemic cell change with nuclear shrinkage, increased eosinophilia of cytoplasm, incrustations and homogenising change. Microvacuolation was not observed.

Necrosis of the vasculature primarily affected the capillaries and post-capillary venules, and to a lesser degree, small venules and arterioles. The latter only tended to become involved in larger lesions. Segmental necrosis was characterised by homogeneous eosinophilic coagulative changes in the walls of affected vessels and surrounding neuropil (Figures 5b, 5c & 6a). Loss of endothelial nuclei was also observed. When present, endothelial nuclei were either swollen or tended to become pyknotic in affected segments. Some cells contained nuclei that had undergone karyorrhexis. In some instances, necrotic arterioles and venules could be distinguished by the presence of clustered, pale, dilated parasitised erythrocytes surrounded by a broad band of homogeneous eosinophilic material (necrotic debris and extra-vascular fibrin polymerisation, Figure 6a). Some necrotic vessels were empty, while others contained erythrocytes, or erythrocytic sludge. Parasitised erythrocytes could not always be demonstrated. Around the zone of extravascular fibrin and necrotic debris was a zone of haemorrhage. The erythrocytes within the haemorrhage tended to stain strongly eosinophilic, and were unparasitised in the majority of cases. Necrotic capillaries tended to have the appearance of eosinophilic smears if sectioned longitudinally (Figures 5b, 5c & 6c).

In some instances, severe oedema of the arteriolar wall was present, with swelling of the cells and shrinkage of nuclei (Figure 6a). Rarely, leukocytoclastic vasculitis was associated with this type of lesion (6% of cerebral cases, Table 3). In contrast, segmental necrosis of microvessels was common (69%, Table 3).

A microglial reaction was observed in some lesions. The earliest microglial response was characterised by influx of rod cells into the affected area (6%). With increasing length of survival, compound granular corpuscles (Gitter cells) predominated in the area of necrosis, and the lesions resembled infarction (3%). There was total necrosis of all tissue elements in the centres of such lesions, the cystic spaces being invaded on the periphery by large numbers of phagocytes.

FIGURE 6: HISTOPATHOLOGY OF REGIONAL LESIONS

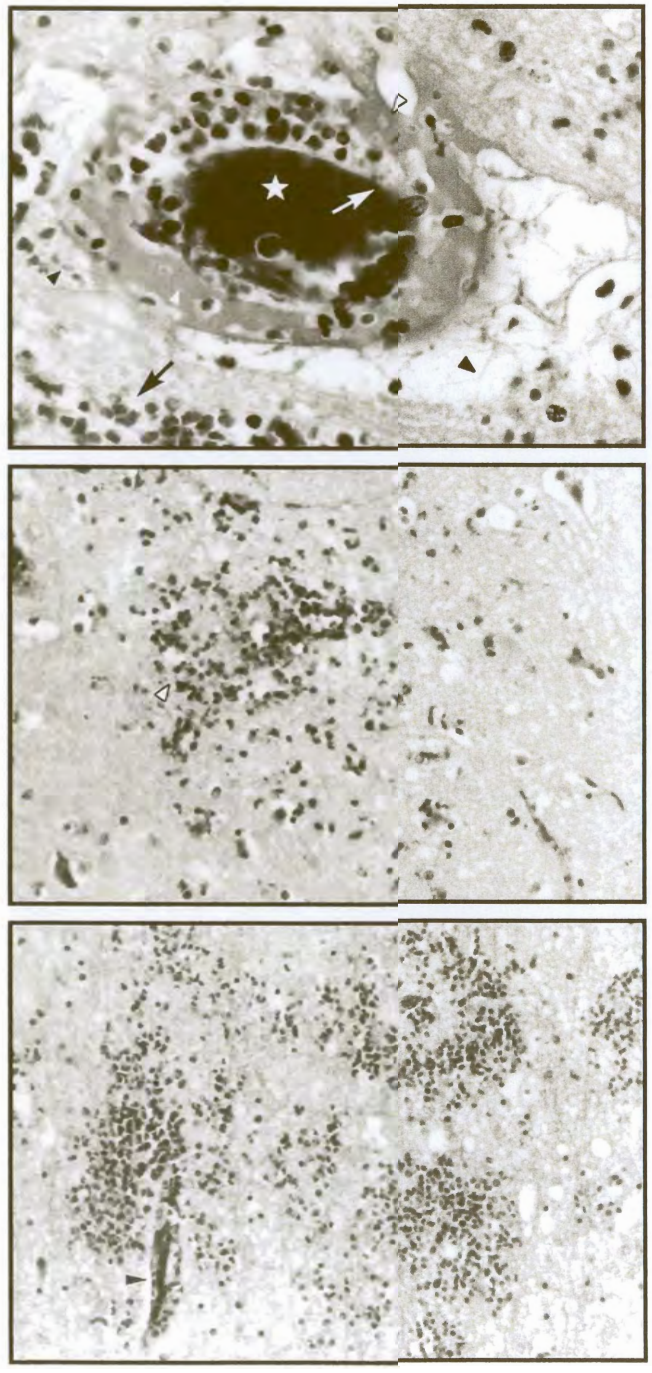

Figure 6a. (Top)
Segmental necrosis of a small vessel. The vessel has undergone coagulative necrosis (white arrowhead) and is identifiable only by the perivascular haemorrhage (black arrow) and a remnant of sludge (star) surrounded by monocytes. A pair of parasitised erythrocytes are visible on the edge of the sludge (white arrow). The poor stainability of these erythrocytes is presumed to be a consequence of haemoglobin loss. The vascular endothelium is no longer discernable and the cellular structure of the vessel wall is lost. Protein-rich fluid (white arrowhead with black edge) and fibrin polymers (black arrowhead) surround the sludge and penetrate into the neuropil. The VR-space is expanded and contains cellular debris (black arrowhead with white edge). (Mag. 400x)

Figure 6b. (Middle)
Area of expansion on the periphery of a severe lesion. Many of the features of an early lesion are demonstrated in this section, such as the local area of oedema and petechial haemorrhage. Unlike an early lesion, a distinct inflammatory infiltrate is present (white arrowhead with black edge).
(Mag.200x)

Figure 6c. (Bottom)
Regional lesion in the white matter. A zone of multifocal micro-haemorrhage and petechiation has expanded to involve the white matter tracts. Characteristically, the haemorrhage tends to form rings rather than spots in the white matter and the degree of coalescent haemorrhage is less in the sub-cortex. The lesion therefore appears more strictly perivascular. Moderate white matter oedema is present. There is a congested capillary in the lower left quadrant (arrowhead). (Mag.200x)

An astrocytic response was often observed in advanced lesions in which necrotic neurons and neutrophils were present. Astrocytes, when observed to react at all, most typically acquired the features of Type 2 Alzheimer cells (31%). Their cytoplasm remained in-apparent, while the nuclei became enlarged and vesicular and showed peripheral displacement of chromatin (Figure 5c). Some nuclei underwent duplication or triplication, and the density of astrocytic nuclei increased in the affected areas (hyperplasia). This reaction of the astrocytes was always restricted to foci of haemorrhage and necrosis, and was never observed as a diffuse cerebral change.

An important feature of advanced lesions, was the presence of small haemorrhages on the periphery of larger zones of injury (Figure 6b). Dense clusters of microhaemorrhage superficially similar in appearance to early lesions, were observed within an area of focal grey matter oedema. An important distinguishing feature of these lesions by comparison with true early lesions, was the presence of ischaemic cell change and homogenising change in associated neurons and local infiltration of neutrophils into uninjured peripheral tissue. These lesions appeared to represent the expanding front of the advanced lesion.

REGIONAL LESIONS IN THE WHITE MATTER

In a few cases, haemorrhage was observed in the white matter (Figure 6c). The extravasation tended to be distinctly perivascular, forming rings around the transected vessels. Often, the affected vessels were necrotic, and surrounded by a zone of fibrin strands.

Haemorrhage in the white matter was found to occur only rarely in cerebral babesiosis (6% of cerebral cases, Table 3). The lesion had a characteristic multifocal distribution, and occurred by extension from extremely severe lesions in the adjacent grey matter. Perivascular ring haemorrhages (Figure 6c) were a distinctive feature of this type of lesion. In some rings, the centrally located capillary or post-capillary venule was clearly discernable, and commonly showed some degree of necrosis with extravasation of fibrin into the VR-space. At the centre of other ring haemorrhages, no vessel was discernable, and the central space may simply have contained a tiny region of homogeneous to fibrillar, eosinophilic-staining material, which might have been necrotic neuropil, or the

remnant of a necrotic capillary. So, a central vessel was not always conclusively demonstrable.

CEREBELLAR LESIONS

Haemorrhages in the cerebellum could be any size, from microhaemorrhage to suggillation. Cerebellar lesions were most commonly observed in the cortex and showed the same perivascular pattern of haemorrhage seen in the cerebrum. Petechiae were observed more frequently than larger areas of haemorrhage. Coalescence of small haemorrhages to involve larger areas, was less frequently observed than in other sites of the brain. Haemorrhage rarely extended into the granule cell layer, but was frequently observed in the molecular layer, or on the border between the molecular layer and the granule cell layer. A tendency for lesions to develop in the depths of cerebellar sulci, similar to that seen in the cerebral cortex, was also noted. Lesions seldom extended into the white matter. The nucleus interpositus showed petechiation in at least one case, which could be mistaken macroscopically for haemorrhage in the white matter. In approximately 30% of cerebral cases, the white matter of the cerebellum showed a teased-out appearance of the axonal tracts, suggestive of vasogenic oedema (Table 3). Necrosis of Purkinje cells was occasionally seen. Severe ventral cerebellar haemorrhage was present in association with brain stem haemorrhage in 2 cases.

SERIAL SECTIONS

Thrombi composed of platelets, fibrin and erythrocytes were not demonstrated in cerebral sections of canine babesiosis. Serial sections from six cerebral lesions failed to demonstrate thrombosis.

Venules draining the haemorrhagic sites were filled with erythrocytic sludge, but thrombi could not be demonstrated in either the arteriolar or venular vasculature associated with severe haemorrhagic lesions. The erythrocytes within the sludge appeared to be fused together, with little distinction between adjacent cells. Sludge could be demonstrated in association with all six lesions examined. Erythrocytic sludging was present in 91% of control cases, 69% of cerebral cases and 78% of all fatal cases (Table 3). Dilated vessels within sulci were also observed in association with locally extensive areas of haemorrhage and necrosis. Extensive sulcal haemorrhage was restricted to individual sites in association with lesions.

ULTRASTRUCTURE

Ultrastructural changes were observed in erythrocytes, vascular endothelium, plasma and cells of the neuropil. Reversible and irreversible changes were present, both in the cells of the microvasculature and in the neuropil.

ERYTHROCYTES

Pathological changes in both parasitised and unparasitised erythrocytes could be subdivided into four groups: Positional abnormalities, morphological abnormalities, abnormal contact with other cells and loss of electron density. Abnormal positions of erythrocytes in vessels were associated with altered cell morphology and altered membrane structure. Close apposition of cell membranes with loss of intercellular space was suggestive of abnormal adhesive contact between cells.

Erythrocytes were observed to occupy abnormal positions in vessels. Normally, they maintain a central position in the lumen of vessels and are surrounded by plasma. In babesiosis, erythrocytes were observed to lie against the vessel wall and appeared to be attached to it. This positional shift was termed margination. Under normal conditions, individual blood cells are separated from each other and the endothelium, by a fine layer of plasma. This layer was absent in many instances and erythrocyte membranes appeared to be fused together. This is thought to cause sludging in vessels. Extensive apposition of the erythrocyte plasmalemma along the endothelial plasmalemma was suggestive of adhesion. Margination and adhesion were observed in both parasitised and unparasitised erythrocytes. Not all erythrocytes were affected in any one case, nor was margination and adhesion present in every case examined.

Margination was observed in all calibers and types of microvessel at the histological level. It was most often observed in smaller caliber vessels at the ultrastructural level. Morphological characteristics of marginated cells included focal electron dense sites of contact between erythrocytes and endothelial cells, extensive flattening of the erythrocyte membrane along the endothelium (adhesion) and squaring of erythrocytes. Points of apparent contact between erythrocytes and endothelial cells were not necessarily present. Under some circumstances, close approximation of the erythrocyte membrane to the endothelial membrane

FIGURE 7: ULTRASTRUCTURAL FEATURES OF ERYTHROCYTES

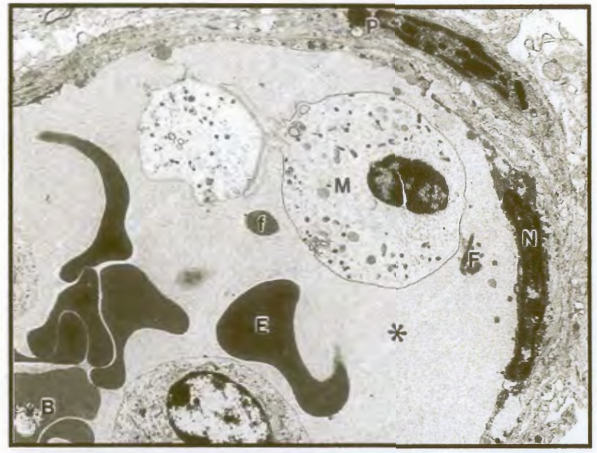

Figure 7a. (Top)
Portion of a small caliber vessel, showing the lumen containing many extensively distorted erythrocytes. Most of the erythrocytes contain a reasonably high concentration of haemoglobin and are electron dense (E). A parasitised erythrocyte (B) is present in the lower left corner of the field, and shows a comparative loss of haemoglobin, as is reflected in the loss of electron density. A macrophage (M) is actively phagocytosing a cellular fragment, which appears to be a fragment of another degranulated phagocyte. An electron dense erythrocyte fragment (f) is present in the plasma (star), adjacent to the macrophage. Fibrin fragments have polymerised in the plasma adjacent to the macrophage (F). The endothelial cell lining the lumen of the vessel is undergoing necrosis. The cytoplasm is starting to fragment resulting in exposure of the basement membrane, and the organelles have condensed. The nucleus (N) is contracted. In contrast, the pericyte (P) contains discernible organelles and structured chromatin in the nucleus. Original magnification 2600X. E854. EM1.98.

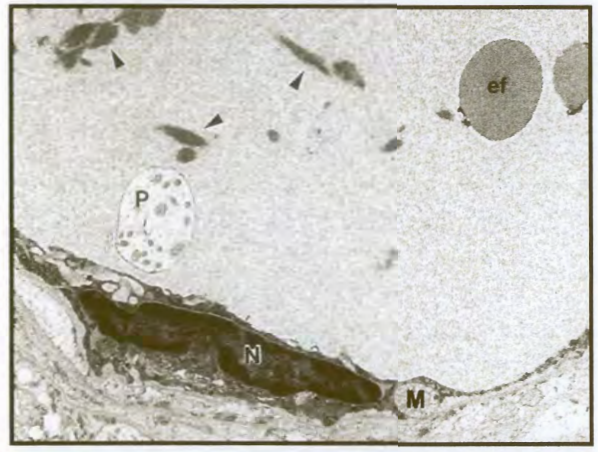

Figure 7b. (Middle)
Venule with fibrin degradation products (arrowheads) and erythrocyte fragments (ef). The erythrocyte fragments have a rounded shape, contain no organelles but consist of a homogenous moderately electron-dense substance, apparently haemoglobin, enclosed in a membrane. Fibrin degradation products are present on the external surface of the erythrocyte fragments. An endothelial cell is present at the bottom, with a clearly defined electron dense nucleus (N). At the right pole of the nucleus is a large mitochondrion (M). In the lumen of the vessel is a platelet (P). Original magnification 3400X. E848. EM1.98.

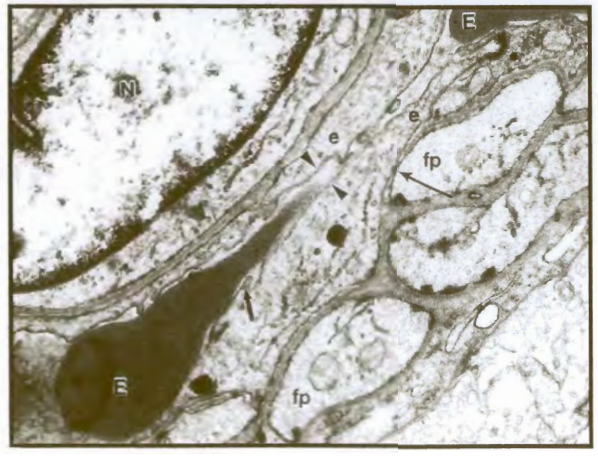

Figure 7c. (Bottom)
Compression of an erythrocyte within a capillary. A swollen pericyte nucleus, (N) bulging into the lumen of a capillary has all but obliterated it. An adjacent erythrocyte (E) has become partially trapped and is compressed in the remaining space (designated by arrowheads between the lining endothelial (e) cells). The endothelial cells show small pseudopodial projections (broad arrow). Swollen astrocyte foot-processes (fp) are present. There is a pore between the astrocyte foot-process and the endothelial cell (slender arrow). Original magnification 10500X. E839. EM1.98

prevented distinction between these two structures, as there was no discernable space present, and membrane integrity appeared disturbed.

Profound distortion of erythrocyte shape was observed in all cases (Figure 7a). Erythrocytes lost their biconcave shape, assuming a wide range of bizarre forms, including general enlargement of the cell, square, rectangular and triangular shapes, severe flattening, bleb formation, doubling over, formation of long slender projections and fragmentation. Fragments of erythrocytes are present in Figures 7a and 7b. Erythrocyte fragments were sometimes attached to the endothelium, but were also observed lying free in the vascular lumen. Erythrocyte fragments were not observed in all cases.

Figure 7c shows a capillary in which the swollen pericyte nucleus has all but obliterated the lumen, causing marked compression of a passing erythrocyte. Such an erythrocyte, on regaining the circulation, could give rise to the distorted free cells observed in Figure 7a.

In addition to the marked morphological distortion of free cells, some erythrocytes appeared to be folded into others, or tightly compressed between neighboring cells in the vessel. Sludge was characterised by clumping of erythrocytes in vessels, loss of the interstitial plasma layer and apparent fusion of adjacent erythrocyte membranes. Sludge consisted of both parasitised and unparasitised erythrocytes, usually in association with macrophages.

Contact Points (Figures 8 & 9)

Erythrocytes formed close contacts with each other, and with endothelial cells. Loss of the interstitial plasma layer was a feature of abnormally close intercellular contact within the vascular lumen. Sites of direct contact varied in size and structure. Zones of contact along lengths of adjacent membranes were observed. Erythrocytes in sludge had abnormally close contact, making distinction between cells difficult. In some instances the membranes appeared to be fused together. Feathery contacts were present in the intercellular space between some erythrocytes in sludge. A fuzzy degradation along the length of the erythrocyte cell membrane was sometimes observed. Membrane apposition in erythrocyte sludge was not dependent on the presence of contact points.

FIGURE 8: INTERCELLULAR CONTACT POINTS

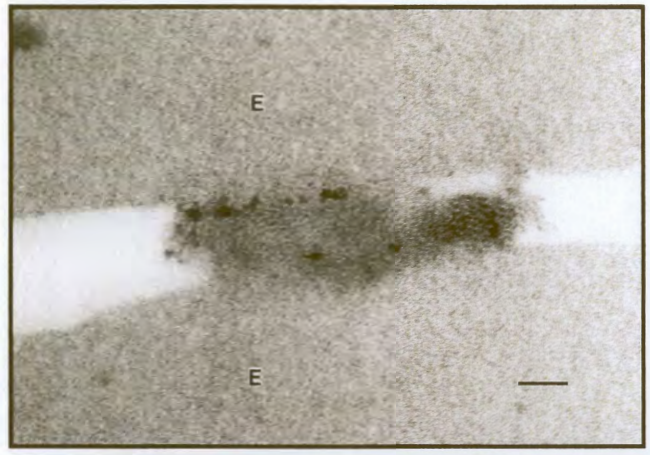

Figure 8a. (Top)
Inter-erythrocytic contact: Detail of two adjacent erythrocytes (E) showing an amorphous granule between the two cells. The material in the inter-erythrocytic space is granular, slightly coarser than the cellular matrix, and also slightly denser. The material has dense granules within it, aligning approximately at the level of the erythrocyte membrane. The plasmalemma is indistinct, and the border of both cells is hazy rather than showing a distinct membranous structure. Bar = 60nm. Original magnification 64 000X. E849. EM1.98.

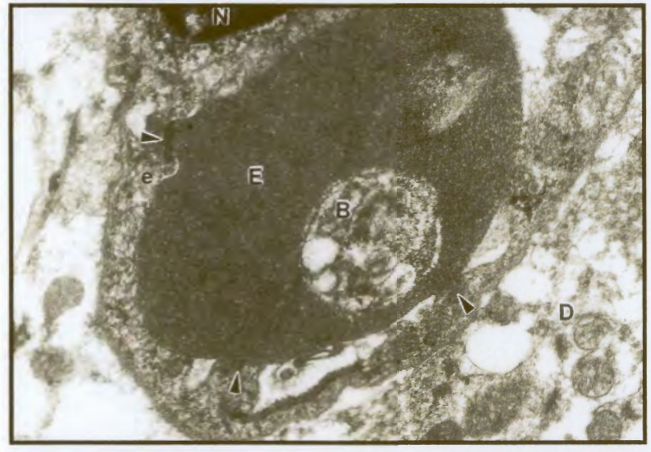

Figure 8b. (Middle)
A parasitised erythrocyte (E) lies within a capillary. A major portion of the erythrocyte surface is in close apposition to the endothelium. At three sites, distinct electron dense contact points are present (arrowheads). N: pericyte nucleus; B: *Babesia* parasite; e: endothelial cell; D: cellular debris. Original magnification 11500X. E905. EM4.98.

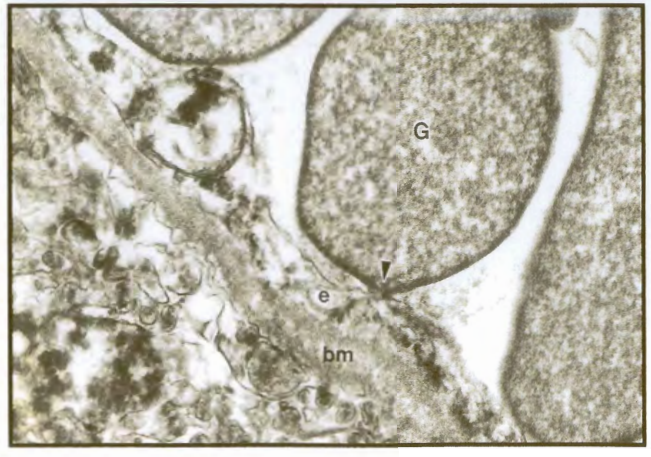

Figure 8c. (Bottom)
An erythrocyte ghost (G) in contact with the endothelium (e) at a single electron-dense site of attachment (arrowhead). bm: basement membrane. Original magnification 15500X. E891. EM3.98.

Two distinct types of contact point were recognised at higher magnifications, one type consisting of an apparently homogeneous, moderately electron dense material (amorphous granules, Figure 8a), the other being composed of highly structured membranous stacks (Figure 9b). Both types of contact point were situated on the outer surface of the erythrocyte membrane. Contact points were present on erythrocytes irrespective of whether cells were parasitised or not and whether or not the cells were adherent to other cells. Membrane stacks were observed between erythrocytes and endothelial cells. They were also observed on the free surfaces of erythrocytes. Amorphous granules were observed in the intercellular space between adjacent erythrocytes and on the free surface of the erythrocyte plasmalemma. They ranged in width from 83nm to 822nm, the majority being about 167nm. The material appeared to be fragmented in some cases, forming a lacework of fine strands in the intercellular space. These fine strands were visible at magnifications of more than 50000x, as a delicate feathering between the cells. These fine strands were approximately 6nm wide.

A fine layer of plasma was lacking between the plasmalemmas of erythrocytes and endothelial cells at sites of erythrocyte margination, although a space of a few nanometres was present between the cells. In some instances, resolution of two distinct membranes was not possible, and a fuzzy contact zone was observed (Figure 9a).

At lower magnifications (5000 – 10000x), membranous stacks were characterised by a high electron density relative to adjacent portions of the membrane (Figures 8b & 8c). The electron dense sites appeared to be fixed contact sites between erythrocytes and endothelial cells (Figures 8b & 8c). At higher magnification (50000x), it was observed that they were limited in width, ranging from 178-2500nm, the majority being in the region of 621nm wide (mode). They were composed of an even number of dark and light bands (4 - 10) with a periodicity of 4,5 - 5nm (Figure 9b). The ends of each membrane were free, and did not curve round to fuse with the next membrane above or below in the stack. In some sites, membranes appeared to split or fuse.

Erythrocyte Ghosts

Numerous electron lucent erythrocytes were observed in individual cases. These were characterised by a spectrum of intra-erythrocytic changes, from dark grey to

pale grey. In some fields, erythrocyte membranes were present, that enclosed strands of flocculent material characteristic of erythrocyte ghosts (Figures 8b & 11b).

ENDOTHELIAL CHANGES

Changes to the cerebral endothelium in canine babesiosis ranged from in-apparent to severe. The majority of endothelial cells examined appeared normal. Damaged microvascular endothelial cells were observed in all cases examined. Some endothelial cells showed reversible changes such as moderate cytoplasmic swelling and nuclear swelling. In some cases cytoplasmic swelling was marked, and there was swelling of rough endoplasmic reticulum as well as an increase in the number of free ribosomes in the cytoplasm. In more severely affected cases, mitochondrial swelling was observed. Endothelial cell necrosis (irreversible injury) was present in most cases, and was characterised by loss of organelles, accumulation of cellular debris and swelling of mitochondria (Figures 10b, 10c & 11b). In some instances, the endothelial plasmalemma was highly convoluted, with long slender processes similar in appearance to pseudopodia, extending into the vascular lumen. These processes were sometimes observed to be in close contact with erythrocytes.

Obliteration of the vascular lumen as a result of nuclear swelling was noted in capillaries (Figure 7c). Severe vasoconstriction with complete occlusion of the vascular lumen, was also observed (Figure 11c). Although marked endothelial cell damage was observed, the zonula occludens of the tight junctions appeared to be intact in many severely affected cells (Figures 10b & 11b). Marked cytoplasmic disruption consequent to endothelial damage was noted repeatedly at sites adjacent to tight junctions (Figure 11b), thus a single cell might be affected and the neighbouring cell spared. In yet other instances, damage was so severe, that numerous adjacent endothelial cells were affected (Figures 10a & 10b).

In some cases, endothelial retraction was marked, resulting in the exposure of the basement membrane. This was not necessarily associated with fibrin deposition (Figures 10c & 11). Leakage of plasma proteins from the vascular lumen into the Virchow-Robbins (VR) space was also observed at sites of endothelial retraction (Figure 10c).

FIGURE 10: ULTRASTRUCTURE - VASCULAR INTEGRITY AND COAGULATION

Figure 10a. (Top)
Fibrin thrombus. An aggregate of parasitised erythrocytes (P) within a small arteriole. Erythrocyte membranes appear fused together. Strands of electron-dense fibers lie between the erythrocytes (arrowheads). They lack the characteristic banding periodicity of fibrin. Two unparasitised erythrocytes are present in the very left of the vessel. They have a higher electron density than most of the parasitised erythrocytes. The vascular endothelial cells (E) are swollen (autolysis). Original magnification 2950X. E912.
EM5.98.

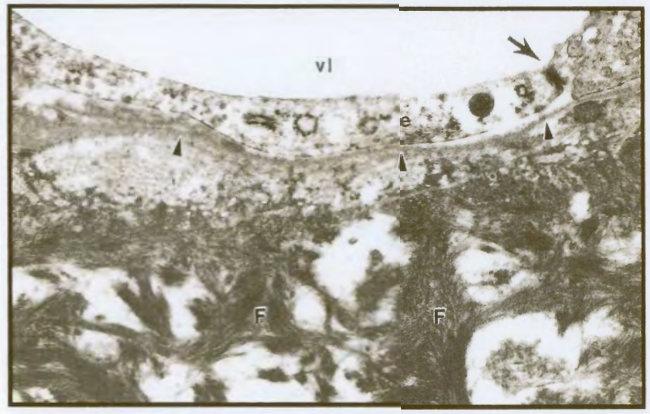

Figure 10b. (Middle)
Polymerisation of fibrin (F) in the VR-space. The endothelial basement membrane is indicated by arrowheads. The endothelial cell (e) shows swelling of the rough endoplasmic reticulum and loss of continuity of the plasmalemma (autolysis). A morphologically intact tight junction is present (arrow).
vl: vascular lumen. Original magnification 8900X. E743. EM27.96.

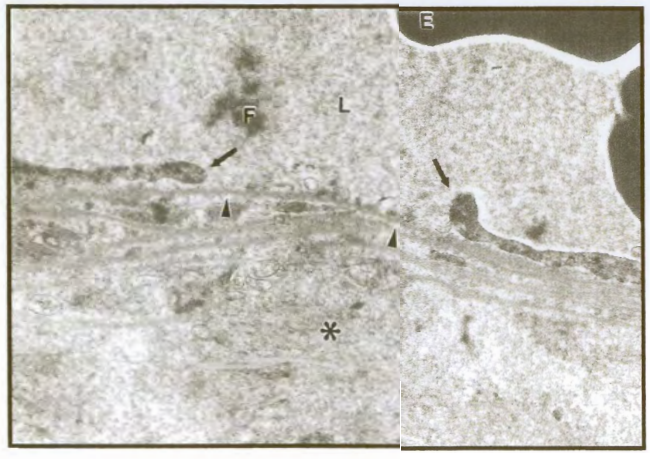

Figure 10c. (Bottom)
Endothelial retraction resulting in exposure of the basement membrane (arrowheads). The arrows mark the slightly swollen free tips of the endothelial cell. Between them lies the breach in the vascular wall. The fine granular material in the vascular lumen (L) is plasma, with a cluster of electron dense material free in the matrix, that might be fibrin degradation products (F). Plasma is present in the intercellular spaces around the venule (star).
E: erythrocyte. Original magnification 5800X. E879. EM6.97.

Endothelial projections, extending into the vascular lumen, were sometimes present (Figure 7c). They varied in length from 0,1 to 1,0µm, and occasionally appeared to be adherent to erythrocytes. Very long, slender pseudopodia were observed extending between erythrocytes, apparently attached to erythrocytes deeper in the lumen. This behaviour of the endothelium was suggestive of phagocytosis, but no erythrocytic material was observed in the cytoplasm of endothelial cells in the cases examined.

CHANGES IN THE EXTRACELLULAR MATRIX

Ultrastructural pathology in the extracellular matrix was particularly suggestive of disturbances in coagulation. Despite fairly substantial damage to the vascular endothelium with exposure of the basement membrane, fibrin deposition and platelet adherence was rarely observed. A region of endothelial retraction with associated exposure of the basement membrane has been sealed by a platelet in Figure 11c. Out of all the vessels examined, platelets were observed in only two instances, suggesting the presence of thrombocytopenia.

An intravascular meshwork of fibrin was observed in several cases. The strands of polymerised fibrin formed a lattice between erythrocytes, which appeared to bind firmly to the red cells, trapping them within the meshes, and against the endothelium. The fibers forming the meshwork were sometimes observed in cross section, lying between adjacent erythrocytes in sludge (Figure 10a). Thrombocytes were not present. Although the strands appeared to be composed of fibrin, they did not always have the characteristic periodic banding of this substance. When banding was present, it had a characteristic bandwidth suggestive of fibrin (19-25nm).

Fibrin fragments (probably degradation products) were also observed in the lumen of capillaries, or filling breaches in the endothelium where the basement membrane had been exposed. Extravasation of fibrin was present with severe vascular wall injury (Figure 10b). As a result of endothelial retraction, plasma was observed in the interstitium. This was a rare observation, but an important indicator of increased vascular permeability.

Polymerisation of fibrin in the VR-space was demonstrated in a case with severe vascular injury (Figure 10b). In contrast, the exposed basement membrane did not show any fibrin deposition in a number of cases. This apparent lack of fibrin

FIGURE 11: ULTRASTRUCTURE: VASCULAR INTEGRITY AND COAGULATION

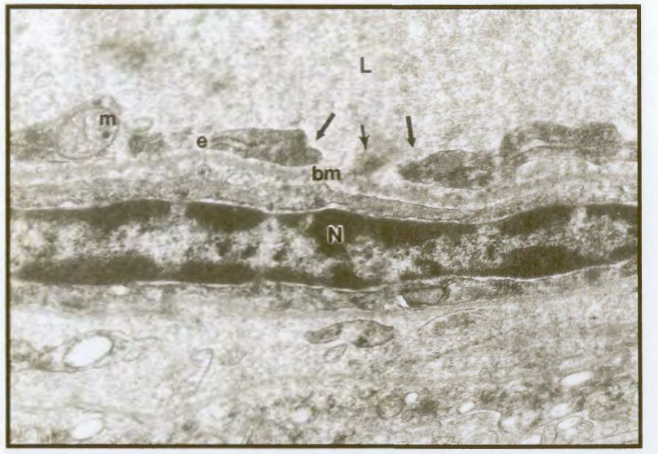

Figure 11a. (Top)
Endothelial (e) retraction (thick arrows) resulting in exposure of the basement membrane (bm). A section of the vascular wall has been severely injured (broad arrows). The slender arrow indicates a tuft of fibrin adjacent to the basement membrane. The endothelial mitochondrion (m) has clearly defined cristae. L: vascular lumen; m: mitochondrion in the endothelial cell; N: pericyte nucleus. Original magnification 10 000X. E928. EM6.97.

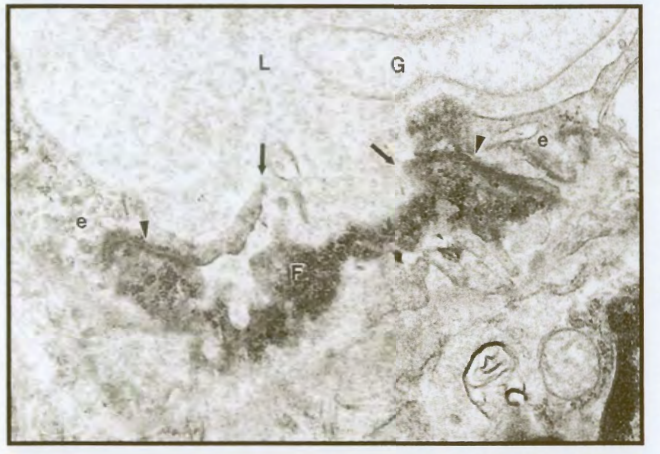

Figure 11b. (Middle)
Detail of the vascular wall showing a breach in endothelial integrity. The arrows indicate the free tips of the endothelial cell (e) where it has lifted and separated off the basement membrane. The latter is not discernable because of the deposition of electron dense granules in the gap (F). The breach lies between two intact tight junctions (arrowheads), suggesting that a second endothelial cell, which has undergone necrosis, may have occupied the intervening space. The dense granules may be fibrin degradation products or necrotic debris from the presumed second endothelial cell. An erythrocyte ghost (G) lies in the capillary lumen (L). Original magnification 4 600x. E847. EM1.98.

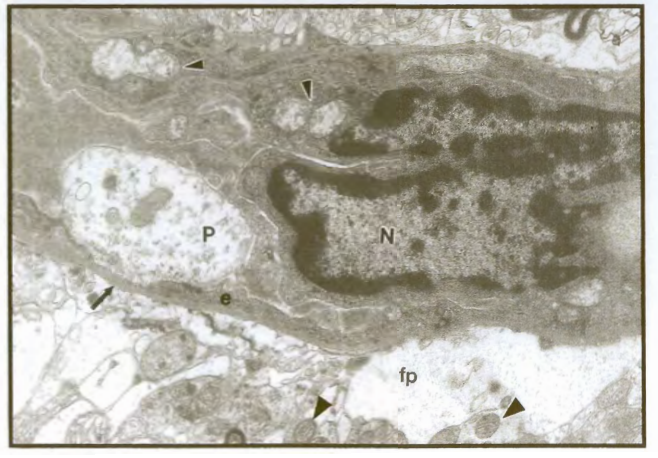

Figure 11c. (Bottom)
Endothelial (e) retraction and vasoconstriction with exposure of the basement membrane (arrow) and occlusion of the vascular lumen respectively. A platelet (P) has filled the gap, and there is no plasma present in the extracellular space, indicating that the seal is effective. A slightly swollen astrocyte foot-process (fp) is present at the bottom right. The endothelial nucleus (N) is enlarged and appears to have completely obliterated the lumen (vasoconstriction). The white-edged arrowheads show swollen mitochondria, which have lost their cristae in the endothelial cell, and adjacent pericyte. In contrast, the mitochondria present in the neighbouring astrocytes (black arrowheads) appear normal. Original magnification 4600x. E927. EM6.97

deposition was associated with the presence of fine fibrillar deposits against either side of the exposed basement membrane, suggestive of fibrin degradation products (Figures 10c & 11a). This finding was accompanied by the presence of granular material on either side of the basement membrane, indicating exudation of plasma into the interstitial space (Figure 10c). Fragments of fibrillar material were sometimes observed in the lumen of vessels in these cases.

CHANGES IN THE CELLS OF THE NEUROPIL

The majority of neurons observed did not show any morphological abnormalities. Mild to moderate swelling of the endoplasmic reticulum was present in the soma of some small neurons in regions of vascular damage. Severe mitochondrial swelling of a large neuron was observed within an area of injury.

Astrocytic changes did not appear to be as advanced as vascular changes in the early stages of lesion development. Endothelial injury was observed adjacent to apparently normal astrocytes (Figure 11c). Swelling of astrocytes was observed around microvessels in severe lesions. In some instances, astrocytic injury was so advanced the astrocytes were no longer discernable.

Some of the myelin sheathes in the white matter showed evidence of fluid accumulation between the membrane layers. Bubble-like spaces between successive layers of myelin occurred in numerous sites within an affected area, a characteristic of myelin-oedema. The axons within the sheaths appeared normal.

DISCUSSION

The pathology of cerebral babesiosis in dogs was described at the gross, histopathological and ultrastructural levels. Lesions are strongly associated with the circulatory system. Global lesions include congestive brain swelling, mild to moderate congestion and diffuse cerebral pallor. The distribution of macroscopically appreciable cerebral oedema, when present, is usually global. Regional lesions are associated with multifocal haemorrhage, malacia and microscopically appreciable oedema. They undergo progressive stages of development. Early lesions are characterised by small (< 100μm) sites of perivascular rarefaction in the neuropil of the grey matter, which may contain a necrotic microvessels (vessels less than 50μm diameter). Intermediate lesions are larger, often containing numerous coalescent, perivascular haemorrhages visible macroscopically as petechiae. Ischaemic cell change is not present despite mild to moderate neutrophil infiltration into the affected area. This stage in the progressive development of lesions is presumably short-lived, as the influx of neutrophils is thought to precipitate further tissue damage (27,31,33,57).

Advanced lesions were suggestive of reperfusion injury and infarction, both of which are thought to be secondary consequences of locally extensive micro-infarction of capillaries and post-capillary venules. Advanced lesions are characterised by multifocal to coalescent areas of perivascular haemorrhage, segmental vascular necrosis of microvessels, arteriolar necrosis with perivascular fibrin deposition, moderate neutrophil infiltration and ischaemic cell change/homogenising change in neurons. Microglial rod cell invasion of affected sites is rarely seen. Astrocytic hyperplasia (Alzheimer type 2 cell response) is often present in lesions of presumably longer duration. The affected areas often show evidence of oedema, which does not extend as a morphologically appreciable change into the surrounding neuropil. Classically, the white matter acts as a barrier that prevents extension of the lesion, which will stop abruptly on the edge of nerve tracts in the majority of cases. Leukocytoclastic vasculitis is a rare finding in regional lesions and tends to occur in more severely affected cases.

In cases with parasitaemia, pRBC (parasitised red blood cells) are present within vessels, while extravasated erythrocytes tend to be unparasitised. Parasitised erythrocytes in haemorrhage are an extremely rare finding.

Histological features of fatal babesiosis that cannot be considered indicative of cerebral babesiosis include widespread endothelial nuclear swelling, pericyte reactivity, uneven vascular filling, intravascular fibrin polymerisation, monocytic leukostasis, mild to moderate congestion (in the absence of regional lesions) and microhaemorrhage in the absence of associated segmental vascular necrosis of capillaries. Red cell changes such as sludging, loss of haemoglobin, cellular enlargement, and changes in cell shape as a result of adhesion to endothelium are common findings in babesiosis in general. Margination and adhesion of erythrocytes can be seen in cerebral sections from cerebral and non-cerebral cases. The significance of such findings as indicators of cerebral babesiosis is therefore questionable. They are likely consequences of systemic inflammation caused by babesial infection. Endothelial reactions such as contraction with nuclear swelling, can be induced by elaboration of inflammatory products such as increased synthesis of free oxygen radicals (26).

It is not known whether early lesions always give rise to advanced lesions given sufficient survival time, or whether advanced lesions develop rapidly from early lesions under specific physiological conditions such as reperfusion.

The ultrastructural study showed that endothelial necrosis is an early event in the development of regional cerebral lesions and that perivascular rarefaction of the neuropil can be due to both vasogenic and cytotoxic oedema (35,75). Ultrastructural pathological changes were interpreted with caution because of the limitations of using field material. Evidence of autolysis was observed in all formalin-fixed cases. The endothelial changes were unexpectedly advanced in comparison with some of the other cell-types, such as neurones and astrocytes. This suggested that endothelial injury had occurred at sites where neuronal injury was morphologically inapparent, and endothelial changes were less likely to be a direct consequence of autolysis.

Membrane-associated structures (contact points) on the surface of erythrocytes (membrane stacks and amorphous granules) were observed in both glutaraldehyde-fixed cases and formalin-fixed cases. They appeared to play a role in adhesive intercellular interactions indicative of sequestration in canine babesiosis. Although contact points differ morphologically from those observed in cerebral babesiosis of cattle and cerebral malaria in man (2,3), they may still

function in a similar manner, and may be responsible for the observed endothelial necrosis.

Lesions of the spinal cord in babesiosis have not previously been demonstrated, although some cases described with peripheral lesions may have had spinal cord injury (55,56). Lesions in the spinal cord show the same structural features as those in the brain, with the same predilection for grey matter microvasculature, suggesting that the pathogenesis of lesions is the same throughout the central nervous system.

Babesiosis is a haemoprotozoan disease and the consequences of infection affect the circulatory system. In cerebral babesiosis, injury to the circulatory system within the CNS can lead to its failure under certain uncharacterised circumstances. Circulatory injury caused by unknown factors leads to increased intracranial pressure either by development of cerebral oedema or congestive brain swelling. This gives rise to the development of some global lesions. Injury to the endothelial cells lining the microvasculature appears to be the initial change that leads to the development of regional lesions. Changes associated with further development of regional lesions are suggestive of reperfusion injury and may be due to microvascular infarction, particularly capillaries and post-capillary venules. The presence of DIC, fibrin thrombi, parasitic emboli, margination and adhesion of pRBC, sludge and endothelial nuclear swelling in control cases suggests that some additional unknown factor is responsible for the pathogenesis of cerebral babesiosis in the dog. Alternatively, a specific combination of events may lead to conditions suitable for the development of lesions.

More than one type of lesion can develop in canine cerebral babesiosis, but all are related in some way to disturbances in the circulation and vascular function of the brain. Congestive brain swelling is a consequence of failure of the autoregulatory responses of endothelial cells in the presence of hypertension (58). Diffuse cerebral pallor may be a consequence of anaemia. Cerebral oedema may be multifocal or diffuse, and reflects a disturbance in the integrity of the blood-brain barrier (26,35). Altered endothelial function will affect the permeability of the blood-brain barrier (38). Regional lesions of cerebral babesiosis in this study, were associated with primary endothelial injury and perivascular haemorrhage.

CONGESTIVE BRAIN SWELLING

In congestive brain swelling, accumulation of intravascular fluid within the cranium causes raised intracranial pressure as a consequence of failure of vascular autoregulation (58). Morphological findings from this study showed widespread sludging of erythrocytes in virtually every capillary and in the vast majority of small vessels in cases with congestive brain swelling. The appearance of sludge at the histological and ultrastructural levels suggests that blood viscosity is raised and there is a reduction in flow rate in vessels containing sludge. Slow blood flow may increase the risk of congestive brain swelling developing. The rate of blood flow could not be measured in this study, but slow flow is inferred, as sludge appears to have a higher viscosity than free erythrocytes: high viscosity would cause slower flow rates (81). An additional or alternative factor influencing severe microvascular congestion may be unresponsive vasodilation (loss of autoregulation). The system failure may be a self-perpetuating combination of factors, in that more vasodilation leads to slower blood flow which in turn causes increased sludge formation. Sludge presumably flows slowly because it is highly viscous and cannot deliver oxygen rapidly enough. Hypoxia develops, with loss of autoregulation (23). The physiological abnormalities governing failure of autoregulation are probably the most important factors influencing development of congestive brain swelling. The physiological conditions present during congestive brain swelling, particularly slow flow rates, would prolong contact times between erythrocytes and facilitate haemagglutination and sludge formation (81). Sludging would therefore be expected to be present to a greater degree in congestive brain swelling than in other conditions of fatal babesiosis. The multifactorial nature of congestive brain swelling is emphasised by the fact that erythrocyte sludging is a common finding in non-cerebral babesiosis. It therefore cannot be considered a primary factor in the pathogenesis of congestive brain swelling which is a rare occurrence in canine cerebral babesiosis.

DIFFUSE CEREBRAL PALLOR

Diffuse cerebral pallor may be a lesion in those cases with severe anaemia, but it is not necessarily a pathological change and should be interpreted with caution. Anaemia was present in 6 of 8 cases with diffuse cerebral pallor, but 3 of the cases had a packed cell volume (pcv) in the range of 20-30%. The diffuse cerebral pallor in these cases could possibly be attributed to anaemia, but could also have been a consequence of bleeding out at necropsy. Cerebral hypoxia as a consequence of

anaemia alone could not be demonstrated experimentally in cerebral babesiosis (54). A shift in the oxygen dissociation curve occurs in canine babesiosis and some cases develop a mixed acid-base imbalance, both of which are an indication of poor oxygen delivery to the brain in anaemic dogs (50). Pulmonary insufficiency may be a more important factor than anaemia in influencing the development of cerebral signs and has been documented as an important cause of cerebral hypoxia (23). A combination of lung oedema and anaemia may be very important in the pathogenesis of hypoxia in cerebral cases with cerebral pallor. In brains with cerebral pallor, histological evidence of hypoxia such as ischaemic cell change and laminar cortical necrosis could not be readily demonstrated.

Cases with severe anaemia (pcv less than 15% (50)) are more likely to develop central nervous signs for reasons related to the anaemia than as a consequence of the presence of the parasite. In cases with cerebral pallor where the patient's pcv is above 15%, it is possible to classify the case as cerebral babesiosis even in the absence of regional lesions, provided the clinical neurological signs are satisfactorily explained as a consequence of the *Babesia* infection, and not some other cause (36,50). Histopathology on such cases may yield early regional lesions.

MILD TO MODERATE CONGESTION

Mild to moderate congestion is a difficult change to interpret, as this is frequently present in cases that lack cerebral signs. It may, however, be the only change observed in cases that have a history of neurological signs and thus cannot be ignored. Like diffuse cerebral pallor, cerebral congestion must be interpreted with caution. Both pallor and congestion can only be interpreted in the light of clinical history, concurrent complications such as pulmonary oedema or systemic haemoconcentration, and histopathology. Histopathology is important in such cases because the lack of grossly visible regional lesions does not exclude the possibility of microscopic regional lesions being present.

CEREBRAL OEDEMA

The fact that cerebral oedema is not a consistent finding in cerebral babesiosis is rather surprising, as increased vascular permeability was considered to be the fundamental process in the pathogenesis of complications in babesiosis

(54,55,56). Cerebral oedema in this disease appears to have a complex pathogenesis, as oedema can be either diffuse or localised, and can be associated with most other types of lesion whether global or regional. Histologically, and from the ultrastructural study, oedema can be either vasogenic or cytotoxic in nature. Cytotoxic oedema is associated with cell swelling and is due to substrate deficiency, while vasogenic oedema is a consequence of vascular injury (35). Both types of oedema occur in association with an ischaemic insult. The period of ischaemia induces cell swelling as a consequence of depletion of ATP and glucose levels, while the reperfusion period is associated with the development of vasogenic oedema, which is largely interstitial as a result of failure of the blood-brain-barrier (35).

In diffuse cerebral oedema associated with cerebral pallor, and in control cases, oedema of the white matter at the histological level was suggestive of vasogenic oedema. Examination of the ultrastructure of the white matter revealed irregular spacing between the layers of myelin in oligodendrocytes, suggestive of myelin-oedema, the axons within the sheaths remaining intact.

In contrast to diffuse oedema, oedema associated with regional lesions appeared to be perivascular and intracellular. Swelling of astrocyte foot processes was observed at the ultrastructural level. Eosinophilic fluid in the VR-space was a rare finding histologically. Astrocyte swelling is indicative of cytotoxic oedema and suggests that the presumed endothelial injury in associated capillary segments led to energy deficits in astrocytes. Hence perivascular rarefaction of the neuropil in early regional lesions may be a consequence of cytotoxic oedema.

Combined vasogenic and cytotoxic oedema, as seen in babesiosis, is not an unusual phenomenon. It has been reported as a consequence of cerebral ischaemia (35,82). In inflammation, cerebral oedema may develop as a consequence of endothelial injury due to the generation of oxygen free radicals (26). Such a process may influence the development of lesion-associated oedema in regional cerebral lesions.

The low frequency of spinal cord lesions suggests that this part of the CNS is more resistant to development of regional lesions than the brain. The spinal cord is

typically listed as the most resistant site in the CNS to hypoxic injury (9). The apparent vulnerability of the sulcal floors and resistance of the spinal cord to regional lesions, suggests that some factor influencing vulnerability to hypoxia (selective vulnerability) may also influence the risk of development of regional lesions in cerebral babesiosis. The combined presence of vasogenic and cytotoxic oedema in some cerebral cases also suggests that hypoxia may influence the development of lesions.

REGIONAL LESIONS OF CEREBRAL BABESIOSIS

The two mechanisms thought to be important in the development of regional lesions are hypoxia and infarction (5,11,54,60,68). There is much evidence from this study to suggest that both these events influence the development of cerebral babesiosis, but they are likely to be secondary events. The primary event in the development of regional lesions appears to be endothelial cell injury. It was beyond the scope of this study to demonstrate this conclusively.

HYPOXIA

The apparent tendency for regional lesions to arise in the floors of sulci and in the caudate nuclei, which are selectively vulnerable to hypoxia (9), suggests that a common factor may determine the site, both of regional lesions and of hypoxia. Transient hypotension may be important in causing hypoxic injury and slow blood flow conducive to sludging, margination and adhesion (14,23,37,72). The sensitivity of the basal ganglia to hypoxia, particularly the caudate nuclei, can be induced by low blood flow in the paleocortex (41).

The ultrastructural study showed that individual endothelial cells undergo necrosis before signs of injury can be detected in astrocytes and neurons. It is possible that, as an increasing number of adjacent endothelial cells become injured, the ability of the microvasculature to maintain its integrity, is decreased. If there is sufficient injury to the endothelium, segmental vascular necrosis is appreciable histologically. This is suggested by the high frequency of segmental vascular necrosis in early lesions, and in cerebral cases as opposed to controls. The difficulty of demonstrating segmental vascular necrosis in histological sections is thought to be a consequence of the minuteness of the lesion in the early stages of its development. This is supported by the ultrastructural observation of individual

endothelial cell necrosis in microvessels that are otherwise intact. Failure of astrocyte function secondary to endothelial cell necrosis is suggested by the presence of histologically visible zones of perivascular rarefaction in the neuropil of affected grey matter. Electron microscopic observations suggest that once several adjacent endothelial cells become necrotic, the remaining endothelium is unable to compensate for the breach in vascular integrity. Erythrocytes can then escape into the perivascular space *per diapedesis* in the early stages of compromised endothelial function. With increasing injury, there is retraction of endothelium and opening of tight junctions. Because of thrombocytopenia, the basement membrane remains exposed and plasma escapes into the interstitium. Thrombocytopenia is a common finding in babesiosis (60,69) and is reflected in the inability of the host animal to compensate for the vascular injury. Fluid shift from the vascular compartment into the interstitium therefore appears to be a combined effect of endothelial injury and a loss of the ability to seal sites of injury.

It is extremely difficult to demonstrate any neuronal injury in early and intermediate lesions, either at the histological or ultrastructural level, in contrast to the apparent advanced degree of capillary necrosis present. The vulnerability of CNS cells to anoxia is well documented (9,29,40,42). Neurons are most vulnerable, followed by glial cells, while endothelial cells are most resistant. Endothelial injury was apparent both at the histological and at the ultrastructural level at sites where neurons were intact, in this study. This is very strong evidence suggesting that the primary lesion of cerebral babesiosis is at the level of the microvascular endothelium and is not due to global hypoxia. The earliest ultrastructurally visible insults appear to be focal, often involving only a single endothelial cell. Adjacent neurons and astrocytes were comparatively unaffected. Observed swelling of neuronal endoplasmic reticulum, originally thought to be indicative of reversible change in neurons, was an artefact attributable to immersion fixation (8). It appears, therefore, that the lesions of reperfusion injury and hypoxia observed in the advanced stages of cerebral babesiosis are secondary events following endothelial injury.

INFARCTION

Endothelial cell necrosis at the ultrastructural level was characterised by shrinkage of the nucleus and fragmentation of the rarefied portion of the cytoplasm. In contrast to injury described as a consequence of infarction in which tight junctions

open (44), tight junctions remained morphologically intact in the majority of lesions of babesiosis. In early lesions endothelial cells were still recognizable, in advanced lesions cells were notably absent, or had ruptured, leaving loose strands of plasmalemma projecting into the lumen. Endothelial cell retraction with opening of tight junctions and exposure of the basement membrane was a feature of advanced but not early lesions. These findings suggest that infarction does not play a role in the initial vascular injury, but is an important secondary factor following endothelial injury. An individual platelet sealing a length of exposed basement membrane was observed in a single instance only. The rare presence of thrombocytes in electron micrographs where obvious endothelial retraction with exposure of basement membrane had occurred, suggests the presence of thrombocytopenia in these cases. Thrombocytopenia was not necessarily measured in these cases, but is a common clinicopathological finding in babesiosis (60,69). The majority of sites where basement membrane was exposed were inadequately filled with fragments of fibrin. Some of the particles were so small and fine, it is possible that they were fibrin degradation products. Extravasation of erythrocytes and plasma was observed at these sites, indicating the presence of increased vascular permeability with development of vasogenic oedema. The extravasated fluid was observed in the interstitium but swelling of astrocyte foot processes was also present, suggesting that both cytotoxic and vasogenic oedema develop in these cases. Ischaemia-hypoxia causes combined vasogenic and cytotoxic oedema in infarction (58). These findings suggest that infarction and hypoxia may play a secondary role in the progressive development of regional lesions.

From this study it appears as if the later evolution of lesions, from the primary early lesion to that of severe multifocal to coalescing haemorrhage and malacia, is a function of reperfusion injury. The term "reperfusion" in itself suggests that there must first be loss of perfusion. Preceding tissue injury (a consequence of perfusion loss) is exacerbated by the influx of oxygen to the injured site when flow is resumed. It appears from the sections examined, that lesions undergo temporal evolution. An initial event gives rise to microvascular injury and the development of early lesions. Following this, perivascular tissue injury apparently ensues, with haemorrhage and extravasation of activated neutrophils. Neutrophils play an important role in the development of oxidative injury during reperfusion (20,31). The tissue injury may become a self-perpetuating cycle (19). This would explain why lesions are multifocal and coalescent, and why early lesions with neutrophils

actively invading the neuropil, are seen on the periphery of advanced lesions. The possibility exists, that activated neutrophils unable to engulf necrotic material in the site of injury, release enzymes into the neuropil. This would be the most likely mechanism by which lesions could expand into the uninjured peripheral tissue. Diffusion of catalytic and proteolytic enzymes released from neutrophils, could occur in the interstitial space and along the VR-space. The diffusion of neutrophil products along the VR-space may in some way influence the development of segmental vascular necrosis and vasculitis (27,31).

Ischaemic Infarction

Ischaemic infarction of the canine brain has been induced experimentally by occlusion of 4 or more major arteries (46,85). The collateral supply to the brain is so efficient, that massive thrombosis would be required in the large ventral arteries, in order to induce the type of large haemorrhagic lesion common to cerebral babesiosis. Such thrombosis has never been demonstrated, but the sludging of erythrocytes within vessels may have a similar effect. Sludge, however, is rarely demonstrable in large arteries in babesiosis. In addition, lesions would resemble ischaemic infarction, and this does not occur. Necrosis of the white matter, a feature of infarction (49), has not been reported in cerebral babesiosis lesions, and observed lesions only show necrosis of all tissue elements (histological definition of infarction (23,46)) in what appears to be the later stages of the disease. Haemorrhagic transformation of infarction also does not explain the haemorrhagic lesions, because by definition, all tissue elements would have become necrotic before haemorrhage occured (46). In early and intermediate lesions, haemorrhage was consistently observed in the absence of neuronal injury (in this study), suggesting that haemorrhagic lesions are not a consequence of infarction, but of primary vascular damage (49).

Since haemorrhagic transformation of infarction cannot explain the regional lesion of cerebral babesiosis, and arterial obstruction was not observed, the possibility of venous infarction should be considered. In venous infarction, venous flow is halted, and back-damming of blood occurs in the region drained by the obstructed vein (23). This type of lesion gives rise to severe, locally extensive haemorrhage in the injured neuropil. This is a common finding in babesiosis. Raised intracranial pressure is a likely consequence of expanding haemorrhagic lesions, cerebral oedema or congestive brain swelling (58). Any one of these events, or all of them,

could result in haemorrhagic infarction. At least in some cases of cerebral babesiosis, haemorrhagic infarcts may be a late development as a consequence of brain swelling with secondary venous occlusion. In particular, the cerebellar haemorrhage observed in some cases, is suggestive of this, as is hypophyseal haemorrhage. Regional lesions developing in the floors of sulci or in the caudate nucleus are not explained by venous infarction. The histological features of early lesions also cannot be explained by haemorrhagic infarction. From this study it can be concluded that venous infarction may occur late in the development of lesions in cerebral babesiosis, but it is an unsatisfactory explanation for the origin of regional lesions.

Venous Infarction

If venous infarction can only explain some of the secondary events in the development of regional lesions, some other mechanism must give rise to the microvascular injury observed. Infarction of capillaries has been suggested by Brumpt (11) who proposed that parasitic emboli disrupt blood flow in babesiosis in a similar manner to that described for cerebral malaria, while Moore and Williams (60) suggested that DIC may be the mechanism responsible for haemorrhagic lesions in babesiosis. Either or both of these mechanisms are likely to influence the pathogenesis of the disease, because both would be capable of inducing endothelial injury, and probably do. DIC and sequestration could act synergistically in inducing microvascular infarction, because localization of pRBCs would promote thrombosis and fibrin thrombi would trap erythrocytes, as has been observed in the electron microscopy study. High-density microvascular infarction in a localised area, or widespread microvascular infarction distributed through a critically high proportion of cerebral tissue, could induce regional lesions. It is beyond the scope of this study to explain why the floors of sulci in the frontal and parietal cortex and the caudate nuclei are more vulnerable to regional lesions than other sites. It is, however, clear from this study, that the unknown conditions suitable for development of lesions, can occur in virtually any site in the central nervous system, but tend to occur more readily in the grey matter than in the white matter. The spinal cord is less likely to be affected than either the neocortex or the paleocortex.

Microvascular Infarction

DIC and sequestration of pRBC have the potential to occur at any site within the vasculature. They have the potential to cause hypoxic injury to endothelium. In addition, mechanical injury to the endothelium may develop as a consequence of adherent contact between pRBC and endothelial cells. Neither DIC nor sequestration need occur simultaneously, although it is possible that either could increase the risk that the other occurs. Once microvascular injury has occurred, thrombolysis and release of sequestered erythrocytes will not prevent lesions from developing, as events following endothelial injury are likely to be independent of vascular obstruction. It is not known why cerebral lesions do not develop in all cases, such as those with DIC or with high cerebral parasitaemias. This is a single, very important reason to disregard microvascular infarction as a factor in the pathogenesis of lesions. It is supported by the fact that lesions similar to cerebral babesiosis do not develop in cases suffering from neoplastic metastatic emboli, or DIC due to other causes, and a case of babesiosis with DIC confirmed histologically did not have lesions in the brain. Intravascular polymerisation of fibrin was seen more commonly in control than cerebral cases, so the formation of fibrin thrombi is less likely to be important in the cerebral form of the disease than was previously thought. Altered enzyme activity in endothelial cells may be induced by binding to pRBC, or exposure to parasite antigens. Endothelial cell surface receptor expression is greatly altered in response to malarial infection (70,77).

Sequestration events alone do not give rise to regional cerebral lesions, as many control cases have demonstrable sequestration. It can be argued that some of these cases may have died before cerebral lesions could develop. However, sequestration appears to be a common event in babesiosis, and cerebral babesiosis is relatively rare. In addition, cerebral babesiosis is often an acute clinical event, suggesting that lesions develop relatively rapidly. Sequestration is seen commonly in subacute control cases. It is therefore proposed that as-yet-unknown parasite-host interactions consequent upon sequestration give rise to the conditions necessary for endothelial cell injury to occur. Once endothelial cell injury occurs, secondary factors determine whether regional lesions will develop to the advanced stage.

Interactions between erythrocytes and endothelial cells were reported by Maegraith *et al.* (54), who observed margination in some of their cases. Adhesion and

apparent firm contact between erythrocytes and endothelial cells mediated by structural alterations of erythrocyte membranes, have never before been reported in canine babesiosis. Histologically, margination and adhesion of erythrocytes were inconsistent findings. The most likely explanation for the variable occurrence of marginating and adhesive behaviour is that it only occurs during a specific stage of the parasite life cycle, and then disappears again (72). It is also possible that *B. canis rossi* induces sequestration, while *B. canis canis* and *B. canis vogeli* do not, or only induce mild sequestration. A third possibility is that erythrocyte surface antigenic variation occurs in canine babesiosis as it occurs in malaria (74) and bovine babesiosis (62). Malarial knob-associated antigens have been shown to bind to ICAM-1, CD-36, VCAM-1 and thrombospondin receptors expressed on activated endothelial cells (15,53,70,77). Contact, mediated by membrane fusion and membrane stacks, between infected erythrocytes and endothelial cells was observed in this study, using electron microscopy on cases that showed margination and adhesion histologically. This suggests that altered membrane receptor expression may influence endothelial-erythrocyte interactions in canine babesiosis.

Membrane-bound vesicles thought to be erythrocyte fragments were attached to the plasmalemma of endothelial cells. Membrane-bound vesicles thought to be pseudopodial projections from the endothelium were attached to the external surface of erythrocyte membranes. These ultrastructural observations strongly suggest that adhesive contact between pRBCs and endothelial cells does occur in canine babesiosis. The significance of these interactions is not well understood, as histological evidence of margination and adhesion were more frequently observed in control than cerebral cases (Table 3). The evidence suggests that sequestration of parasitised erythrocytes occurs in canine babesiosis, but that it is not important for the pathogenesis of cerebral babesiosis. It may, however, be an important predisposing factor leading to the development of lesions under specific conditions. The precise nature of these conditions is yet to be elucidated.

PATHOGENESIS OF REGIONAL LESIONS

The regional lesions of canine cerebral babesiosis are unique to this disease in the dog, suggesting that pRBC must play some role in the pathogenesis of lesions. The difficulty in finding a logical explanation for regional lesions in cerebral babesiosis lies less with the role of the parasite in the development of lesions than in the lack of lesions in the majority of cases with parasites. Some additional factor,

therefore, must determine whether lesions are going to develop or not. It is most likely that there are several additional factors both of host origin and parasite origin, that act together to produce the lesions of cerebral babesiosis. A complex multifactorial pathogenesis for the development of cerebral lesions would best explain the rarity of the condition in canine babesiosis.

It has been shown in this study that localised endothelial cell injury is the primary event leading to the development of regional lesions in cerebral babesiosis. The mechanism by which endothelial cells are injured is unknown. A number of possible explanations exist, and will require further investigation. Mechanical obstruction of individual capillaries by sequestered pRBC may lead to endothelial hypoxia and necrosis as a consequence of loss of blood flow. Total obstruction of capillaries by erythrocyte sludge and adherent erythrocytes would give rise to microvascular infarction. The spatial distribution of microvascular infarcts within the cerebral tissue, may influence the final outcome determining whether or not lesions will develop.

Alternatively, partial obstruction of capillaries may result in abnormally high wall shear stresses in small caliber vessels. Wall shear stress can generate frictional forces sufficient to injure endothelial cells (81). Under circumstances of combined adherence and partial obstruction of some vessels within an individual capillary bed supplied by a single arteriole, in the presence of total obstruction of other capillaries within the same capillary bed, wall shear stresses in the semi-patent capillaries rise to very high levels and would be capable of damaging endothelial cells. The presence of erythrocyte fragments attached to endothelial cells, free fragments in the vascular lumen and vesicles thought to be endothelial pseudopodial projections attached to erythrocytes, all suggest that under conditions of high wall shear stress, adherent cells may be forcefully separated, leading to endothelial cell injury.

A third mechanism involved in endothelial cell injury would be the presence of a theoretical "*Babesia* toxin". Such a substance, secreted by the parasite in the sequestered site, could cause individual necrosis of adjacent endothelial cells. Under circumstances of sequestration in microvessels, a parasite-derived substance could accumulate to toxic levels. This theory is attractive in terms of explaining why complications of the disease occur so seldom. The conditions necessary for sufficient levels of toxic build-up to develop within capillaries would

be rare. Soluble parasite antigens synthesised by *B. canis canis* are currently under investigation (71).

All the mechanisms suggested thus far are dependent on a sequestration event within the microvasculature leading to microvascular infarction. The assumption that sequestration is important in the pathogenesis of regional lesions is based on the fact that lesions are strictly vascular-associated. Individual endothelial cell injury and segmental vascular necrosis tend to occur in the microvasculature, where sequestration is also commonly observed. Irreversible endothelial cell injury could either occur through the process of necrosis or through apoptotic mechanisms. Babesial toxins or inflammatory mediators could potentially induce endothelial cell apoptosis.

An anatomical study cannot readily address the biochemical events taking place in the course of a disease process, and this was not investigated in this study. However, the intermediate and advanced lesions of cerebral babesiosis are suggestive of reperfusion injury. The presence of haemorrhage supplies a source of free iron to the injured site (20). The influx of neutrophils provides a source of catalase (19,33). Hypoxia is known to induce cerebral endothelial cells to convert the enzyme xanthene dehydrogenase to xanthene oxygenase (19,20). Xanthene oxygenase synthesizes superoxide, a moderately active reactive oxygen species, which is readily neutralized by cellular antioxidant mechanisms (20). However, in the presence of neutrophil-derived catalase, hydrogen peroxide is produced, which, in the presence of free iron and superoxide radicals, leads to the synthesis of hydroxyl radicals (20). This is the so-called Haber-Weiss reaction, and the hydroxyl radicals produced are highly toxic and may give rise to necrotising vasculitis (27). It is possible during the course of babesiosis infection in the dog, that conditions arise which are suitable for the Haber-Weiss reaction to occur in the affected brain tissue, leading to the development of intermediate and advanced lesions. Expansion of the lesions on the periphery may be a consequence of diffusion of radicals along the VR-space in association with neutrophil chemotaxis. This theory remains to be tested.

Finally, the astrocytic response in advanced lesions requires comment. Alzheimer type 2 cells are a characteristic astrocytic response to hepatic encephalopathy as a result of hyperammonaemia (43). Such a response is normally disseminated throughout the cerebral tissue, unlike the regional cerebral lesions of canine

babesiosis where Alzheimer type 2 cells are only present in association with lesions. Although hepatic injury is a fairly common sequel to babesial infection (54,60), cerebral babesiosis has never been attributed to hepatic encephalopathy. The fact that the brain lesions are regional rather than diffuse and that the astrocytic response is directly associated with the affected foci, suggest that local changes in astrocyte function are influenced by the local tissue injury. Whether this is a consequence of changes in tissue pH, release of glutamate-type neurotransmitter substances related to ammonium metabolism or an effect of astrocyte antioxidant function (48,59), is unknown.

The pathogenesis of cerebral babesiosis is complex and multifactorial. Each different manifestation of cerebral disease is determined by the co-action of a multitude of variable factors. No single factor can be held responsible for the development of lesions. Under circumstances where a critical combination of factors occurs at a given moment in a given patient, cerebral babesiosis ensues. The exact factors remain to be elucidated. Further research in canine babesiosis should be directed at the immunology of the disease, especially the interactions between soluble parasite antigen, erythrocytes, lymphocytes, monocytes and neutrophils. Activation of cerebral microvascular pericytes was observed in both control and cerebral cases, suggesting that these antigen presenting cells may be important in cerebral immune and inflammatory responses. The primary cause of endothelial injury is not clear, but may be a consequence of inflammation-induced apoptosis, or a direct sequel to microvascular infarction (necrosis secondary to hypoxia, accumulation of metabolic waste products and depletion of energy substrates). Microvascular infarction could be caused by sludging of erythrocytes, or by margination and adhesion of erythrocytes to endothelial cells. Since all these phenomena are present in control cases, the events leading to the individual endothelial injury are poorly explained. Further investigation should be aimed at the biochemical level and should involve an in-depth investigation of immune and inflammatory mechanisms.

The role of intercurrent disease and multiple organ failure in cerebral babesiosis should be investigated further. An experimental investigation of therapeutic diamidine therapy in severely compromised patients should be conducted to establish whether they are at higher risk of developing cerebral disease. Further studies of the pathogenesis of canine babesiosis should be aimed at investigating the role of soluble parasite antigens or "babesial toxins", inflammatory mediators,

cytokines, reactive oxygen species, complement and coagulation factors in endothelial cell injury.

CONCLUSIONS

The aims of this study were:

1). To describe the cerebral lesions of canine babesiosis at the macroscopic and light-microscopic level.

It was found that gross lesions could be either global (diffuse cerebral pallor, congestive brain swelling) or regional (multifocal haemorrhage and malacia) with or without cerebral oedema. Histological findings distinctive for cerebral babesiosis were associated with regional lesions only. Histological features suggested that regional lesions develop over time in cerebral babesiosis. The primary site of injury appears to be at the level of the endothelial cell.

2). To determine what ultrastructural pathology is present in canine cerebral babesiosis, and whether changes are comparable or not to those seen in either bovine cerebral babesiosis or cerebral malaria in man.

The ultrastructural features of cerebral babesiosis suggest that endothelial cell injury occurs early in the development of lesions. Membrane stacks between erythrocytes and endothelial cells suggest that abnormal adhesive contact is induced between these cells during *Babesia canis* infection in dogs.

3). To improve current understanding of the pathogenesis of cerebral babesiosis.

The findings of this study suggest that an unknown mechanism, possibly inflammatory or mechanical, or a combination of both, induces endothelial cell injury in cerebral babesiosis. This leads to the development of regional lesions, a consequence of combined hypoxic and oxidative injury. Intermittent microvascular obstruction may increase the risk of reperfusion injury following localised hypoxia.

REFERENCES

1. Aikawa, M. (1988). Human cerebral malaria. *American Journal of Tropical Medicine and Hygeine* **39:** 3-10.

2. Aikawa, M., Pongponratn, E., Tegoshi, T., Nakamura, K., Nagatake, T., Cochrane, A., and Ozaki, L. S. (1992). A study on the pathogenesis of human cerebral malaria and cerebral babesiosis. *Memorias do Instituto Oswaldo Cruz* **87:** 297-301.

3. Aikawa, M., Rabbege, J., Uni, S, Ristic, M., and Miller, L. H. (1985). Structural alterations of the membrane of erythrocytes infected with *Babesia bovis*. *American Journal of Tropical Medicine and Hygeine* **34:** 45-49.

4. Aikawa, M., Suzuki, M., and Gutierrez, Y. (1980) Pathology of Malaria. in: *Malaria Vol. 2*, Kreier, J. P. (eds.). Academic Press. New York. p: 47-102.

5. Basson, P. A. and Pienaar, J. G. (1965) Canine babesiosis: A report on the pathology of three cases with special reference to the "cerebral" form. *Journal of the South African Veterinary Medical Association* **36:** 333-341.

6. Botha, H. (1964). The cerebral form of babesiosis in dogs. *Journal of the South African Veterinary Medical Association* **35:** 27-28.

7. Brierley, J. B, Brown, A. W., and Meldrum. B. S. (1971). The nature and time course of the neuronal alterations resulting from oligaemia and hypoglycaemia in the brain of *Macaca mulatta*. *Brain Research* **25:** 483-499.

8. Brierley, J. B, Meldrum, B. S., and Brown, A. W. (1973). The threshold and neuropathology of cerebral "anoxic-ischemic" cell change. *Archives of Neurology* **29:** 367-374.

9. Brown, A. W. (1977). Structural abnormalities in neurones. *Journal of Clinical Pathology* **30, Supplement:** 155-169.

10. Brown, A. W. and Brierley, J. B. (1968). The nature, distribution and earliest stages of anoxic-ischaemic nerve cell damage in the rat brain as defined by the optical microscope. *The British Journal of Experimental Pathology* **49:** 87-106.

11. Brumpt, E. (1919). Transmission de la piroplasmose canine francaise par le *Dermacentor reticulatus*. Embolies parasitaires dans les capillaires del'encephale. *Bulletin de la Societe de Pathologique Exotique* **12:** 651-664.

12. Clark, I. A., Hunt, N. H., and Cowden, W. B. (1986). Oxygen derived free radicals in the pathogenesis of parasitic disease. *Advances in Parasitology* **25:** 1-30.

13. Colly, L. P. and Nesbit, J. W. (1992). Fatal acute babesiosis in a juvenile wild dog (*Lycaon pictus*). *Journal of the South African Veterinary Association* **63:** 36-38.

14. Commins, M. A., Goodger, B. V., Waltisbuhl, D. J., and Wright, I. G. (1988). *Babesia bovis*: studies of parameters influencing microvascular stasis of infected erythrocytes. *Research in Veterinary Science* **44:** 226-228.

15. Cooke, B. M., Berendt, A. R., Craig, A. G., and MacGregor, J. (1994). Rolling and stationary cytoadhesion of red blood cells parasitised by *Plasmodium falciparum*: separate roles for ICAM-1, CD36 and thrombospondin. *British Journal of Haematology* **87:** 162-170.

16. Cuillé, M. J. and Darraspen, E. (1927). Formes atypiques et formes chroniques de la piroplasmose du chien. *Revue Generale de Medicine Veterinaire* **36:** 433-443.

17. Dale, J., Ohlsson, K., Nordstoga, K., and Aasen, A. O. (1980). Intravascular hemolysis and ultrastructural changes of erythrocytes in lethal canine endotoxin shock. *European Surgical Research* **12:** 39-51.

18. Dürck, H. (1917). Über die bei Malaria perniciosa comatosa auftretenden Veränderungen des Zentralnervensystems. *Archiv für Schiffs- und Tropen-Hygiene* **21:** 117-132.

19. Farber, J. L., Kyle, M. E., and Coleman, J. B. (1990). Mechanisms of cell injury by activated oxygen species. *Laboratory Investigation* **62:** 670-679.

20. Fridovich, I. (1983). Superoxide radical: An endogenous toxicant. *Annual Review of Pharmacology and Toxicology* **23:** 239-257.

21. Garcia, J. H. and Anderson, M. L. (1991) Circulatory disorders and their effects on the brain. in: *Textbook of Neuropathology*, 2. ed., Davis, R. L and Robertson, D. M. (eds.). Williams and Wilkins. Baltimore. p: 621-718.

22. Garcia, J. H., Kamijyo, Y., Kalimo, H., Tanaka, J., Viloria, J. E., and Trump, B. F. (1975). Cerebral ischaemia: The early structural changes and correlation of these with known metabolic and dynamic abnormalities. Whisnant, J. P. (eds.). p: 313-323.

23. Graham, D. I. (1992) Hypoxia and vascular disorders. in: *Greenfield's Neuropathology*, 5. ed., Adams, J. H. and Duchen, L. W. (eds.). Edward Arnold. London. p: 153-268.

24. Griffiths, J. A. (1922). Studies on animal diseases in south-central Africa. 1. A review of the clinical aspects of canine piroplasmosis. Royal College of Veterinary Surgeons. Fellowship of the Royal College (Dissertation, unpublished). 4-22.

25. Gutierrez, Y., Aikawa, M., Fremount, H. N., and Sterling, C. R. (1976). Experimental infection of *Aotus* monkeys with *Plasmodium falciparum*. Light and electron microscopic changes. *Annals of Tropical Medicine and Parasitology* **70:** 25-44.

26. Hariri, R. J. (1994). Cerebral Oedema. *Neurosurgery Clinics of North America* **5:** 687-706.

27. Heeringa, P., Foucher, P., Klok, P. A., Huitema, M. G., Tervaert, J. C., Weening, J. J., and Kallenberg, C. G. M. (1997). Systemic injection of products of activated neutrophils and H_2O_2 in myeloperoxidase-immunized rats leads to necrotizing vasculitis in the lungs and gut. *American Journal of Pathology* **151:** 131-140.

28. Hemmer, R. M., Wozniak, E. J., Lowenstine, L. J., Plopper, C. G., Wong, V., and Conrad, P. A. (1999). Endothelial cell changes are associated with pulmonary edema and respiratory distress in mice infected with the WA1 human *Babesia* parasite. *Journal of Parasitology* **85:** 479-489.

29. Hicks, S. P. (1968) Vascular pathophysiology in acute and chronic oxygen deprivation. in: *Pathology of the Nervous System*, Minckler, J. (eds.). McGraw-Hill. New York. p: 341-350.

30. Hildebrandt, P. K. (1981) The organ and vascular pathology of babesiosis. in: *Babesiosis*, Ristic, M. and Kreier, J. P. (eds.). Academic Press. London. p: 459-473.

31. Hoff, E. J. and Vandevelde, M. (1981). Case Report: Necrotizing vasculitis in the central nervous system of two dogs. *Veterinary Pathology* **18:** 219-223.

32. Ibiwoye, M. O., Howard, C. V., Sibbons, P., Hasan, M., and van Velzen, D. (1993). Cerebral malaria in the rhesus monkey (*Macaca mulatta*): Observations on host pathology. *Journal of Comparative Pathology* **108:** 303-310.

33. Ikeda, Y. and Long, D. M. (1990). The molecular basis of brain injury and brain oedema: the role of oxygen free radicals. *Neurosurgery* **27:** 1-11.

34. Irwin, P. J. and Hutchinson, G. W. (1991). Clinical and pathological findings of *Babesia* infection in dogs. *Australian Veterniary Journal* **68:** 204-209.

35. Ito, U., Ohno, K., Nakamura, R., Suganuma, F., and Inaba, Y. (1979). Brain edema during ischemia and after restoration of blood flow. Measurement of water, sodium, potassium content and plasma protein permeability. *Stroke* **10:** 542-547.

36. Jacobson, L. S. and Clark, I. A. (1994). The pathophysiology of canine babesiosis: new approaches to an old puzzle. *Journal of the South African Veterinary Association* **65:** 134-145.

37. Jacobson, L. S., Lobetti, R. and Vaughan-Scott, T. (2000). Blood pressure changes in dogs with babesiosis. *Journal of the South African Veterinary Association* **71**: 14-20.

38. Janzer, R. C. (1993). The blood-brain barrier: cellular basis. *Journal of Inherited Metabolic Diseases* **16:** 639-647.

39. Jardine, J. E. (1996). Personal communication. Department of Pathology, Facutly of Veterinary Science, University of Pretoria.

40. Jenkins, L. W. (1979). Complete cerebral ischaemia. An ultrastructural study. *Acta Neuropathologica* **48:** 113.

41. Jones, T. H., Morawetz, R. B., Crowell, R. M., Marcoux, F. W., FitzGibbon, S. J., DeGirolami, U., and Ojemann, R. G. (1981). Thresholds of focal cerebral ischemia in awake monkeys. *Journal of Neurosurgery* **54:** 773-782.

42. Jubb, K. V. F. and Huxtable, C. R. (1993) The nervous system. in: *Pathology of Domestic Animals*, 4. ed., vol:1. Jubb, K. V. F., Kennedy, P. C., and Palmer, N. (eds.). Academic Press Inc. New York. p: 336.

43. Jubb, K. V. F. and Huxtable, C. R. (1993) The nervous system. in: *Pathology of Domestic Animals*, 4. ed., vol:1. Jubb, K. V. F., Kennedy, P. C., and Palmer, N. (eds.). Academic Press Inc. New York. p: 305-306.

44. Kamijyo, Y., Garcia, J. H., and Cooper, J. (1977). Temporary regional cerebral ischemia in the cat. A model of haemorrhagic and subcortical infarction. *Journal of Neuropathology and Experimental Neurology* **36:** 338-350.

45. Knuth, P. and du Toit, P. J. (1921) Tropen-krankheiten der Haustiere. in: *Handbuch der Tropenkrankheiten*, 2. ed., Mense, C. (eds.). Johann Ambrosius Barth. Leipzig. p: 411-421.

46. Koshu, K., Seki, H., Yoshimoto, T., and Suzuki, J. (1981). Experimental hemorrhagic thalamic infarction in the dog. *Surgical Neurology* **16:** 274-279.

47. Kreier, J. P. (1980) Preface. in: *Malaria*, 1. ed., vol:2. Kreier, J. P. (eds.). Academic Press. New York. p: xii.

48. Landis, D. M. D. (1994). The early reactions of non-neuronal cells to brain injury. *Annual Review of Neuroscience* **17:** 133-151.

49. Laureno, R., Shields, R. W., and Narayan, T. (1987). The diagnosis and management of cerebral embolism and haemorrhagic infarction with sequential computerized cranial tomography. *Brain* **110:** 93-105.

50. Leisewitz, A. L., Guthrie, A. J., and Berry, W. L. (1996). Evaluation of the effect of whole-blood transfusion on the oxygen status and acid-base balance of *Babesia canis* infected dogs using the oxygen status algorithm. *Journal of the South African Veterinary Association* **67:** 20-26.

51. Lewis, B. D., Penzhorn, B. L., Lopez-Rebollar, L. M., and De Waal, D. T. (1996). Isolation of a South African vector-specific strain of *Babesia canis*. *Veterinary Parasitology* **63:** 9-16.

52. Lobetti, R. G. (1994). The comparative role of haemoglobinaemia and hypoxia in the development of nephropathy in the dog. University of Pretoria. MMedVet(Med).

53. Macpherson, G. G., Warrell, M. J., White, N. J., Looareesuwan, S., and Warrell, D. A. (1985). Human Cerebral Malaria. *American Journal of Pathology* **119:** 385-401.

54. Maegraith, B., Gilles, H. M., and Devakul, K. (1957). Pathological process in *Babesia canis* infections. *Zeitschrift für Tropenmedizin und Parasitologie* **8:** 485-514.

55. Malherbe, W. D. (1956). The manifestations and diagnosis of *Babesia* infections. *Annals of the New York Academy of* **64:** 128-146.

56. Malherbe, W. D. and Parkin, B. S. (1951). Atypical symptomatology in *Babesia canis* infection. *Journal of the South African Veterinary Medical Association* **22:** 25-36.

57. McCord, J. M. (1985). Oxygen-derived free radicals in postischemic tissue injury. *The New England Journal of Medicine* **312:** 159-163.

58. Miller, J. D. and Adams, J. H. (1992) The pathophysiology of raised intracranial pressure. in: *Greenfield's Neuropathology*, 5. ed., Adams, J. H. and Duchen, L. W. (eds.). Edward Arnold. London. p. 69-105.

59. Montgomery, D. L. (1994). Astrocytes: form, functions, and roles in disease. *Veterinary Pathology* **31:** 145-167.

60. Moore, D. J. and Williams, M. C. (1979). Disseminated intravascular coagulation: a complication of *Babesia canis* infection in the dog. *Journal of the South African Veterinary Association* **50:** 265-275.

61. Naudé, T. W., Basson, P. A., and Pienaar, J. G. (1970). Experimental diamidine poisoning due to commonly used babesiacides. *Onderstepoort Journal of Veterinary Research* **37:** 173-184.

62. O'Connor, R. M., Lane, T. J., Stroup, S. E., and Allred, D. R. (1997). Characterization of a variant erythrocyte surface antigen (VESA1) expressed by *Babesia bovis* during antigenic variation. *Molecular and Biochemical Parasitology* **89:** 259-270.

63. Okoh, A. E. (1978). A case of cerebral babesiosis in the dog. *Bulletin of Animal Health and Production in Africa* **26:** 118-119.

64. Oo, M. M., Aikawa, M., Thjan, T., Aye, T. M., Myint, P. T., Igarashi, I., and Schoene, W. C. (1987). Human cerebral malaria: a pathological study. *Journal of Neuropathology and Experimental Neurology* **46:** 223-231.

65. Piercy, S. E. (1947). Hyper-acute canine babesia. *Veterinary Record* **59:** 612-613.

66. Purchase, H. S. (1947). Cerebral babesiosis in dogs. *Veterinary Record* **59:** 269-270.

67. Purnell, R. E. (1981) Babesiosis in various hosts. in: *Babesiosis*, Ristic, M. and Kreier, J. P. (eds.). Academic Press. New York. p: 45-48.

68. Reuße, U. (1954). Zur klinik und patologie der hunde-babesiose. *Zeitschrift für Tropenmedizin und Parasitologie* **5:** 451-469.

69. Reyers, F., Leisewitz, A. L., Lobetti, R. G., Milner, R. J., Jacobson, L. S., and van Zyl, M. (1998). Canine babesiosis in South Africa: more than one disease. Does this serve as a model for falciparum malaria? *Annals of Tropical Medicine and Parasitology* **92:** 503-511.

70. Rowe, J. A., Moulds, J. M., Newbold, C. I., and Miller, L. H. (1997). *P. falciparum* rosetting mediated by a parasite-variant erythrocyte membrane protein and complement-receptor 1. *Nature* **388:** 292-295.

71. Schetters, T. P. M., Kleuskens, J., Scholtes, N., and Bos, H. J. (1995). Strain variation limits protective activity of vaccines based on soluble *Babesia canis* antigens. *Parasite Immunology* **17:** 215-218.

72. Schetters, T. P. M., Kleuskens, J., Scholtes, N., and Gorenflot, A. (1998). Parasite localization and dissemination in the *Babesia*-infected host. *Annals of Tropical Medicine and Parasitology* **92:** 513-519.

73. Schetters, T. P. M., Kleuskens, J., Scholtes, N., Pasman, J. W., and Bos, H. J. (1993). Vaccination of dogs against *Babesia canis* infection using antigens from culture supernatants with emphasis on clinical babesiosis. *Veterinary Parasitology* **52:** 219-233.

74. Smith, J. D., Chitnis, C. E., Craig, A. G., Roberts, D. J., Hudson-Taylor, D. E., Peterson, D. S., Pinches, R., Newbold, C. I., and Miller, L. H. (1995). Switches in expression of *Plasmodium falciparum* **var** genes correlate with changes in antigenic and cytoadherent phenotypes of infected erythrocytes. *Cell* **82:** 101-110.

75. Stewart, P. A., Hayakawa, K., Farrell, C. L., and DelMaestro, R. F. (1987). Quantitative study in microvessel ultrastructure in human peritumoral brain tissue. *Journal of Neurosurgery* **67:** 697-705.

76. Suzuki, J., Yoshimoto, T., Tnanka, S., and Sakamoto, T. (1980). Production of various models of cerebral infarction in the dog by means of occlusion of intracranial trunk arteries. *Stroke* **11:** 337-341.

77. Udomsangpetch, R., Taylor, B. J., Looareesuwan, S., White, N. J., Elliot, J. F., and Ho, M. (1996). Receptor specificity of clinical *Plasmodium falciparum* isolates: Nonadherence to cell-bound E-selectin and vascular cell adhesion molecule-1. *Blood* **88:** 2754-2760.

78. Uilenberg, G., Franssen, F. F. J., Perie, N. M., and Spanjer, A. A. M. (1989). Three groups of *Babesia canis* distinguished and a proposal for nomenclature. *Veterinary Quarterly* **11:** 33-40.

79. Valli, V. E. O. (1993) The Haemopoietic System. in: *Pathology of Domestic Animals*, 4. ed., vol:3. Jubb, K. V. F., Kennedy, P. C., and Palmer, N. (eds.). Academic Press Inc. New York. p: 190.

80. van der Lugt, J. J. and Jardine, J. E. (1994). Cerebral Lesions. Hoechst canine babesiosis symposium. *Proceedings of the XIXth World Congress of the World Small Animal Veterinary Association* . Verstraete, F. J. M. (eds.). p: 758.

81. Weiss, H. J. (1995). Flow-related platelet deposition on subendothelium. *Thrombosis and Haemostasis* **74:** 117-122.

82. Westergaard, E., Go, G, Klatzo, I., and Spatz, M. (1976). Increased permeability of cerebral vessels to horseradish peroxidase induced by ischemia in Mongolian gerbils. *Acta Neuropathologica* **35:** 307-325.

83. Wozniak, E. J., Lowenstine, L. J., Hemmer, R., Robinson, T., and Conrad, P. A. (1996). Comparative pathogenesis of human WA1 and *Babesia microti* isolates in a syrian hamster model. *Laboratory Animal Science* **46:** 507-515.

84. Wright, I. G. (1972). An electron microscopic study of intravascular agglutination in the cerebral cortex due to *Babesia argentina* infection. *International Journal for Parasitology* **2:** 209-215.

85. Yoshimoto, T., Sakamoto, T., and Suzuki, J. (1978). Experimental cerebral infarction Part I: Production of thalamic infarction in dogs. *Stroke* **9:** 211-214.

86. Yu, W. A., Yu, M. C., and Young, P. A. (1974). Ultrastructural changes in the cerebrovascular endothelium induced by a diet high in linoleic acid and deficient in vitamin E. *Experimental and Molecular Pathology* **21:** 289-299.

APPENDIX A

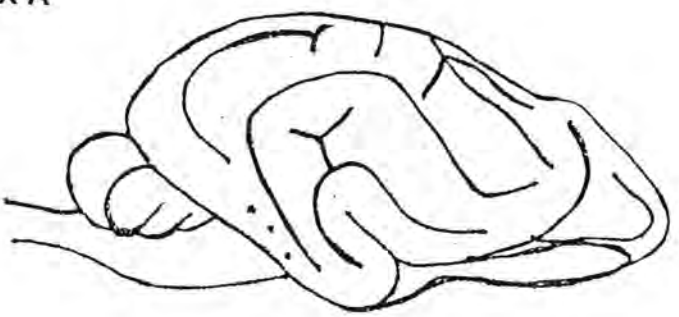

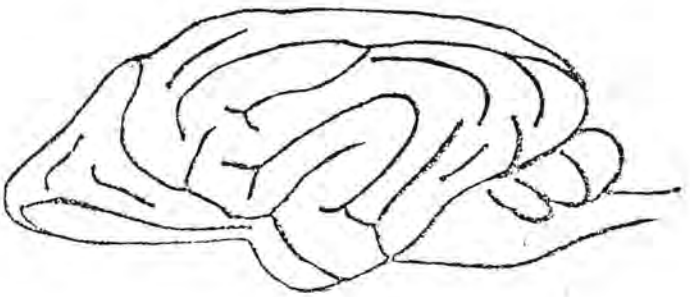

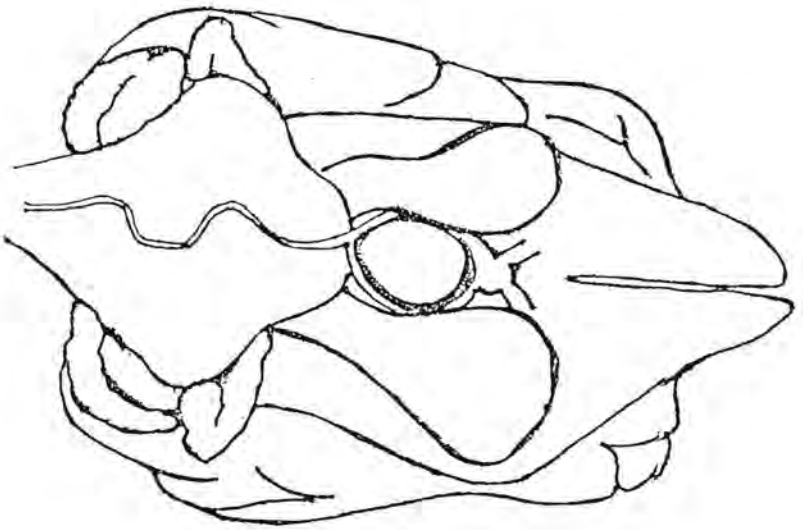

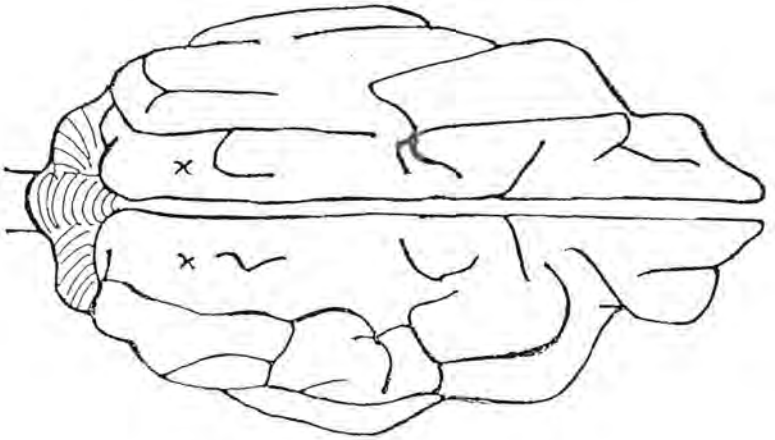

APPENDIX B

Haematoxylin – Eosin Staining technique

Solutions

1.	Haematoxylin (Lillie-Mayer)	10 liters
	Distilled water	7000 ml
	Haematoxylin (Merck)	50 gm
	Ammonium Alum	500 gm
	Glycerol	3000 ml
	Acetic Acid (Glacial)	200 ml
	Sodium Iodate ($NaIO_3$)	5 gm

Heat the water to approximately 40° C, then add and dissolve each ingredient in the sequence as given above. The stain will be ready for use in 18-24 hrs.

2. Acid-Alcohol

   10ml HCl (concentrated) in 1000 ml 70% alcohol

3. Eosin

Distilled water	1400 ml
96% alcohol	3600 ml
Eosin (Merck)	25 gm
When dissolved, add Glacial Acetic Acid	25 ml

Method

Formalin fixed – paraffin sections – 4 micron

1.	Deparaffinate & hydrate	
2.	Stain in Haematoxylin (Solution 1)	8-10 mins.
3.	Rinse in tap water	
4.	Differentiate in solution 2	10-15 secs.
5.	Blue in running tap water	10 mins
6.	70% alcohol	rinse
7.	Eosin (solution 3)	2.25-2.5 mins.
8.	96% alcohol	1.5 mins.
9.	Absolute alcohol	3 mins.

10. Xylol
11. Mount in Pernount

Results

Nuclei – blue

Cytoplasm – pink

Giemsa for sections

Solutions

1. Giemsa stain

   80 ml H_2O + 10 ml acetone. Add this to 10 ml Giemsa solution.

2. Differentiating solution

   1-2 ml of a saturated solution of Collophonium resin in acetone per 100 ml 96% alcohol.

Method

1. Deparaffinize and hydrate
2. Stain in solution 1 for 3-4 hours at 37°C
3. Without decanting, wah off stain with running tap water. Leave sections here. *From this point onwards, sections are handled singly.*
4. Rinse in H_2O.
5. Rinse in 96% alcohol for 1 minute.
6. Differentiation: Set up 3 coplin jars with solution 2. Transfer sections from step 5 to the first of these where most of the stain is washed out. Transfer to second jar for further differentiation and then to the third jar. In this way, final differentiation is done in a clear solution. Differentiate until section background is a light pink.
7. 100% alcohol for 1-2 mins.
8. Xylol and mount with Permount.

Results

Nuclei – blue

Cytoplasm – pink

APPENDIX C

FULL GROSS PATHOLOGY RESULTS TABLE

Abbreviations

ID no: identification number

Macro: gross pathology classification

- s/a: subacute
- GIT: gastro-intestinal form
- Haemoconc. Haemoconcentration form
- s/clinical: subclinical
- MOF: multiple organ failure

Histo: histopathology classification

- n/c: not cerebral
- C: cerebral

Clinical signs:

- ARDS: acute respiratory distress syndrome
- ARF: acute renal failure
- IMHA: immune-mediated haemolytic anaemia
- SIRS: systemic inflammatory response syndrome
- MODS: multiple organ dysfunction syndrome
- HBC: hit by car

Neuro signs: clinical neurological signs.

Rx: antibabesial therapy

- U: untreated
- T: Trypan Blue
- B: diminazene aceturate
- F: imidocarb

Ht: haematocrit

Par: parasitaemia

- Y - present
- N - absent

E/D:

- E: euthanasia
- D: died

ISA: in-saline agglutination

- P: positive
- N: negative

Tfn: blood transfusion

- Y: yes
- N: no

Breed

- Staffie: Staffordshire bull terrier
- Dob/Pin: doberman pinscher
- MinPin: miniature pinscher
- Boston Ter: Boston terrier
- GSD: German shepherd dog

Age:

- W: weeks
- M: months
- Y: years
- A: adult

Sex:

- F: female
- M: male

Included:

- M: gross pathology study
- H: histopathology study
- S: sequestration study

Final classification:

- N/C: not cerebral
- C: cerebral
- comp: other complications of babesiosis concurrently present

ID no	PM No	Macro	S No	Histo	F No	History	Neuro signs	Rx	Ht	Par	SI	E/D	ISA	Tfn	Breed	Age	Sex	Owner	Included	Final classification
1	598.96	s/a	1692.96	0	P	found dead	unknown	U	0	Y	0	D	0	0	Staffie	0	F	Q Withfield	M	N/C
2	619.96	pallor,s/a	742.96	n/c	P	0	0	U	0	Y	0	0	0	0	Dob/Pin	1Y	F	van der Wahl	M,H	N/C
3	646.96	s/a	1800.96	0	58962	s/a	0	T	16	0	0	D	0	0	Staffie	4Y	F	P S Roos	M	N/C
4	736.96	s/a	1994.96	0	0	s/a	0	0	0	0	0	D	0	0	Staffie	A	F	de Jager	M	N/C
5	754.96	s/a	0	0	0	s/a	0	U	28	0	0	D	0	0	Maltese	3Y	M	0	M	N/C
6	838.96	GIT	2242.96	0	5946	GIT	0	T	12	0	0	0	0	Y	Maltese	7M	M	W A Richards	M	N/C comp
7	886.96	haemo-c.	2477.96	0	59575	haemo-c	0	T	60	0	0	D	0	0	MinPin	1Y	F	T J van Wyk	M	N/C comp
8	915.96	s/clinical	2568.96	0	58947	HBC	No	U	0	Y	0	0	0	0	Maltese	5Y	M	W J Bergh	M	N/C
9	947.96	oedema	2641.96	0	0	s/a	0	U	0	Y	0	E	0	0	Fox Terrier	1Y	F	Vermaak	M	N/C comp
10	985.96	pulmonary	2788.96	0	51372	s/a ARDS	0	U	0	0	0	D	0	0	Pekingese	A	M	M J Eybers	M	N/C comp
11	996.96	pallor	2849.96	0	58640	s/a	0	U	11	Y	0	E	0	0	Fox Terrier	3Y	M	M L van Biljon	M	N/C
12	1038.96	pulmonary	2953.96	n/c	0	ARDS	No	B	52	Y	0	D	0	0	Boston Ter	2Y	M	Papenfus	M	N/C comp
13	1069.96	pulmonary	3016.96	0	60106	ARDS	No	T	16	Y	0	D	N	Y	Chihuahua	0	M	J H Liebenberg	M	N/C comp
14	1144.96	s/a pulmonary	3224.96	0	0	s/a	No	T	18	Y	0	D	0	0	Chihuahua	7Y	M	Wallace	M	N/C comp
15	1146.96	MOF	3226.96	n/c	P	s/a and IMHA	No	T	28	Y	0	D	P	0	GSD	0	F	De Gough	M,H	N/C comp
16	1165.96	s/a	3285.96	n/c	49962	IMHA	No	B	27	Y	0	D	P	0	Roltweiler	5Y	M	H Breedt	M	N/C
17	1221.96	s/a pulmonary oedema	3282.96	0	P	found dead	unknown	U	0	Y	0	D	0	0	Staffie	3Y	F	M Bester	M	N/C comp

ID no	PM No	Macro	S No	His to	F No	History	Neuro signs	R x	Ht	Par	SI	E/D	ISA	Trn	Breed	Age	Sex	Owner	Included	Final classification
18	1239.96	subacute; pulmonary	3407.96	0	60584	myocardial	No	T	15	N	0	D	0	Y	Dachshund	4Y	M	M Janse van Rensburg	M	N/C comp
19	1260.96	s/a	3482.96	0	60667 O/P	s/a	No	U	0	Y	0	E	0	0	Toy Pom	17Y	F	J P Fourie	M	N/C
20	87.97	s/a	184.97	n/c	61115	subacute	No	B	34	Y	0	0	0	Y	Boer bull	3W	M	Stoltz	M,H	N/C
21	154.97	s/a	0	0	O/P	collapse, ARDS	No	U	0	Y	0	D	0	0	Cocker Spaniel	9M	M	E Bronkhorst	M	N/C comp
22	182.97	acute; pulmonary	511.97	0	53607	haemo-c., collapse	N	T	55	Y	0	0	0	0	Dachshund	1Y	F	D van Staden	M	N/C comp
23	283.97	pulmonary	1959.97	n/c	0	ARDS	No	U	5	Y	0	E	0	0	Fox Terrier	1Y	F	G W Heck	M,H	N/C comp
24	405.97	MOF	1215.97	n/c	62025	SIRS;MODS;DIC	No	B	11	Y	0	0	N	Y	Boerbull	1Y	F	P du Toit	M,H	N/C comp
25	536.97	pulmonary	1618.97	n/c	59565	ARDS	No	F	8	Y	0	0	0	0	Rottweiler	A	M	H Crafford	M,H	N/C comp
26	541.97	subacute	1635.97	n/c	48688	IMHA	No	B	9	Y	0	0	P	0	Bull Terrier	8Y	M	G Collyer	M,H	N/C comp
27	847.97	pulmonary	2427.97	0	63217	MODS	No	0	0	Y	0	E	0	0	Boxer	1Y	F	Jacobs	M	N/C comp
28	890.97	s/a	2517.97	0	P	s/a	No	F	0	Y	0	D	0	0	GSD	6W	M	Delport	M	N/C
29	913.97	s/a	2573.97	0	63457	s/a	No	U	13	Y	0	0	N	0	GSD	4M	M	J J Venter	M	N/C
30	1086.97	pulmonary	3052.97	0	40334	ARDS	No	B	10	Y	0	0	0	Y	Staffie	5Y	M	RMJ Britz	M	N/C comp
31	687.97	haemo-c.	2535.97	n/c	62765	haemo-c.	No	0	0	Y	0	0	0	0	Rottweiler	3Y	M	J A Jordaan	M,H	N/C comp
32	538.98	s/a	1391.98	0	P1307 85 Medunsa	ARDS	No	T	10	Y	0.83	0	0	0	Crossbred	0	F	Lebeloane	M,S	N/C comp
33	OPT II	subacute	672.98	n/c	0	s/a	Unknown	U	9	Y	0.96	0	0	0	0	0	0	0	M,H,S	N/C
34	OPT III	cardiac	1344.98	0	P	s/a	No	U	0	Y	0.76	0	0	0	Chow chow	3M	M	0	M,S	N/C comp
35	668.96	s/a; cerebellar prolapse	0	0	59016		No	T		Y	0				Maltese x Collie	10 W	M	Beyleveldt	0	cerebral
36	842.96	muscle		0	0	0	yes	U	12	Y	0	0	0	0	Boer bull	8M	F	0	M	cerebral comp.
37	857.96	cerebral	201.98	C	0	haemo-c.	yes	T	46	Y	0	D	0	0	Labrador	4M	M	J H Murray	M,H	cerebral comp.
38	1074.96	mild congestion	3024.96	C	60120	ARDS	No	U	0	Y	0	E	0	0	Staffie	6Y	F	W S Humphries	M	cerebral
39	1130.96	Cerebral	3157.96	C	O/P	haemo-c.	none noted	T	61	Y	0	0	0	0	Labrador, crossbred	5Y	M	H J Sleyn	M,H	cerebral
40	1148.96	Cerebral oedema and pallor. Subacute, pulmonary	3228.96	C	60336	weakness	Yes, not specified	U	6	Y	0	D	N	0	Labrador	2M	F		M,H	cerebral comp.
41	1163.96	s/a; cerebral oedema and pallor	3264.96	0	P	0	0	U	0	Y	0	D	0	0	Rottweiler	A	M	Fitzpatrick	M	cerebral

ID no	PM No	Macro	S No	Histo	F No	History	Neuro signs	Rx	Ht	Par	SI	E/D	ISA	Tfn	Breed	Age	Sex	Owner	Included	Final classification
42	7.97	cerebral and muscle	4.97	C	80629	collapse	No	T	0	Y	0	0	0	0	GSD	2M	F	J Heyns	M,H	cerebral comp.
43	178.97	cerebral and haemo-c.entrated	460.97	0	61385	MODS	Yes: seizures	B	40	Y	0	D	0	0	Chow chow	2Y	F	L Barkhuizen	M	cerbral comp.
44	205.97	pulmonary	551.97	0	O/P	acute cerebral	Yes: seizures	U	0	Y	0	E	0	0	Fox terrier	1Y	M	Vermaak	M,H	cerebral comp.
45	231.97	GIT	598.97	C	61514	GIT	semi-coma	T	24	Y	skin	D	N	Y	Husky	6M	F	van Bosch	M,H	cerebral comp.
46	237.97	cerebral and pulmonary	975.97	C	37680	depression	Yes: depression and disorientation	F	28	Y	0	D	0	0	Cocker Spaniel	3M	M	Swanepoel	M,H	cerebral comp.
47	268.97	subacute with cerebral pallor and generalised oedema	1391.97	C	O/P	subacute cerebral	Yes: opisthotonus and extensor rigidity	U	8	Y	0	0	0	0	GSD	4M	M	B du Preez	M,H	cerebral comp.
48	284.97	acute	1960.97	C	57775	cerebral	Yes: coma	B	31	Y	0	E	0	0	Chihuahua	3Y	F	F Els	M,H	cerebral
49	314.97	cerebral and pulmonary	923.97	C	61737	MODS ; cerebral and pulmonary	Yes: coma	U	0	Y	0	D	0	0	Crossbred	1Y	M	N Roelofse	M,H	cerebral comp.
50	338.97	cerebral and spinal compression fracture	965.97	C	61662	Haemo-c.. Spinal fracture and history of babesiosis that was treated. Berenil given.	Yes: Opisthotonus, vertical nystagmus and generalised seizures	B	51	N	0	D	0	0	Borzoi	7Y	M	B C Stoop	M,H	cerebral .comp.
51	466.97	Cerebral and pulmonary	1430.97	n/c	60988	IMHA	No	F	16	Y	0	D	P	Y	Bull Terrier	9M	M	H L Terblanche	M,H	cerebral comp.
52	682.97	Congestive brain swelling and thalamic petechiae. Haemo-c..	0	0	58197	ARDS ,ARF, anuria, IMHA	No	B	50	Y	0	D	P	N	Bulldog	2Y	M	MC Jacobs	M	cerebral
53	918.97	cerebral and pulmonary	2575.97	C	O/P	subacute bab	Yes: coma	B	10	Y	0.99	D	0	0	Border collie	5W	F	Pearson	M,H,S	cerebral comp.
54	983.97	cerebral and myocardial	2709.97	n/c	658	babesiosis	Yes: head pressing	B	37	Y	0	E	0	0	Bull Terrier	3Y	M	I G van Aswegen	M,H	cerebral comp.
55	1046.97	cerebral and haemo-c.	2868.97	C	63844	peracute with haemo-c.	No: none recorded	B	55	Y	0.69	0	0	0	Chow chow	A	M	P Moltasi	M,H,S	cerebral comp.
56	1085.97	cerebral and haemo-c.	3051.97	C	57182	MODS with haemo-c.	No, none recorded	B	44	Y	0.93	E	0	0	Bull Terrier	8Y	F	L Kruger	M,H,S	cerebral comp.
57	1.98	cerebral and haemo-c.	4.98	C	50986	acute	None noted	U	60	Y	0	D	N	N	Cocker spaniel	10Y	M	T J Potgieter	M,H	cerebral comp.
58	13.98	cerebral. Disseminated petechiation	24.98	C	58590	acute babesiosis - suspected cerebral babesiosis terminally.	Suspected cerebral babesiosis terminally, but no neurological signs specified.	B	35	Y	0.87	E	0	0	Boxer	6M	M	JS Prinsloo	M,H,S	cerebral
59	50.98	cerebral	150.98	C	58513	acute, cerebral signs, ARDS	opisthotonus progressing to coma	B	45	Y	0.93	D	N	0	Boxer	9M	F	F de Kock	M,H,S	cerebral comp

Id no	PM No	Macro	S No	Hist o	F No	History	Neuro signs	Rx	Ht	Par	SI	E/D	ISA	Tfn	Breed	Age	Sex	Owner	Included	Final classification
60	70.98	GIT with cerebral pallor	152.98	n/c	746	MODS	coma	B	25	Y	0.99	0	0	0	Bull terrier	4Y	F	CR Fourie	M,H,S	cerebral comp.
61	105.98	GIT with cerebral oedema	307.98	n/c	54445	ARDS and cerebral signs	opisthotonus, collapse and trembling	B	21	Y	-4	D	N	Y	Boerbull	4Y	F	MM Botha	M,H,S	cerebral comp,
62	106.98	s/a	305.98	C	P	found dead	Unknown	U	0	Y	0.96	D	0	0	Rottweiler	6M	F	G Strauss	M,H,S	cerebral
63	113.98	cerebral with haemo-c.	331.98	C	64395	haemo-c. and ARDS	not noted	B	60	Y	0.97	E	0	N	Bulldog	3Y	M	M Weber	M,H,S	cerebral comp.
64	OPT. I	cerebral	274.98	C	0	subacute babesiosis	unknown	0	0	Y	0	0	0	0	0	0	0	0	M,H,S	cerbral subac.
65	119.98	cerebral and myocardial	348.98	C	49397	cerebral	seizures	B	0	Y	-15	D	0	0	Pug	1Y	M	J van Rensburg	M,H,S	cerebral comp.
66	148.98	cerebral and muscle	426.98	C	64495	MODS: haemo-c. and ARF	apparent blindness	B	58	Y	0.83	D	0	N	Chow chow	2Y	F	Adlam	M,H,S	cerebral comp.
67	186.98	cerebral and pulmonary	815.98	C	P	none	unknown	U	0	Y	0	D	0	N	Staffie crossbred	0	0	van Rooyen	M,H	cerebral comp.
68	311.98	cerebral and muscle; acute babesiosis	675.98	C	O/P	haemo-c	no neurological signs noted	U	0	Y	0.15	0	0	0	Pug	1Y	F	W A Engelbrecht	M,H,S	comp. cerebral
69	325.98	acute cerebral and muscle	925.98	C	0	MODS: renal and GIT	None noted	T	0	Y	0	0	0	0	crossbred	8M	F	Boucher	M,H	comp. cerebral
70	384.98	haemo-c. with cerebral lesions	1094.98	C	0	peracute	ataxia, blindness and head pressing	B	37	N	0	D	0	0	Staffie	4Y	M	Kitching	M,H	comp. cerebral
71	397.98	acute cerebral babesiosis with cerebral oedema and cerebral flush; haemo-c. form	1112.98	C	102650	cerebral babesiosis	seizures	B	58	Y	1	D	0	N	Bull Mastiff	1Y	F	D C Spooner	M,H,S	acute cerebral
72	450.98	pulmonary	1207.98	pre-cerebral	O/P	acute	No	B	0	Y	0.45	0	0	0	Maltese	11M	F	van Staden	M,H,S	cerebral comp,
73	452.98	cerebral and haemo-c.	1214.98	0	0	suspected poisoning: in retrospect this was peracute babesiosis	seizures	U	0	Y	0.84	D	0	0	Boerbull	A	F	I H Willemse	M,S	cerebral comp.
74	473.98	cerebral and pulmonary; severe cerebral oedema pressure on the cerebellum	1268.98	C	103281	Bite wounds on head	collapse and coma	B	27	Y	0	0	0	0	Ridgeback	4M	M	JA Rademeyer	M,H,S	cerebral comp.
75	475.98	oedema form with pulmonary lesions. No macroscopically visible cerebral lesions	1270.98	n/c	103306	cerebral and ARDS	seizures and blindness	B	11	Y	0	0	N	Y	crossbred	2M	M	A Brits	M,H	cerebral comp.
76	564.98	Congestive brain swelling. Cerebral and GIT.	1480.98	0	P	found dead	unknown	U	0	Y	0.85	D	0	N	Staffie	5Y	F	S Sheppard	M,H,S	cerebral comp

APPENDIX C

REGIONAL LESIONS TABLE

Key to Abbreviations:

Lesion Type

G	global lesion
R	regional lesion

Lesion Symmetry

A	asymmetrical lesion
B	bilateral lesion
S	symmetrical lesions
U	unilateral lesion

Treatment

D	diminazene aceturate
I	imidocarb
T	trypan blue
U	untreated
0	treatment status unknown

Macro group

CBS	congestive brain swelling
E	ecchymosis(es)
H	haemorrhage
Hy	hydrocephalus
M	malacia
O	oedema
Pet	petechiae

Cerebral cortex (Site of lesions)

B	bilateral
E	ecchymosis(es)
GC	lesions in gyral crests
H	haemorrhage
LCN	laminar cortical necrosis
M	malacia
Pet	petechiae
SF	lesions in sulcal floors
U	unilateral

Lobe

F	frontal lobe
O	occipital lobe
P	parietal lobe
T	temporal lobe

Olfactory tract

Ped	olfactory peduncle
Tub	olfactory tubercle

Border Zone

r/m rostral-middle cerebral arteries

r/c rostral-caudal cerebral arteries

m/c middle-caudal cerebral arteries

Artery

C	caudal cerebral artery
M	middle cerebral artery
R	rostral cerebral artery
rc	rostral cerebellar artery
cc	caudal cerebellar artery
v	vertebral artery

ID no	PM no.	Lesion type	Lesion symmetry	treatment	Macro group	Site of lesions												
						Cerebral cortex	Lobe	Cerebellum	Caudate nucleus	Colliculus	Tthalamus	Pyriform lobes	Lateral geniculate nucleus	Hypophysis	Medulla oblongata	Olfactory tract	Border Zones	Artery
1	857.96	R	B A	T	M H	SF GC H. infarct frontal lobe malacia	F P T O	Rostral vermis: central culmen	U Caput corpus	caudal						Ped Tub	r/c	R M C rc
2	1130.96	R	B A	T	M H	SF, GC, E frontal lobe LCN, Sub-ventricular M (Occipital lobe) no H	F O		B Caput cauda							Tub		R M
3	1148.96	G		U	Pallor Oedema													
4	7.97	R	B & S	T	M H Oedema Mild Hy	E Pet GC	F P T	Caudal vermis Nodulus uvula	B caput corpus cauda			Pet				Tub	r/m B	M cc

ID no	PM no	Lesion Type	Symmetry	Antibabesial Treatment	Macro group	Site of lesions									
						Cerebral cortex	Lobe	Cerebellum	Caudate nucleus	Colliculus	Tthalamus	Pyriform lobes	Lateral geniculate nucleus	Hypophysis	Medulla oblongata	Olfactory tract	Border Zones	Artery
5	237.97	R	B A rost S caud	I	M H	SF splenial GC Rhinal sulcus	F P T/ O	Nodulus Uvula Ansiform	B Corpus		Pet						R/m	R, M C cc
6	314.97	R	B A	U	M H	SF GC M	F O	Ventral paramedian lobe M		U caudal							r/m	R M C cc
7	466.97	R	B S	I	Pallor M H	spared		E lingula	E cauda	Pet caudal	Pet				Pet			M rc v
8	624.97			0	Normal brain													
9	682.97	G R		D	CBS						Pet							R M C
10	918.97	R	B A	D	M (H)	GC (tectum)	O	Pet lingula	U E cauda	Dorsal rostrals Caudals								C M rc

ID no	PM no	Lesion Type	Symmetry	Antibabesil Treatment	Macro group	Site of lesions									
						Cerebral cortex	Lobe	Cerebellum	Caudate nucleus	Colliculus	Tthalamus	Pyriform lobes	Lateral geniculate nucleus	Hypophysis	Medulla oblongata	Olfactory tract	Border Zones	Artery
11	1046.97	R	B A	D	M H	SF GC	F P O				E			E			r/m r/c	R M C
12	1085.97	R	B S	D	moderate congestion of surface. M, H				B caput	Rostral caudal	Pet		Pet		Pet			M v
13	1.98	R	U	U	M H	SF GC	F	Focal E	B corpus	rostral	Pet		Pet		Pet		cc/rc	R M rc cc v
14	13.98	R	B	D	M H Dissemina ted Pet E	Frontal Ventral SF GC	F P T O	Uvula nodulus (floculono dular lobe)	B Corpus Left cauda	Caudal rostral tectum		≡	Pet			Tub	m/r	R M C cc
15	50 98	R	B A	D	M H Pet,E	SF GC Frontal haematoma	F P O	Nodulus Uvula L paramedi an lobule R central lobule E	B corpus								r/m	R M C cc rc

Site of lesions	Artery		M	M	R	R M C
	Border Zones					r/c r/m
	Olfactory tract					Ped
	Medulla oblongata					
	Hypophysis			Focal E		
	Lateral geniculate nucleus		M			
	Pyriform lobes					
	Tthalamus					
	Colliculus					
	Caudate nucleus			B caput		
	Cerebellum					
	Lobe		P		F	F P T
	Cerebral cortex		SF			GC SF
Macro group		Pallor	Pallor Oedema M	M, H Pallor Oedema Mod. Hy	M H	M H
Antibabesil Treatment		D	D	D	D	D
Symmetry			U	B S		B A
Lesion Type		G	G R	R	R	R
PM no		70.98	105.98	113.98	119.98	148.98
ID no		16	17	18	19	20

Site of Lesion	Artery	M	R M	R M C cc
	Border Zones		r/m r/c	r/c r/m
	Olfactory tract			
	Medulla oblongata			
	Hypophysis			
	Lateral geniculate nucleus			
	Pyriform lobes			
	Tthalamus	U M E	B M	
	Colliculus		B caudal	
	Caudate nucleus	B M H		
	Cerebellum			Pet Caudal lobe Pyramis Uvula
	Lobe	T	F P T	F P
	Cerebral cortex	No superficial lesions SF Focal M	SF GC	SF (GC) E, Pet
Macro group		Pallor M H	M H	M H
Antibabesil Treatment		0	U	T
Symmetry		B A	B A (S)	B A (S)
Lesion Type		R	R	R
PM no		186.98	311.98	325.98
ID no		21	22	23

ID no	PM no	Lesion Type	Symmetry	Antibabesil Treatment	Macro group	Site of Lesion												
						Cerebral cortex	Lobe	Cerebellum	Caudate nucleus	Colliculus	Tthalamus	Pyriform lobes	Lateral geniculate nucleus	Hypophysis	Medulla oblongata	Olfactory tract	Border Zones	Artery
24	384.98	R	B S (A)	D	M H Oedema Mod U Hy	SF (congestion)	P	compress ion	B Caput corpus						Severe compressi on	Tub Ped		M
25	397.98	G R	B S	D	CBS M H Severe oedema Mild Hy	SF & sides GC E & P	F P T O	Severe compress ion Focal E lingua	B Corpus U Caput left	Rostral, right Caudal right E	Pet						r/m r/c m/c	R M C rc
26	473.98	R	B S	D	H M Oedema Mild Hy	Total cortical haemorrhage. GC SF E S	F P T O	Paramedi an lobule (uvula) E	B Caput cauda	U Caudal right	Pet E B					Tub	r/c	R M cc
27	475.98	G		D	Pallor													
28	OPT I	R	B S (A)	0	Pallor M H Mild Hy	No superficial lesions. SF	F P O		B Caput cauda	U Caudal left	M E	B E					r/m	R M

APPENDIX C

Histopathology Results Table

Key:

a-O:	autolysis minimal.	ICC:	ischaemic cell change.	sc:	spinal cord.
A2:	Alzheimer Type 2 astrocytes.	imp:	immunoperoxidase staining.	uvf:	uneven vascular filling.
CBS:	congestive brain swelling.	ivFt:	intravenous fibrin thrombi.	S-a:	severe autolysis.
ens:	endothelial nuclear swelling.	m-a:	mild autolysis.	SNC:	severe neuronal change.
evF:	extravascular fibrin.	M-a:	moderate autolysis.	svn:	segmental vascular necrosis.
fc:	foamy pericytes.	M+A:	margination and adhesion.	VR-space:	Virchow-Robbins space.
H:	haemorrhage.	Mlk:	monocytic leukostasis.		
HE:	ecchymosis	NN:	neuronal necrosis.		
HM:	microvascular haemorrhage.	Og:	oedema of grey matter.		
	HP: petechiae	Os:	oedema of white matter		
HR:	perivascular haemorrhage.	pRBC:	parasitised erythrocytes.		
HC:	homogenising change	RCC:	red cell changes		

1	48.96	Multifocal ens. RCC. Monocytes, plasma cells, lymphocytes. HM. ivFt. uvf. **E. canis**	++	n/c Ex
2	248.96	RCC. Os. Mlk. M+A. M-a. **E. Canis**	++	n/c Ex
3	808.96	RCC. Mlk. Lymphocyts +. M+A. uvf.	+	n/c (histo)
4	1438.96	ens. Microvascular congestion. uvf. Mlk. RCC. Sludge in microvessels. Og. HM. HP. Neutrophil invasion. Focal ischaemia. M-a.	-	C
5	1679.96	Severe congestion. uvf. ens. Mlk Few plasma cells. Lymphocytosis fc. Os. RCC. ivFt. HM. M-a **E. canis.**	-	n/c Ex
6	1682.96	Ens and necrosis svn and vasculitis: cortex and subcortex, caudal colliculus, thalamus, brain stem. evF. HR. HP. HE. Mlk. Severe neutrophilia and neutrophil infiltration. Astrocytosis. Microgliosis. NN. ICC. HC. Og. ivFt.	-	C
7	1767.96	Died on day of treatment. Moderate acute purulent myelitis and septicaemic microabscessation. **Septicaemia.**	-	n/c Ex
8	1742.96	Ens.Mlk. M+A. RCC. fc. Purkinje cells HC. m-a. ivFt.	++	n/c
9	1778.96	Mlk. Neutrophilia. RCC. Multi-focal grey matter oedema and mild microglial reaction. perivascular. ivFt. m-a. Phagocytosis of parasites by neutrophils. **Parvo.**	+	n/c Ex
10	1780.96	ens. fc. uvf. Mlk. Sludging in microvasculature. High protein serum iv. M-a.	-	n/c
11	1785.96	uvf. Mlk. ivFt. m-a. **Parvo.**	-	n/c Ex
12	2104.96	ens. Mlk. uvf. Margination of unparasitised erythrocytes. Microvacuolation. Rare neutrophil in circulation. Monocytic and neutrophilic cuff. HR. Ischaemia. Very fresh.	-	n/c
13	2612.96	Multifocal HM - artifact. M-a. Os **Suspected diamidine toxicity.**		n/c Ex
14	2788.96	Mlk. M+A. Mild RCC. M-a. HM of sc.	++	n/c
15	2849.96	Ens. Mild RCC. Rare monocytes and lymphocytes	++	n/c

16	2953.96	Ens. M+ but no adhesion. RCC. Mlk. fc.	+	n/c
17	2965.96	Multifocal HE + malacia. ICC.	++	C
18	3024.96	Ens. Svn. M+A. RCC. Severe congestion. HP.ICC. A2. **E. canis**	+	C Ex
19	3066.96	ens. HM. HP. Severe congestion. Mlk. fc. Focal infarction. ICC + H. HP: sulcal depths and gyral crests. uvf: some arterioles empty. Hypoxia. CBS. **E. canis.**	-	C Ex
20	3067.96	Lymphoplasmacytic meningitis. **E. canis.**	-	n/c Ex.
21	3157.96	Focal ens. fc. RCC. M+A. Mlk. Os. svn. Og. HE deep sulcal cortex. Neutrophil infiltration. ICC. HC. Astrogliosis. evF. Cerebellum: vasculitis. HE, HC Purkinje cells. ivFt. a-0. sc: HP & HC.	+	C
22	3168.96	Multifocal HE + ICC. Protein rich oedema. Neutrophil cuffs. Few lymphocytes.	+	C
23	3226.96	Endothelial nuclear swelling (ens). Margination and adherence (M+A). Red cell changes + (RCC). Foamy cells (fc). uvf. Mlk. Neutrophilia. SNC. Moderate autolysis. M-a	+++	n/c
24	3228.96	Multifocal ens.+ svn. SNC + ICC + HC. Cerebellar + periventricular HP. Os. uvf. sc: HP. m-a.	++++ +	C
25	3285.96	Multifocal ens. RCC. uvf. Mild Os. Monocytosis and neutrophilia - mild. fc. ivFt. m-a.	+	n/c
26	3427.96	**E. canis**	0	n/c (histo) Ex
27	3542.96	Organisms in depths of sulci. HP - multifocal to coalescing. Monocytic leukostasis (Mlk). **E.canis**		C Ex
28	4.97	Mlk. RCC. HR. HE. HP. Advanced lesions. svn. A2. ICC also with incrustations. HC. Large granular lymphocytes. Og. Free organisms. Cerebellar sulcal depths. ivFt. HM subcortex.	++++	C
29	184.97	Severe congestion. Mlk. RCC. HM. HR. ivFt. S-a.	+++	n/c
30	424.97	**Granulomatous meningo-encephalitis.** *B. canis* - associated?	-	n/c Ex
31	559.97	**E. canis**	-	n/c Ex
32	598.97	Mlk. uvf. svn. HM with extravasation of pRBC. Early lesions. HM sc. ivFt. putrefaction. S-a. Hypophyseal adenitis and necrosis (true cerebral lesion).	+	pre-cerebral
33	702.97	Mlk. HE. ICC. Perivascular neutrophilic cuffing and neutrophil infiltration. S-a. **E. canis**	-	C Ex
34	923.97	ens. svn. Margination. RCC. Mlk. Microvascular congestion. HM. HR. HP. Og. *ICC but no neutrophils, monocytes or gliosis.* M-a	+	C
35	946.97	Mlk. fc. Margination. svn. Og. HR Subcortex necrosis of neuropil. HM hippocampus. M-a. **E. canis**	+	pre-cerebral Ex
36	965.97	Severe congestion of microvasculature. fc. Os. Mlk. HP white matter. sc: HE. **Spinal injury**	-	n/c Ex
37	974.97	Mlk. RCC. M+A. Lymphocytes. Neutrophils. HM. Multiple parasites in erythrocytes. Severe congestion.	++++ +	n/c (histo)
38	975.97	RCC. M+A. HE. HR. HP deep sulcal. Perivascular neutrophilic cuffing. Rare monocytes. SNC. Advanced lesion caudate nucleus. sc: HM.	+	C
39	1215.97	Mlk. Moderate congestion. RCC. sc perivascular lymphoplasmacytic cuffing & HM.	++	n/c
40	1216.97	**E. canis**		Ex
41	1391.97	Ens. Mlk. RCC. Margination. uvf. Os. Og. Neutrophilia. Svn. HM. Early cerebral lesions. M-a.	++	C
42	1430.97	Multifocal ens. Mlk. Lymphocytosis. ivFt. HM. RCC. M+A. Os. sc: HM.	++++ +	n/c
43	1484.97	Focal ens. HM. Lymphoplasmacytic perivascular cuffing. Mild lymphoplamacytic meningitis. **E. canis**	+	n/c Ex
44	1503.97	Multifocal ens. svn. RCC. Mlk. Lymphocytosis. Plasma cells. uvf. HM. ivFt. m-a. Margination of neutrophils. **E.canis**	++	n/c Ex
45	1553.98	Focal ens. RCC. uvf. ICC (hypoxia). M-a **Intussusception Recovered from *B. canis***	-	n/c Ex

46	1618.97	Multifocal ens. RCC. M+A. Deep sulcal and meningeal margination. Multiple organisms in individual cells HM. Free organisms.	++++	n/c
47	1635.97	uvf. HP. HM. ivFt.	+	n/c
48	1636.97	ens. Mlk. M+A. HM. Oedema. uvf. RCC. ivFt. M-a. Focal malacia in sulcus. Gitter cells and gemistocytes. Microglial and astroglial infiltration. Lesion of long duration. **E. canis**	+	C Ex
49	1800.97	Mlk. RCC. ens. uvf. Lymphocytic leukostasis. HM. **Septicaemia**.	-	n/c Ex
50	1835.97	ens. RCC. M+A. Mlk. Lymphoplasmacytosis. uvf. Og. HM cerebellum, subcortex and hippocampus. Early lesions, SNC. m-a. **E. canis**	++	C Ex
51	1839.97	RCC. HM. Os. Mlk. Microvascular congestion. **E. canis**	++	n/c Ex
52	1953.97	S-a. Mlk. **E. canis**	-	n/c Ex
53	1959.97	ens. Microvascular congestion. Mlk.	-	n/c
54	1960.97	RCC. Margination. Microvascular congestion. Perivascular lymphocytic cuffing. iv haemoglobin globules. Og. Multiple parasites in individual cells. HE. Distemper imp negative.	+++	C
55	1970.97	svn. Moderate microvascular congestion. fc. Mlk. Os. M+A. HM. HP. HR. Neutrophil infiltration. A2. Og. pRBC in haemorrhage.	++	C
56	2005.97	Mlk. Plasma cells. RCC. HE. Many free parasites. Sever haemorrhage and coagulative necrosis of hypophysis (advanced lesion). **E. canis**	++++	C Ex
57	2098.97	**E. canis** and metastatic neoplasia (to CNS).	-	Ex
58	2203.97	M-a. Lymphoplasmacytic infiltration. Distemper imp negative. Suspect **E. canis**.	-	Ex
59	2534.97	Mlk. Lymphocytosis. Neutrophila. Margination. HM. A2?. Early lesions. Perivascular lymphoplasmacytic meningitis. **E. canis**	+	C Ex
60	2535.97	RCC. Advanced lesion HE. Og. SNC. ICC. NN and gemistocytes.	-	C (histo)
61	2560.97	Moderate microvascular congestion. RCC. Mlk. Os. Intravascular protein droplets. uvf. HM. ivFt. svn in hypophysis. **E. canis**	-	n/c Ex
62	2567.97	RCC. Advanced lesions with Gitter cells and gemistocytes.Vasculitis. Axonal degeneration and necrosis. HE. HM. **E. canis**	-	C Ex
63	2575.97	ens. Margination. RCC. HP cerebellum. Spinal cord early lesion HM. HE caudal colliculus.Mlk Lymphocytic infiltration.	++++	C
64	2600.97	Mlk. svn. HM. HR. Lymphocytes. Oedema. Margination. **E. canis**	++	C Ex
65	2611.97	RCC. Margination. uvf. svn. Og. Mlk. HM of white matter. Few plasma cells. Lymphocytes. Neutrophilia. ivFt. M-a.	+++	n/c
66	2709.97	Ens. RCC.Mlk. fc. HP & HM in white matter of occipital lobe. Og. Lymphocytes. Neutrophils.	-	n/c
67	2868.97	Ens. Microvascular congestion. Mlk. fc. RCC. Margination. Os. Svn. Og. HP. HE. HM. Perivascular neutrophilic cuffing. Intermediate lesions. Neutrophil infiltration. Advanced lesions. ICC. NN. no svn on edge of lesion. Paired parasites in red cells.	+	C
68	3051.97	Mild ens. Severe congestion of meninges. RCC. Mlk. fc. HP. HM. Grey-white junction. svn. HE olfactory bulb. Advanced lesion ICC, HC. ivFt. **E. canis**.	++	C Ex
69	4.98	Mlk. Monocytic cuffing. Monocytic infiltration. Free parasites. Margination. ens. uvf. HM. HR. HP. HE. Og. ICC.	+++	C
70	24.98	ens. Mlk. Margination. RCC. HP. svn. Neutrophilia and neutrophil invasion of parenchyma. ICC on periphery of haemorrhagic area. M-a. Single area parasitaemia 4+.	+	C
71	150.98	Meningeal congestion. ens. Mlk. svn. HP. HE. Og. Os. Neutrophil infiltration. Necrosis of the subcortex. ICC. Leukocytoclastic vasculitis. A2. Gemistocytes. Flattening of gyri. Haemorrhage does not penetrate white matter tracts in some sites, in others, HE. pRBC do not extravasate, or are confined to VR-spaces.	+++	C
72	151.98	ens. Moderate microvascular congestion. fc. HM. Os. Parasitic proliferation in capillaries of white matter. svn. **E. canis**	++	n/c Ex
73	152.98	Ens. uvf. Mlk. RCC. Congestion of larger caliber vessels. fc. ivFt. HM. HR. Sulcal haemorrhage.	+-	n/c
74	201.98	RCC. Mlk. uvf. fc. Og. Os. svn. Vasculitis. HM. HP. HE. HR in white matter. Perivascular monocytic and neutrophilic cuffing. Neutrophil infiltration. Vascular necrosis with no neuronal change and no haemorrhage in cerebellum. SNC in deep sulcal cortex. M-a.	+	C

75	274.98	ens. Mlk. RCC. uvf. Os. Svn. HE. ICC. Neutrophil infiltration. Og. A2. Vascular necrosis with adjacent normal neurons. No haemorrhage in white matter. M-a.	++	C
76	305.98	ens. Og. uvf. RCC. Moderate microvascular congestion. Os. HM. HP. HE. ICC. Neutrophiiic leukostasis. Neutrophil infiltration. Petechiation of the grey/white junction. M-a.	+++	C (histo)
77	307.98	Mild ens, focal. Mlk. RCC. uvf. Os. Og-focal, deep sulcal. ivFt. Focal periventricular cyst in white matter with gemistocytes, microglial infiltration. Survival post-infarction. M-a.	+	n/c
78	331.98	ens. Mlk. Fc. svn. Advanced lesions. HE. ICC. Vasculitis. Neutrophil infiltration. A2. Microglial rod cells SNC. Og.	++	C
79	348.98	Mlk. ens. HM. RCC but no sludging. M+A. Neutrophil leukostasis. Os. Og. HP. Neutrophil infiltration. ICC *No ICC present in haemorrhagic site where neutrophil extravasation was absent.* HR in grey matter.	+	C
80	426.98	ens. Mlk. RCC. M+A. svn. Og. Os. Leukocytoclastic vasculitis, endothelial cells ok. Advanced lesions. HP. HE. ICC. NN. A2. Cerebellar Purkinje cells ICC, HCC. Spinal cord advanced lesion. "Venous infarction"	+	C
81	427.98	Mild microvascular congestion. Mild ens, fc. Mlk. M+A. RCC. Os.Toxic neutrophilia. HM. **Pancreatitis**	-	n/c Ex
82	672.98	Ens. uvf. Os. ivFt. M+A. RCC.	+++	n/c
83	815.98	RCC. Margination. Os. Og. HE. Neutrophil infiltration. Empty vessels. Advanced lesions with HE. neutrophils. Gitter cells. A2, cystic lesions. S-a.	+++	C
84	875.98	Ens. Mlk. Svn. RCC. Margination. Necrosis of pial vessels. Congestion of meninges. Advanced lesions. HE. Neutrophil infiltration. ICC. NN. Vascular necrosis. ivFt. "Venous infarction".	++++ +	C
85	925.98	Ens. Mlk. RCC. fc. HP. svn. Vasculitis. HE. Astrogliosis (sulcal floors). Neutrophil infiltration but no neuronal necrosis (mod MSB;LFB Holmes;LFB PAS). ivFt. **Primary vasculitis.**	++	C
86	1031.98	ens. Mlk. Mild congestion. Neutrophilia. HM. HR. HP. RCC. Axonal injury in spinal cord. **E. canis**	+	n/c Ex
87	1094.98	Ens. Mlk. Mild congestion. Severe Os and cerebellar compression, fc. *HE lenticular nucleus with sparing of internal capsule.* Leukocytoclastic vasculitis. Svn. ICC. NN. HR in grey matter. Og. ivFt.	-	C
88	1112.98	RCC. Severe multifocal microvascular congestion (lesion associated). fc. Svn. Og. Os. HR. **Arterial congestion is a feature of this case.** Caudal colliculus - advanced lesion. HE. Neutrophil infiltration. ICC. NN. Severe og. Mlk. Vascular wall necrosis.	+	C
89	1207.98	Severe congestion. ens. fc. RCC. Mlk. svn. HP. HM. Granule cell layer has HP. ivFt. Og. Early lesion capillary necrosis and associated oedema.	++	pre-cerebral
90	1268.98	Mlk. ens. RCC. svn. HP. Og. Perivascular monocytic cuffing. Advanced lesion. HE. Neutrophil infiltration. ICC. EvFt. A2. Caudal compression of cerebellum. *Low parasite density in capillaries.* ivFt.	+++	C
91	1270.98	Mlk. ens. RCC. M+A. Moderate congestion. pRBC abound in capillaries but not in larger vesseis. HM. Mild Os. m-a.	+++	n/c

APPENDIX C FULL RESULTS TABLE - ULTRASTRUCTURE

CASE	EM NUMBER	HISTORY	MACROSCOPIC PATHOLOGY	HISTOPATHOLOGY	ULTRASTRUCTURAL PATHOLOGY
1	26.96	Peracute haemoconcentrating babesiosis with central nervous excitation. Archival case.	Severe cerebral oedema and congestion.	Congestion and endothelial activation.	Endothelial - erythrocyte contact. Intererythrocytic contact. Necrosis of neuropil, with free erythrocytes, mitochondrial and other organellar debris and swelling of astrocyte foot processes.
2	27.96	Cerebral babesiosis. Archival case.	Ecchymotic haemorrhage of brain stem and spinal cord.	Perivascular haemorrhage and vascular necrosis of brain stem. Neuronal necrosis.	Advanced neuronal ischaemic cell changes, immersion artifacts in neurons. Endothelial cell necrosis and autolysis in some cells. Severe astrocytic swelling. Intravascular inter-erythrocytic sites of contact.
3	6.97	Peracute babesiosis with no neurological signs clinically. Glutaraldehyde fixed (direct).	Bilateral, asymmetrical haemorrhage in caudate nuclei. Locally extensive myocardial necrosis.	Segmental vascular necrosis. Advanced lesions with ischaemic cell change and foci of malacia.	Severe vascular injury with exposure of basement membrane, loss of plasma into perivascular space, intact tight junctions, endothelial cell necrosis. Microvascular vasoconstriction. Swelling of pericyte nuclei causing luminal obstruction. Fibrin degradation products. Inter-erythrocytic contact points. Cytoplasmic vesicles on erythrocyte membranes. Intravascular monocytic activation. Neutrophilia.
4	1.98	Severe generalised seizures.	Multifocal cerebral haemorrhage. Cardiac form.	Erythrocyte margination and adherence. Multifocal petechiation with perivascular oedema of grey matter. Mild focal neutrophilic perivascular cuffing. No neuronal necrosis. Low endothelial reactivity.	Marked plastic deformation of erythrocytes. Loss of electron density. Erythrocyte fragmentation. Inter-erythrocytic contact points: amorphous granules. Endothelio-erythrocytic contact points. Focal endothelial necrosis. Focal endothelial nuclear swelling with microvascular occlusion. Endothelial pseudopodia formation - luminal aspect. Phagocytosed erythrocyte fragments. Plasma in perivascular space. Loss of swollen astrocyte foot-process contact with basement membrane. Condensation of organelles in endothelial cells. Individual endothelial cell necrosis. Neuronal changes very variable. From intact, through early reversible change to irreversible change with loss of nucleoli, nuclear swelling, loss of ribosomes and presence of mitochondrial dense bodies. Astrocytic syncytial swelling observed adjacent to intact neurons. Oedema of myelin sheathes.

CASE	EM NUMBER	HISTORY	MACROSCOPIC PATHOLOGY	HISTOPATHOLOGY	ULTRASTRUCTURAL PATHOLOGY
5	3.98	Cerebral babesiosis	Multifocal cerebral haemorrhage and muscle form.	Severe vascular necrosis with vasculitis. Neuronal necrosis could not be demonstrated using modified MSB, LFB-Holmes or LFB PAS stains. Perivascular neutrophilic cuffs and focal infiltration.	Endothelial-erythrocytic contact. Membrane stacks between erythrocytes and endothelial cells. Margination of erythrocytes against endothelium with apparent fusion of erythrocyte and endothelial membranes. Sludging of erythrocytes with apparent fusion of adjacent membranes. Endothelial cell retraction with exposure of underlying basement membranes. Endothelial cell necrosis. Perivascular polymerisation of fibrin with complete necrosis of endothelial cells. Tight junctions morphologically intact, lysis of organelles.
6	4.98	Subacute babesiosis with respiratory distress. Glutaraldehyde fixed (direct).	Pulmonary oedema.	Very high parasitaemia, rare microhaemorrhage. Margination of parasitised erythrocytes and swelling of endothelial nuclei.	Erythrocyte sludging, loss of electron density and inter-erythrocytic contact. Endothelial-erythrocyte contacts. Severe nuclear swelling. Focal endothelial necrosis. Retraction of endothelial cells with exposure of basement membrane.
7	5.98	Subacute babesiosis. AIHA.	External pallor, internal bilateral ecchymoses of caudate nuclei. Pulmonary form.	Sludging, margination of erythrocytes. Very high parasitaemia. Microhaemorrhage.	Apparent fusion of adjacent erythrocyte membranes. Erythrocyte squaring in capillaries, or marginating. Apparent fusion of erythrocyte-endothelial plasmalemma. Endothelial necrosis with condensation of organelles. Intravascular fibrin polymerisation. Endothelial pseudopodia. Endothelial-erythrocyte contact.

APPENDIX D ARTERIAL SUPPLY FIELDS OF THE CANINE BRAIN.

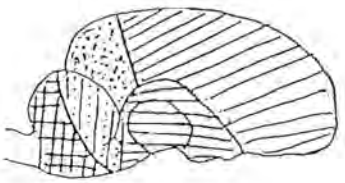

Medial

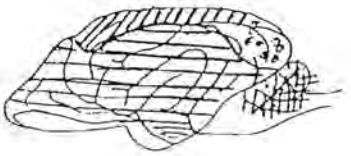

Lateral

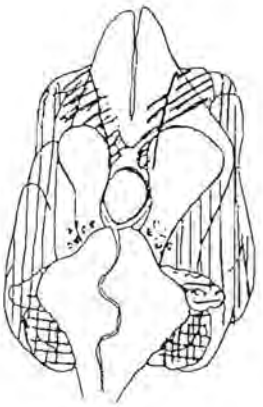

Ventral

Dorsal

Key:

Rostral cerebral artery

Middle cerebral artery

Caudal cerebral artery

Rostral cerebellar artery

Caudal cerebellar artery

APPENDIX E

Table of Excluded cases

Exclusion criterion	Frequency (%)	Cumulative frequency
Ehrlichia canis co-infection	28 (65.1)	65.1
Septicaemia	2 (4.7)	69.8
Parvoviral enteritis	3 (7)	76.8
Pancreatitis	1 (2.3)	79.1
Warfarin toxicity	1 (2.3)	81.4
Granulomatous meningo-encephalitis	1 (2.3)	83.7
Metastatic cerebral neoplasia (with concurrent *Ehrlichia canis* infection)	1 (2.3)	
Splenic tortion	1 (2.3)	86
Acute heart failure	1 (2.3)	88.3
Babesia canis not confirmed	2 (4.7)	93
Intussusception	1 (2.3)	95.3
Spinal injury	1 (2.3)	97.6
Suspected diamidine toxicity	1 (2.3)	99.9
TOTAL	43	